Polyserine-Tau Interactions Modulate Tau Fibrilization

by

James Pratt

B.S., Loyola Marymount University, 2018

A thesis submitted to the

Faculty of the Graduate School of the

University of Colorado in partial fulfillment

Of the requirement for the degree of

Doctor of Philosophy

Department of Biochemistry

2025

Committee Members:

Roy Parker

Deborah Wuttke

Marcelo Sousa

Christopher Link

Alexandra Whiteley

Pratt, James (Ph.D., Biochemistry)

Polyserine-Tau Interactions Modulate Tau Fibrilization

Thesis directed by Professor Roy Parker, Ph.D.

The aggregation of tau is observed across several neurodegenerative diseases classified as tauopathies. While tau has been studied extensively for several decades, little is known about the molecular mechanisms driving tau aggregation. One possible mechanism is the formation of cytoplasmic speckles, assemblies of mislocalized nuclear speckle proteins that contain polyserine domains, which creates a preferred site of tau aggregation. However, the nature of the interaction between tau and these polyserine containing assemblies, and the impact on developing tau pathology, are unknown.

My goal was to characterize the nature and consequence of tau-polyserine interactions, leading to a mechanistic understanding of tau aggregation with polyserine. Specifically, I performed a series of *in vitro* experiments with recombinant proteins and cell culture models to characterize the tau-polyserine interaction. I found that polyserine is capable of self-assembly, and that these assemblies interact directly with tau. This interaction increases the rate of formation and growth of seeding competent tau fibers. In cells, I found that polyserine-rich domains can enrich in tau aggregates independent of exacerbating tau aggregation. I used a series of separation of function polyserine variants to show that polyserine assembly and polyserine targeting to tau aggregates are distinct functions. Using a polyserine fusion protein that blocks polyserine self-assembly in cells, I show that polyserine assembly is necessary for increasing tau aggregation.

I also briefly discuss how the SARS-CoV-2 pandemic may result in increased diagnoses of tauopathies. I summarize previous viral pandemics and how they lead to tauopathy sequelae and propose a mechanism in which viral infection triggers neuroinflammation and tau aggregation.

Acknowledgements

The work presented in this thesis would not be possible without the support and mentorship I have received over the years.

First, I would like to thank Roy Parker. I would not have had the opportunity to write this thesis and perform this research if not for your generous support and mentorship. You have believed in me and my abilities from the moment I joined your lab, and you have worked incredibly hard to make my experience as great as possible. Thank you for the mentorship, training, and balloons.

To my thesis committee, it has been an absolute joy getting to work with you all. To Marcelo Sousa, teaching our first semester of core, writing and proctoring my qualifying exams, and easing my transition into graduate school from day one, I am extremely grateful. To Debbie Wuttke and Alex Whiteley, the opportunity to work with you both in progressing my research has been a great joy, and collaborating with both of you in getting Diversity Equity and Inclusion initiatives started and supported made working in the Biochemistry Department a better place. Finally, to Chris Link, you have read every piece of writing I have produced in graduate school, and you have provided necessary feedback and suggestions before you sat on my committee, you make this work exciting, and your passion for research is infectious. Thank you all for working with me.

I have had the great pleasure of working with an incredible cohort, we have had a rather unconventional graduate school experience, and I couldn't have made it without our pandemic movie nights, Dungeons and Dragons games, and late-night gaming sessions. I would specifically like to thank Victor Passanisi, my first friend in Colorado, you have forever changed the way I drink coffee and think about science.

I would also like to thank all the members of the Parker Lab that I have had the pleasure of working with. The opportunity to work with you all makes coming into the lab every day a joy.

To the Tau Team, none of the work in this thesis would be possible without our long conversations, brainstorming sessions, and collaborations, thank you so much for helping with every step of the way.

My passion for research started when Sarah Mitchell accepted me into her lab at Loyola Marymount University. I was a naïve Junior, but Sarah made doing science into something truly fun, exciting and accessible. Sarah, you ignited my passion for research.

I would also like to thank my partner, Meaghan Van Alstyne. I have been in awe of your talent and drive since the moment you interviewed. You have pushed me to be a better scientist, and a better man. I wouldn't be writing this without your support, training, and mentorship in lab and in life. You make everything better just by being there with me. I'm so excited to keep growing with you.

Finally, I would like to thank my family. To my mom and dad, you taught me how to ask questions, and how to think critically about everything. Even if you didn't know exactly what I was doing in the lab, you were able to support me when it was tough, and celebrate all of the small wins with me along the way. You have both worked so hard to make sure I have a good life; I am forever grateful for you both. To my sister Christine, our weekly calls have given me something to look forward to every week, you help me put my work into perspective, help me laugh, and have helped keep me close to our family, even when I feel so far away. I love you all so much.

CONTENTS

FIGURES

TABLES

CHAPTER I

In Vitro and Cellular Mechanisms of Tau Misfolding and Aggregation

Contribution Statement: This chapter is adapted from a review titled **Diverse influences on tau aggregation and implications for disease progression**, authored by Meaghan Van Alstyne, James Pratt, and Roy Parker, published in *Genes and Development*.

SUMMARY

As the population on average becomes older, more and more people will be diagnosed with neurodegenerative diseases. Several of these diseases share the hallmark aggregation of tau. In Alzheimer's Disease, symptom severity correlates with increased tau pathology, providing further support that tau aggregation drives disease. While there have been several decades of research on how tau aggregates and contributes to neurodegeneration, the molecular mechanisms of aggregation, and the specific toxicities of tau are unknown. Herein, we review our developing understanding of tau folding and aggregation *in vitro* and in cells. First, we describe the biology of tau, from isoform expression and cellular functions. Second, we summarize prevalent neurodegenerative diseases in which tau aggregates, termed tauopathies. Third, we review how modulation of the biochemical state of tau due to ionic conditions, post-translational modifications, co-factors and other interacting molecules or assemblies can affect the formation and structure of tau fibrils. Finally, we continue our discussion of how cellular factors contribute to tau aggregation, possibly through formation of ribonuclear protein assemblies.

INTRODUCTION

Several observations support that the misfolding of tau into fibrillar aggregates is causative in over 25 different neurodegenerative diseases termed tauopathies. This was foreshadowed by the discovery that tau is the key protein in neurofibrillary tangles (NFTs) – the second pathological hallmark of Alzheimer's disease (AD) (Brion et al. 1985b). Critically, identification of mutations in the tau encoding gene (*MAPT*) in frontotemporal dementia (FTD) provided the first genetic link supporting a causal role for tau in disease (Hutton et al. 1998; Poorkaj et al. 1998; Spillantini et al. 1998). Since then, over 50 genetic mutations and variants in *MAPT* have been associated with familial forms of FTD including Pick's disease (PiD), progressive supranuclear palsy (PSP), and corticobasal degeneration (CBD) (Forrest et al. 2018; Strang et al. 2019). Expression of human *MAPT* with pathogenic mutations in mice and rats also recapitulate aspects of human disease (Dujardin et al. 2015). Moreover, pathogenic variants of tau can be more prone to forming fibers *in vitro*, in cell lines, and in mouse models emphasizing the importance of tau fibrillization in disease (Yoshiyama et al. 2007; Chen et al. 2023; Holmes et al. 2014).

Tau aggregates identified in disease are composed of filaments of tau organized in β-sheet fibrillar structures (Crowther 1991; Fitzpatrick et al. 2017). Tau fibers can develop within a given cell in a 'prion-like' manner where small "seeds" of a fiber can template the misfolding of additional tau monomers into the same structure. In support of this mechanism, tau fibers are able to induce folding of naïve tau monomers into fibrils in solution (Dinkel et al. 2015; Fichou et al. 2018). Further, tau fibrils can also propagate between cells as injection of tau seeds into mouse brain can induce aggregation across connected brain regions reflecting the patterning observed in human pathologies (Guo and Lee 2011; Iba et al. 2013; Clavaguera et al. 2009). Another shared characteristic of prions and tau is that distinct strains defined by morphology can be stably propagated through multiple rounds of transmission between both cellular and mouse models

(Sanders et al. 2014; Kaufman et al. 2016). Thus, the ‘prion-like’ spread of tau pathology is an important aspect of disease.

In this review, we focus on the biochemical and cellular mechanisms influencing the transition of tau from a normal state into a misfolded and aggregation-prone toxic form. We also review the formation of ribonuclear protein assemblies and how these assemblies influence tau aggregation. Given the breadth of the field, we apologize to those whose work we were not able to include due to space constraints.

BIOLOGY OF TAU

Tau isoforms, domain architecture and expression

Tau is predominantly expressed in neurons with seven alternatively spliced isoforms (Figure 1.1).

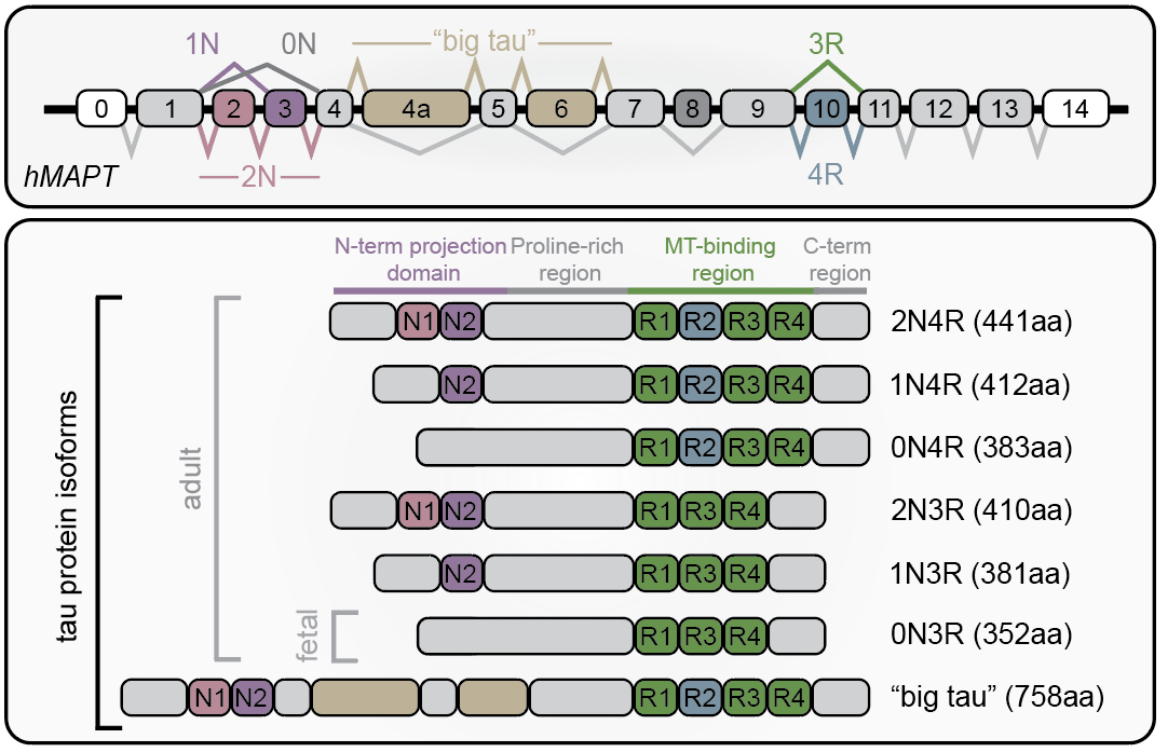

Figure 1.1 MAPT gene and tau protein isoforms. Transcripts derived from the human MAPT gene (*hMAPT*) can undergo alternative splicing to generate various tau protein isoforms. Inclusion or exclusion of exons 2 and 3 determine 0, 1, or 2N isoforms while exon 10 determines 3 or 4R isoforms. Big tau is characterized by inclusion of exon 4a and 6. All protein isoforms are expressed in adult human brain while 0N3R is the predominant fetal isoform.

These isoforms are defined by the inclusion of 0, 1, or 2 N terminal inserts (N), and either 3 or 4 pseudo-repeats (3R or 4R) in the microtubule binding region (MTBR) (Goedert et al. 1989a, 1989b). Alternative splicing controls the inclusion of exons 2, 3 (0, 1, or 2N) and 10 (3R vs 4R) (Andreadis et al. 1992). In embryonic and early developmental stages, tau is predominately expressed as a 3R isoform while in adult brains there is a 50:50 balance between 3R:4R tau (Goedert et al. 1989a). A larger tau isoform – referred to as big tau – includes additional exons (4A and 6) in the N terminal region and is expressed more highly in less vulnerable brain regions. (Oblinger et al. 1991; Chung et al. 2024).

Tau has four distinct domains, an N-terminal projection domain, a proline rich region (PRR), the microtubule binding region (MTBR), and a C-terminal region. The N-terminal projection domain has no affinity for microtubules and orients away from the microtubule surface (Hirokawa et al. 1988). The PRR upstream of the MTBR has been reported to drive phase separation of tau *in vitro* and in cells (Zhang et al. 2020b). The PRR is also highly post-translationally modified and contains a majority of phosphorylation sites on tau (Martin et al. 2013b). The MTBR of tau is composed of 3 (in 3R tau) or 4 (in 4R tau) imperfect repeats of 30-31 amino acids that differentially mediate roles in microtubule polymerization and stability (Panda et al. 2003).

Tau is highly expressed in the brain, most predominantly in neurons where it localizes to axons (Binder et al. 1985). The cellular spatial organization of tau is regulated by selective transport as well as localized translation and degradation (Aronov et al. 2002; Nakata and Hirokawa 2003). A change in the cellular localization of tau is part of the pathogenic process as the mislocalization and aggregation of tau in the somatodendritic space of neurons is observed in disease (Braak et al. 1994). In addition to neurons, tau can also be expressed to a lesser degree in other central nervous system (CNS) cell types such as oligodendrocytes and astrocytes (Ezerskiy et al. 2022; Torii et al. 2023).

Cellular roles of tau

Tau was first described as a microtubule-associated protein (MAP) that promoted microtubule polymerization *in vitro* (Weingarten et al. 1975; Cleveland et al. 1977; Panda et al. 1995). In cells tau also increases microtubule polymerization and stabilizes microtubules (Drubin and Kirschner 1986). Moreover, in primary neurons tau regulates microtubule dynamics, organization, and growth cone ordering and growth (Biswas and Kalil 2018). However, the stabilization of neuronal microtubules by tau in mice appears redundant since tau knockout mice

do not show strong microtubule impairments (Harada et al. 1994; Dawson et al. 2001; Takei et al. 2000), but double-knockout mice lacking both tau and MAP1b have greater defects in neuronal axons (Takei et al. 2000). Thus, tau binds and stabilizes microtubules and is at least partially functionally redundant with other MAPs.

The interaction of tau with microtubules suggests it may influence axon transport. Neurons are unique as they can have long axons and require transport of proteins and organelles over long distances. Several observations suggest this process, termed fast axonal transport (FAT), is modulated by tau (Combs et al. 2019). For example, tau can associate in dense regions along a microtubule that hinder kinesin processivity (Siahaan et al. 2019), leading to enhanced dynein activity (Chaudhary et al. 2018). Such roles for tau may also be particularly important for the transport of components that are required for proper function and maintenance of synapses (Guedes-Dias and Holzbaur 2019).

Tau has also been proposed to have roles in protecting DNA and RNA from damage. One observation is that TUNEL staining in Tau knockout mice show increased susceptibility to DNA and RNA damage during heat stress (Violet et al. 2014). Similarly, knockdown of tau in primary neurons increases double stranded breaks induced by etoposide (Asada-Utsugi et al. 2022). This role may be direct as tau has been observed in the nucleolus of cultured cells (Maina et al. 2018; Bou Samra et al. 2017), and in mice 1N isoforms of tau are enriched in soluble nuclear fractions (Liu and Götz 2013). Such a role might be relevant since tau has nanomolar affinity for DNA (Wei et al. 2008) and RNA (McMillan et al. 2023). Thus, a less explored role for tau is in the regulation of nucleic acids.

TAUOPATHIES

Primary Tauopathies

Primary tauopathies are diseases caused by mutations in the gene *MAPT* and are classified based on the primary pathological feature of tau deposition. These mutations can be coding or non-coding, and alter tau dynamics, localization, and structure.

Disease Associated Mutations in Tau

There are over 50 missense-coding mutations in *MAPT*, several of which are causative of severe FTD (Strang et al. 2019). These missense-coding mutations can contribute to disease through several mechanisms which generally lead to increases in tau aggregation. For example, mutation of P301S/L increases the ability for tau to aggregate as proline residues inhibit β-sheet formation (Strang et al. 2019). Further, several disease-linked tau missense mutations lead to impaired microtubule binding and reduced effects on microtubule polymerization *in vitro* which may increase the concentration of free tau available for aggregation (Strang et al. 2019). Interestingly, the S320F mutation, which promotes spontaneous tau aggregation, may work by both decreasing tau-microtubule interactions, and by increasing exposure of necessary regions for incorporation into a fiber (Rosso et al. 2002; Chen et al. 2023) – a mechanism shared by P301L/S mutations (Chen et al. 2019).

Tau mutations can also alter the ratios of tau isoforms which can affect aggregation and disease development. The missense mutation S285R increases inclusion of exon 10, resulting in higher expression of 4R tau (Ogaki et al. 2013). Additionally another class of mutations in *MAPT* are silent or noncoding variants causing increased inclusion of exon 10, resulting in higher expression of 4R tau (Skoglund et al. 2008; Stanford et al. 2000; Spillantini et al. 2000; D'Souza et al. 1999). Many of these non-coding mutants are in intron 10 and cause destabilization of a stem loop near the exon 10 splice site, which leads to increased inclusion and disruption in the

balance of 3 and 4R tau isoforms contributing to pathology (Qian and Liu 2014; Buchholz and Zempel 2024).

Pathology

Primary tauopathies differ in where pathology starts and spreads, general presentation of symptoms, and aggregation of 3R or 4R tau.

FTD exists on a spectrum with primarily tau aggregation driven disease on one side, and primarily TDP-43 aggregation driven diseases (ALS) on the other (Ling et al. 2013; Götz et al. 2019). Other primary tauopathies, such as progressive supranuclear palsy (PSP), corticobasal degeneration (CBD), and Pick's Disease (PiD) (discussed below), exist on the tau side of the FTD-spectrum (Götz et al. 2019). FTD-tau can be both sporadic and familial, with mutations such as P301L/S and S320F being causative (Rosso et al. 2002; Bugiani et al. 1999; Sperfeld et al. 1999). Aggregation of tau in FTD occurs in the cortex, basal ganglia, and brainstem (Van Swieten and Spillantini 2007). Different tau mutations present with specific symptoms. For example, G272V and P301L typically present with early dementia and personality changes (Bird et al. 1999). Mutations like N279K, and intronic mutations that increase inclusion of exon 10, present with more parkinsonism symptoms, including gait impairment, tremor, and rigidity (Wszolek et al. 1992; Pickering-Brown et al. 2002; Miyamoto et al. 2001).

PSP is a 4R primary tauopathy with early characteristic atrophies allowing for diagnosis in patients (Shi et al. 2021; Pandey 2012). PSP presents as progressive paralysis, loss of control of eye motion, and eventually loss of control over breathing (Dickson et al. 2007). Neuropathologically, PSP presents as atrophy of the pons, creating a characteristic hummingbird shape (Pandey 2012). This occurs alongside tufted astrocytes and globular tau aggregation in

neurons (Dickson et al. 2007). Tau pathology spreads from initial atrophy in the pons into cortical areas through the fronto-parietal to temporal, to occipital lobes (Kovacs et al. 2020).

CBD is a rare 4R primary tauopathy (Zhang et al. 2020a). Symptomatically, CBD presents with motor, behavioral, sensory, and cognitive defects and is usually diagnosed during autopsy (Kouri et al. 2011). Cortical and substantia nigra atrophy and ballooning of neurons burdened with tau aggregation is observed in patient autopsy. Additionally, aggregation of tau is observed in neurons, and in astrocytes as plaques (Chung et al. 2021).

PiD is the only known primary 3R tauopathy (Falcon et al. 2018). This disease presents with more severe personality deterioration and cognitive impairment with less severe motor function deficit compared to other tauopathies (Dickson 1998). Atrophy of the hippocampus, entorhinal cortex and amygdala is common. Tau aggregation in this disease is distinct in that only 3R aggregates are observed, and these aggregates spread from the hippocampus and amygdala through the subcortical regions into the primary motor cortex and finally in the visual cortex (Irwin et al. 2016). Additionally, AT8 staining of patient tissue shows Pick's Bodies, or round, bulbous inclusions of aggregated tau in early phases of the disease (Irwin et al. 2016).

Secondary Tauopathies

Secondary tauopathies also feature tau aggregation, however this occurs subsequent to additional insults or pathological features. Secondary tauopathies include AD and CTE, subacute-sclerosing pan encephalopathy (SSPE), and in rare cases, HTT and SCA8.

The cause of tau aggregation in secondary tauopathies is disease specific. For example, CTE is caused by repetitive head trauma, AD through some unknown amyloid-β-tau axis, SSPE arises as a sequelae to measles, and HD and SCA8 through completely unknown mechanisms (Chung et al. 2021; Bloom 2014; Chen 2018; Bancher et al. 1996; Jiang et al. 2023; Gratuze et

al. 2016). A convergent hypothesis is that these preceding insults trigger neuroinflammation altering the neuronal microenvironment to enhance tau aggregation. CTE and AD are specifically interesting in that disease symptoms and pathology correlate with tau burden (Tommasi et al. 2021; Alosco et al. 2021). This implies that while tau is not the primary cause of the disease, the misregulation of tau is the main driver of disease.

The way in which tau becomes pathogenic in CTE is unknown. One way in which this may happen is through TDP-43 loss of function. In several cases of CTE, TDP-43 accumulation is also observed (McKee et al. 2016). This accumulation occurs in the same brain regions as tau pathology (McKee et al. 2013). TDP-43 has been proposed to regulate tau mRNA stability and splicing of exon 10 (Gu et al. 2017b, 2017a). Thus, aggregation and loss of function of TDP-43 in CTE may contribute to the development of tau pathology via increased inclusion of exon 10, and increased expression of tau (Chen 2018). How tau aggregation occurs in cases of CTE without TDP-43 pathology is unknown.

AD is a secondary 3R/4R tauopathy that impacts millions of people globally (2024). Tau aggregation in AD correlates with disease symptoms and tau may be required for disease progression (Leroy et al. 2012; Tommasi et al. 2021). Classically, amyloid-β aggregation is thought to be the cause of AD, as a SNP in *APP* was the first identified risk factor for AD (Goate et al. 1991). However, PET imaging of non-demented aged brains have shown aggregation of amyloid-β with no tau pathology (Weigand et al. 2019). Further support that tau is the driver of AD comes from characterization of the protective ApoE Christchurch mutation (Wardell et al. 1987). Patients with the Christchurch variant of ApoE, R136S, show amyloid-β plaque accumulation with no tau pathology or severe symptoms of AD (Wardell et al. 1987; Sepulveda-Falla et al. 2022). It is widely accepted that amyloid-β aggregation is upstream of tau aggregation and induces the conversion of healthy tau to a hyperphosphorylated, oligomeric state, and the exact mechanism, and how this axis is mediated by ApoE, is unknown. Regardless, experiments in tauopathy mouse models

have shown that injection of amyloid-β fibers into the brain induces fivefold increase in NFT accumulation (Götz et al. 2001). Additionally, *in vitro* models have shown that treatment of cultured neurons with synthetic or patient derived amyloid-β fibers results in increased hyperphosphorylated tau and dystrophy of the neuron (Jin et al. 2011). The actual mechanism of how amyloid-β aggregation induces tau aggregation is unknown.

SSPE is a secondary 3R/4R tauopathy that is a sequela to measles virus (Okuno et al. 1989; Wisniewski et al. 1991). Here, long-term infection with measles results in increased neuroinflammation that in turn exacerbates tau pathology (Miyahara et al. 2022). SSPE is characterized by severe nerve loss and demyelination, and hyperphosphorylated tau in NFTs found in the cerebral cortex, oculomoter nuclei, and locus coreuleus (Corsellis 1951; Miyahara et al. 2022). The development of secondary tauopathy after viral infection may be more prevalent. For example, previous pandemics, such as the 1918 flu, and more recently, SARS-CoV-2, result in increased diagnoses of tau aggregation and dementia (Buée-Scherrer et al. 1997; Qi et al. 2024). These viral induced secondary tauopathies may be driven through neuroinflammation, independent of direct viral infection of the central nervous system.

Tau Fiber Structures in Disease

Cryogenic electron microscopy (cryo-EM) structures from post-mortem samples have shown that different tauopathies have specific tau fiber structures observed in multiple patients with a given disease (Shi et al. 2021; Fitzpatrick et al. 2017; Falcon et al. 2019, 2018; Zhang et al. 2020a) (Figure 1.2; Table 1.1).

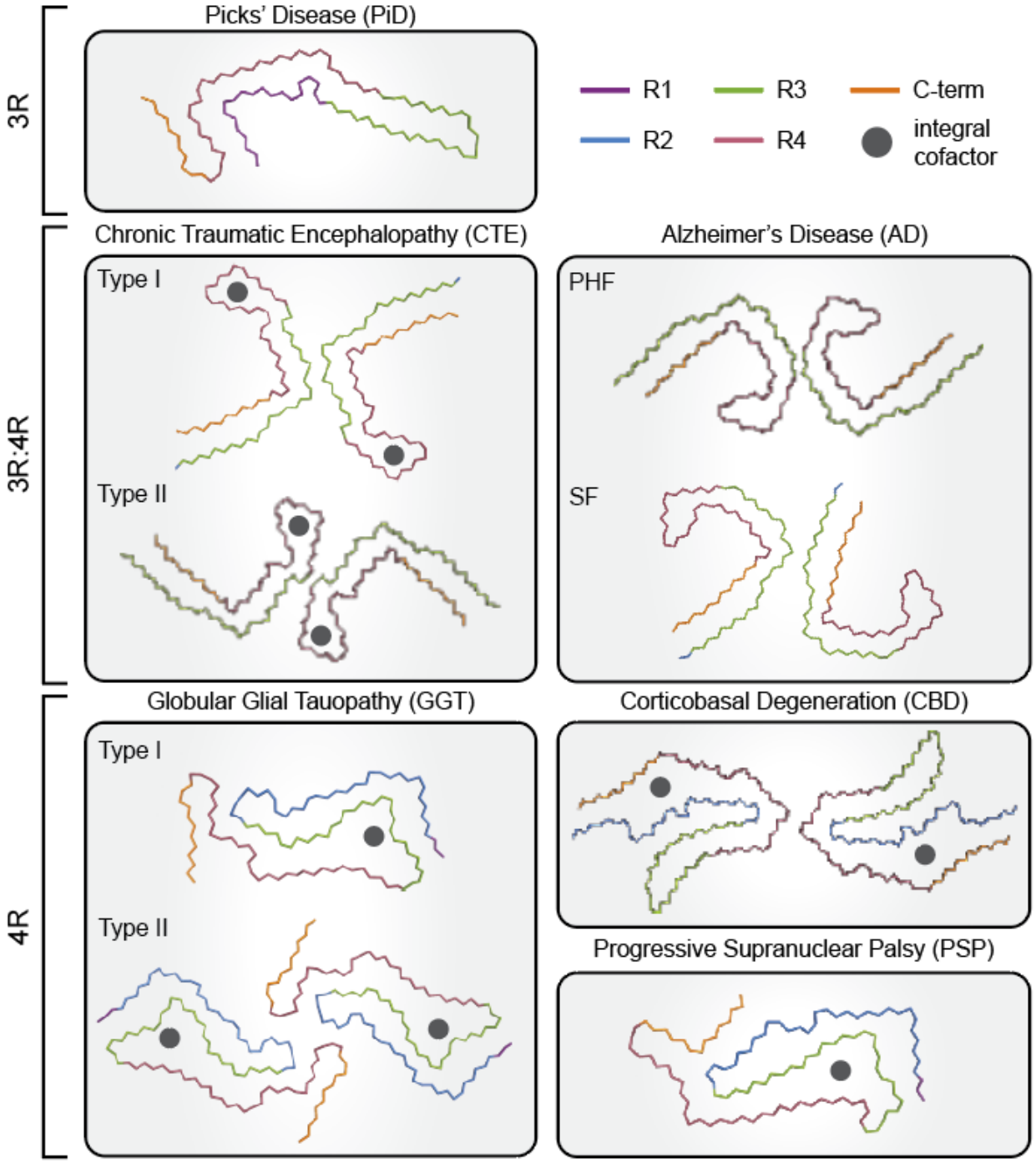

Figure 1.2 Tau Fiber structures in disease. Representations of a subset of tau structures solved from several tauopathies involving inclusions of 3R, 4R or 3 and 4R tau. Notably, solved structures are conserved across multiple patients with a given disease and multiple structures have been solved for some tauopathies including AD which represent paired helical filaments (PHF) or straight filaments (SF) or are classified as distinct fiber types for CTE and GGT. While tau fibers across diseases share involvement of the microtubule repeat domain region of tau, the precise

amino acids involved in the core fiber differ and their distinct structures highlight the diversity of tau fibril forms. Further, several disease relevant tau fiber structures contain non-proteinaceous cofactors which are integral to the fiber core (see Table 1.1).

Disease	Amino Acids in Structure (3R/4R)	Unknown Integral Cofactor	Citation
Alzheimer's Disease (AD)	306-378 (3R/4R)	N/A	Fitzpatrick et al 2017
Chronic Traumatic Encephalopathy (CTE)	305-379 (3R/4R)	Hydrophobic	Falcon et al 2019
Cortical Basal Degeneration (CBD)	274-380 (4R)	Possible Polyanion	Zhang et al 2020a
Progressive Supranuclear Palsy (PSP)	272-381 (4R)	Internal Cofactors between N279 and G323 likely hydrophobic; K294 and D314 likely solvent; K317, K321, K340 likely polyanion 30Å^3.	Shi et al 2021
Globular Glial Tauopathy (GGT)	272-379 (4R)	Internal Cofactors between N279 and G323 likely hydrophobic; K317, K321, K340 likely polyanion, 50Å^3.	Shi et al 2021
Pick's Disease (PiD)	254-378 (3R)	N/A	Falcon et al 2018

Table 1.1 Tau structures from tauopathies. Tau structures which have been solved by cryo-EM from various tauopathies highlighting the amino acids involved in the fibril structures and observation of integral cofactor.

In each case, the stable fiber core is composed of portions of the microtubule binding domain and, in some diseases the C-terminus of tau, arranged in distinct geometries. Outside of the fiber core, tau remains structurally undefined and is described as a "fuzzy coat" observed in 2D-class averages (Fitzpatrick et al. 2017). Interestingly, the tau fiber structures for CTE and CBD contain extra electron density that is not covalently bound to the tau fiber (Falcon et al. 2019; Zhang et al. 2020a). In CTE, the extra density is described as hydrophobic and extends through the tau fiber from end to end (Falcon et al. 2019). In CBD, the extra density is found surrounded by positively

charged amino acids suggesting a negatively charged cofactor (Zhang et al. 2020a). Despite RNA being associated with NFTs (see below), this density appears too small to be RNA. In some diseases more than one tau fiber structure is resolved in cryo-EM. For example, in CTE, there are two related folds, and globular glial tauopathy (GGT) and PSP have three known fiber structures (Shi et al. 2021). These findings raise the possibility that distinct neuronal cell types or regions of the brain might preferentially form different tau structures. This is also suggested by spectral analyses that tau fibers from a single PiD patient have different properties in neurons, oligodendrocytes, and astrocytes (Yang et al. 2023).

The diversity of tau fibers suggests the specific structure that predominates in a given disease is dictated by the biochemical conditions and cell type where disease initiated, and that many tau fiber structures are sufficient to cause neurotoxicity. In support of this, different buffer conditions and cofactor presence can lead to several distinct tau fiber structures from the same tau isoform *in vitro* (Lövestam et al. 2022). Interestingly, mutations in tau do not solely dictate the resulting fiber fold, as P301S tau from two mouse models have distinct folds (Schweighauser et al. 2023). Thus, a summation of the biochemical conditions, expression, splice isoform, and intracellular conditions likely drive tau folding in disease.

BIOCHEMISTRY OF TAU AGGREGATION

Biochemical steps of tau fibrillization

In principle, the formation of tau aggregates proceeds through a series of stages, which can be overlapping. The process initiates with the formation of a "seed", more specifically, a state of tau that shifts the equilibrium away from monomeric tau, towards aggregated tau. Subsequently, the seed develops into a tau “oligomer”, which can be broadly defined as soluble tau multimers that interact with "oligomer-specific" antibodies raised against soluble, seeding

competent tau (Kopeikina et al. 2012; Lasagna-Reeves et al. 2012). Importantly, while the term oligomer is utilized to refer to an intermediate tau aggregate species there is a need to more rigorously define the biochemical and structural properties in a consensus manner. Nonetheless, tau oligomers and resulting fibers can serve as nucleators for additional fibers. Tau fibers can also accumulate together into larger paired helical filaments (PHF) or straight filaments (SF), that bundle into NFTs (Crowther 1991). The formation of larger aggregates of multiple tau fibers can be understood to occur by the increased avidity of long fibers to aggregate, even when individual interactions are weak. Finally, a fiber can produce secondary seeds, presumably through a process of fiber fragmentation. Each of these processes can be affected by the folding and concentration of free tau monomers.

Dynamics of tau folding

Disordered proteins – such as tau – have no highly stable well-folded structure and instead can rapidly exchange between different monomer states with relatively low energy barriers (Trivedi and Nagarajaram 2022). This suggests tau will be distributed between multiple states, which has key implications for tau fibrillization (Figure 1.3).

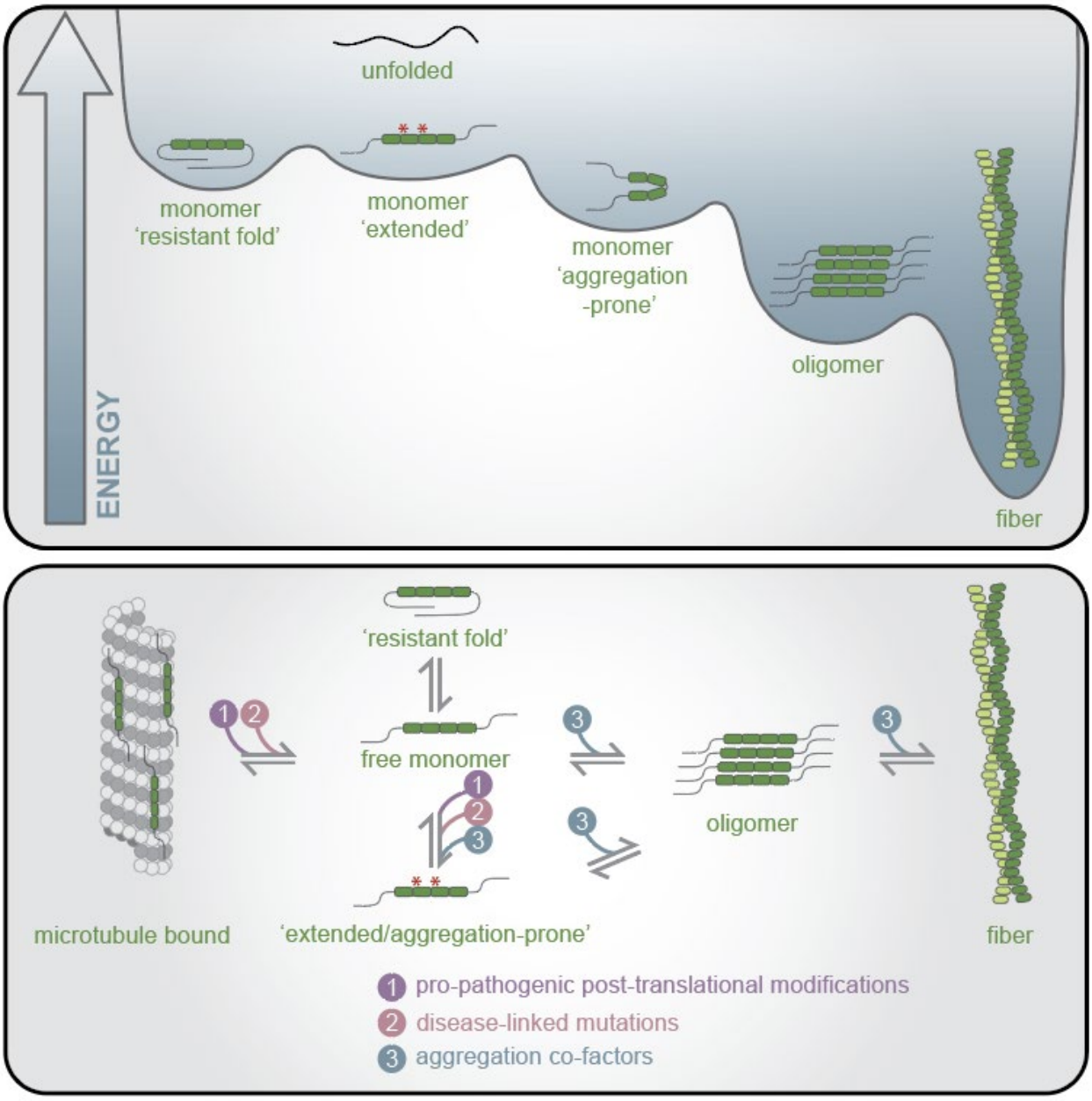

Figure 1.3. Tau folding landscape. Tau can exist in a diversity of unfolded or folded states. For example, a free tau monomer can be in a form resistant to integration into a fiber by adopting a 'paperclip-like' fold or adopt an extended conformation where the PHF6 and PHF6* sequences are exposed (denoted with asterisk) which promotes incorporation into a fibrillar structure. Critically, pathogenic fibrillar forms of tau represent particularly energetically stable states (see top panel). These states of tau exist in equilibrium and additional influences from pro-pathogenic post-translational modifications, disease-linked mutations, or cofactors which facilitate aggregation can affect the balance of tau states shifting the equilibrium toward fibrillar forms (see bottom panel).

First, some folded states are resistant to initiating fiber formation. For example, tau can adopt a ‘paperclip-like’ fold wherein the N and C termini fold over and block the aggregation prone $_{306}$VQIVYK$_{311}$ sequence (referred to as PHF6) in the MTBR, which is the minimal sequence required to nucleate fibrilization *in vitro* (Andronesi et al. 2008; Mukrasch et al. 2009; Li and Lee 2006). Additionally, the different folded states of tau monomers can influence the structure of the resulting fibril. For example, the ability to form the CTE (or AD) fiber structure *in vitro* is dependent on different salt concentrations that stabilize specific monomer folds (Lövestam et al. 2022). Finally, as tau can exist in several folds, biochemical conditions that bias the folding of tau into the same fibrilization prone state should increase the rate of tau aggregation.

The distribution of tau monomers into different folded states can be influenced by several factors acting in cis (Figure 1.3). First, modification or mutation of the tau protein monomer itself can alter fibrillization propensity. This can occur in the form of pathogenic mutations such as S320F which alters interactions within tau reducing the ‘paperclip-like’ fold leading to an extended conformation with increased exposure of the PHF6 region (Chen et al. 2023). This can also be regulated through post-translational modifications biasing folding and thereby either promoting or inhibiting fibrillization (Boyko and Surewicz 2023; Xia et al. 2020; Haj-Yahya et al. 2020).

Initiation of fiber formation:

A key step of fibril formation is the initial formation of a seed that can then incorporate additional monomers. In the simplest model, tau proteins fold into the same conformation, bind together, and initiate a β-sheet rich amyloid fiber, which can then grow by the addition of more tau monomers. The hexapeptide motifs $_{306}$VQIVYK$_{311}$ and $_{275}$VQIINK$_{280}$ (PHF6 and PHF6*, respectively) in the tau MTBR are both necessary and sufficient to form tau fibers *in vitro*. (Li and Lee 2006). Thus, a fold in which these regions are exposed in multiple tau proteins would promote

formation of a β-sheet rich tau fiber in this manner (Li and Lee 2006). In fact, the exposure of these sequences can be the first observed physical change in tau that leads to tau fiber formation (Pavlova et al. 2016).

A variant model for the formation of seeds is that an individual tau monomer undergoes a chemical transition to a relatively stable conformation that is sufficient to serve as a seed for tau fibrillization. This is based on identification of a stable fraction of monomeric tau from AD brains that can serve as a seed (Mirbaha et al. 2018). A potential explanation for this observation is that this seeding-competent monomer is produced by a non-enzymatic chemical change to tau such as isomerization of proline, serine, or aspartate amino acids without breaking the backbone chain thus altering aggregation propensity. For example, L- to D- isomerization of serine and aspartate residues in the MTBR of tau altered structural properties and/or fibril formation while cis- trans proline isomerization was shown to promote spontaneous tau aggregation potentially via destabilizing shielding of the PHF6 motif (Chen et al. 2019; Tochio et al. 2019).

Studies using time resolved cryo-EM demonstrated that *in vitro* tau fibers can initiate with a shared filamentous intermediate that than adopts different related structures over time, with the final predominant fiber type in a population being the most thermodynamically stable under the reaction conditions (Lövestam et al. 2024). We note these *in vitro* fibrillization reactions are done at high tau concentrations with no competing protein interactions. This creates conditions where even weak interactions between tau monomers and fibers can contribute to additional fiber formation. In contrast, in cells the tau concentration is lower and there is competition with the large excess of other components that can disrupt weak homotypic interactions (Protter et al. 2018). Thus, whether this process can occur in cells remains to be established.

<u>Cofactors can mediate tau fiber formation</u>

Cofactors are often used to increase the rate of tau fiber initiation and fibrilization *in vitro* and are expected to alter tau fibrilization in neurons as well (Figure 1.3). Cofactors used *in vitro* are typically polyanions such as heparin, RNA, and some fatty acids (Lövestam et al. 2022; Montgomery et al. 2023; Dinkel et al. 2015; Fichou et al. 2018). Generally, polyanions are thought to increase tau fiber formation through neutralization of positive charges in the MTBR (Sibille et al. 2006; Fichou et al. 2019).

In principle, cofactors could act in three manners to increase the rates of initiation and fibrilization of tau fibers (Figure 1.4).

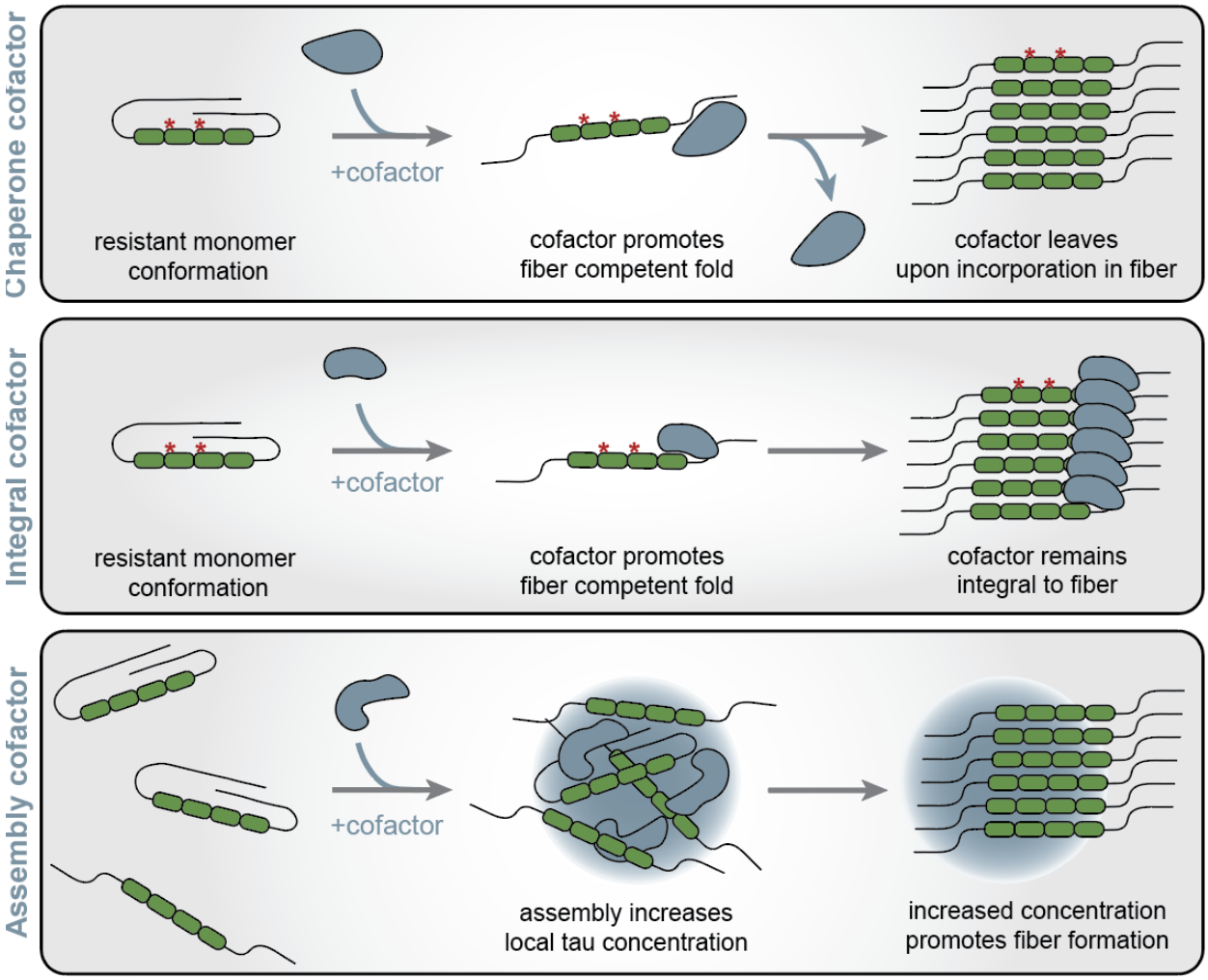

Figure 1.4. Models of tau aggregation cofactor mechanisms. Cofactors may facilitate tau aggregation through various mechanisms. First, a cofactor may serve to promote a fiber competent fold of a tau monomer and leave once tau undergoes incorporation into a fiber. Second a cofactor may promote a fiber competent fold and become integral to the fiber structure. Third, a cofactor promotes tau fibrillization by increasing local concentrations of tau through the formation of assemblies through processes such as liquid-liquid phase separation.

First, cofactors could act essentially as chaperones and stabilize tau folds prone to forming fibers. For example, the ClearTau fibrilization system has shown that immobilized heparin produces tau fibers without heparin being incorporated into the fiber (Limorenko et al. 2023). Similarly, even though heparin can induce the formation of a seeding competent tau monomer, no stable biochemical interaction is observed between tau and heparin in some experiments (Mirbaha et

al. 2018). Second, cofactors may be integral to the final fiber as a structural component as fibers prepared with heparin, or RNA, have been reported to depolymerize when treated with heparinase or RNAase, respectively (Fichou et al. 2018). Moreover, seeding-competent tau forms from AD patient brain are reduced by treatment with RNase suggesting RNA may be relevant to the transmission of seeds in patients (Zwierzchowski-Zarate et al. 2022). Third, cofactors could act to create high local concentrations of tau monomers. For example, tau and cofactors can undergo liquid-liquid phase separation (LLPS) creating high local concentrations of tau and increasing fibrilization rates (Zhang et al. 2017; Kanaan et al. 2020). The LLPS of tau and cofactors is likely formed and maintained through several weak interactions between individual tau proteins and tau with cofactors, allowing for more protein refolding events. The chaperone and concentration effects of cofactors can be coupled such that the interaction of tau with polyanions both concentrates and stabilizes a fold that promotes fibrillization, thus enhancing the rate of initial seed formation.

It is unclear which specific cofactors in a cell can influence tau fibrilization. The structure of CBD, PSP, GGT, and CTE fibrils contain relatively small non-proteinaceous unidentified densities indicating the presence of potential lipid or negatively charged co-factors that are integral to the fiber (Zhang et al. 2020a; Falcon et al. 2019). Other commonly utilized *in vitro* cofactors, such as RNA and heparin, may similarly influence tau fiber formation in a cellular context. In support of this, NFTs stain with RNA dyes, and tau aggregates purified from mice and cell models contain RNA with an enrichment of snRNAs and snoRNAs (Lester et al. 2021; Ginsberg et al. 1997). Additionally, endogenous heparan sulfate proteoglycans (HSPG) have also been identified in tau tangles in AD (Su et al. 1992; Spillantini et al. 1999). There are also numerous other polyanions in cells that can stimulate tau fibrilization *in vitro*, but whether these can affect tau fibrilization in cells is unknown (Montgomery et al. 2023).

Tau Liquid Liquid Phase Separation

Liquid liquid phase separation (LLPS) is a phenomenon in which upon reaching a critical concentration, proteins and other large molecules will condense into a liquid like droplet separate from the bulk liquid phase. Several non-membranous organelles in cells have been proposed to form through LLPS, such as stress granules, nuclear speckles, cajal bodies, and P-bodies (Hyman et al. 2014), but do not necessarily retain liquid-like properties upon formation. These phase separated condensates may contribute to disease (Alberti and Dormann 2019). For example, Tar-DNA Binding Protein 43kDa (TDP-43) mislocalizes from the nucleus and interacts with cytoplasmic stress granules leading to its aggregation and loss of function (Bentmann et al. 2012). TDP-43 can also aggregate within myo-granules in muscle, contributing to muscular dystrophy (Vogler et al. 2018). Recently, other amyloidogenic proteins, such as tau and amyloid-β have been observed to undergo phase separation, however whether this contributes to development of pathology is unclear (Zhang et al. 2025).

Tau has been shown to undergo liquid liquid phase separation *in vitro* and in cells (Fichou et al. 2019; Lin et al. 2019; Zhang et al. 2017, 2020b). This has been described as both on pathway towards pathogenic tau aggregates (Fichou et al. 2019), and off pathway in complex-coacervates (Lin et al. 2019). Additionally, incubation of tau with RNA or heparin results in tau fibrilization or phase separation, dependent on relative concentrations and buffer conditions (Lin et al. 2019). Interestingly, tau fused to a Cry2 oligomerization domain and exposed to blue light in cells phase separates, and the liquid like nature of the assembly is mediated by phosphorylation of the proline rich region which may contribute to microtubule assembly and stability (Zhang et al. 2020b). However, phase separation of wild type tau in cells has not been observed (Zhang et al. 2020b).

INTRACELLULAR INFLUENCES ON TAU AGGREGATION

Post-translational modification and processing

Within a cell, tau is subject to extensive post-translational modifications (PTMs). Tau PTMs are of significant interest as certain modifications are enriched in tau aggregates and accumulate with the progression of pathology in tauopathies such as AD (Wesseling et al. 2020) (Figure 1.5).

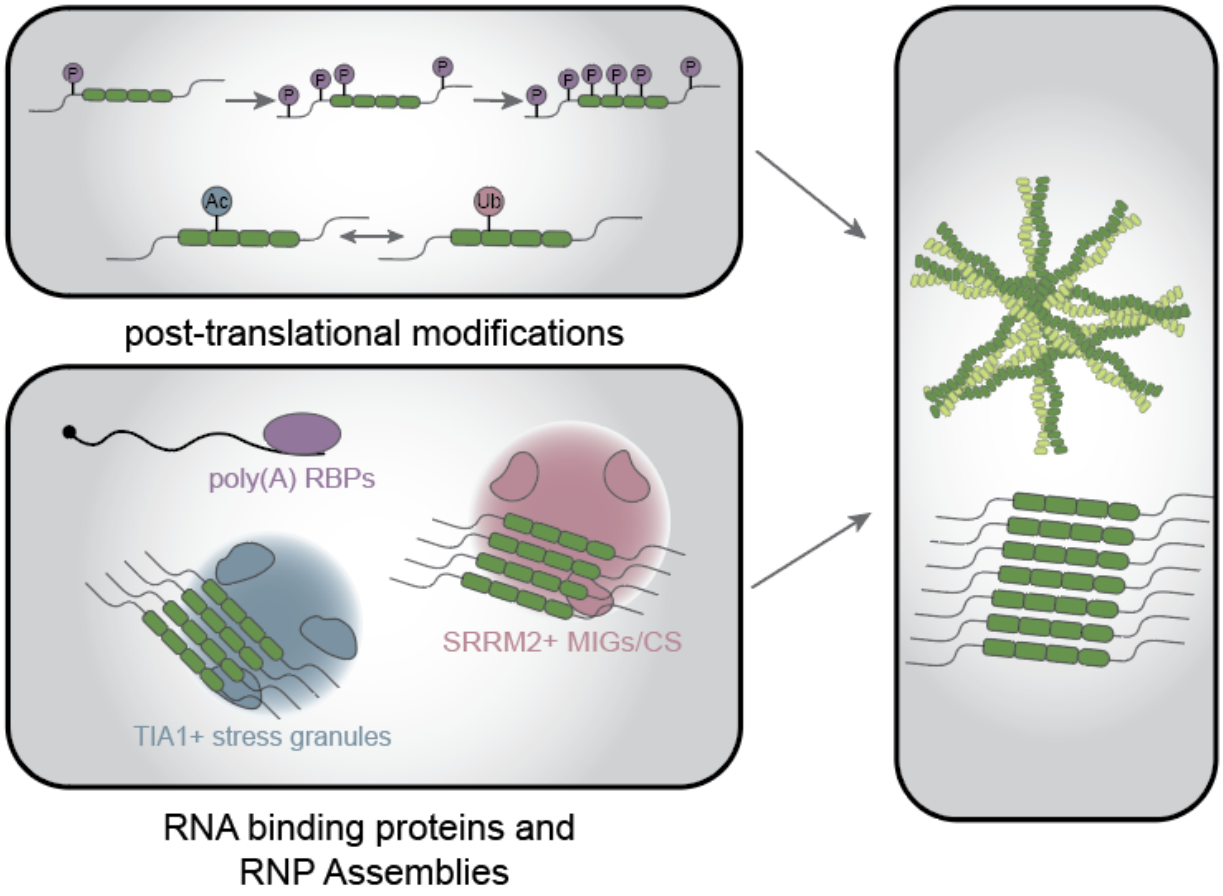

Figure 1.5. Intracellular influences on tau aggregation. In cells, tau can be highly post-translationally modified, and/or interact with several RNA binding proteins or RNP assemblies. Tau aggregates are hyperphosphorylated, however it is unclear whether this phosphorylation drives aggregation in disease. *In vitro*, the effect of phosphorylation on tau fibrilization is site and context specific. In addition to phosphorylation, tau can be acetylated, changing binding affinity with microtubules and competing with sites of ubiquitination. Tau is also highly poly-ubiquitinated in aggregates, likely as a signal for protein degradation as tau aggregates. Finally, tau can interact with several RNA binding proteins and RNP-assemblies with different effects on tau aggregation in cells.

For modifications associated with pathogenic tau, it is important to consider whether they accrue during disease and are thus a feature but do not directly affect the pathogenic cascade, or whether they alter the biochemical properties of tau in a manner which actively modulates tau aggregation. In this section, we will discuss a few notable examples of tau PTMs, a topic that has previously been extensively reviewed (Alquezar et al. 2021).

Phosphorylation

The phosphorylation of tau is the most extensively studied post-translational modification spurred on by the finding that fibrillar forms of tau present in AD are ‘hyperphosphorylated’ (Grundke-Iqbal et al. 1986). Furthermore, phosphorylation of tau at certain epitopes is often utilized as a marker of pathology (Götz et al. 2010). Several kinases and phosphatases which act on tau have been identified and investigated for contributions to pathology and therapeutic potential as reviewed previously in more detail (Martin et al. 2013a, 2013b). A key example which is supportive of phosphorylation playing a role in pathology, includes the knockdown or activation of cyclin dependent kinase 5 (CDK5) – a major tau kinase – which reduced or increased aggregation of tau in mouse models, respectively (Piedrahita et al. 2010; Castro-Alvarez et al. 2014; Noble et al. 2003). Similarly, inhibition of a related tau kinase glycogen synthase kinase 3 (GSK-3) reduces tangle formation in transgenic mice (Hurtado et al. 2012). However, such kinases often phosphorylate tau at multiple sites and have many other cellular targets warranting more direct biochemical investigation of the effects of tau phosphorylation specifically.

Despite the observation that tau aggregates are hyperphosphorylated, the effect of tau phosphorylation on fibrilization and aggregation is more nuanced. For example, while phosphorylation in the MTBR leads to a reduction in microtubule affinity, it also inhibits aggregation kinetics in *in vitro* assays and reduces seeding in cells (Haj-Yahya et al. 2020; Powell

et al. 2024; Kellogg et al. 2018). While such a phosphorylation modification may not directly increase fibrillization rates, phosphorylation could modulate the concentration of cellular tau unbound to microtubules available for aggregation. In contrast, phosphorylation of residues in the PRR have been directly linked to increased aggregation *in vitro* and in cells (Xia et al. 2020; Despres et al. 2017). Ultimately, the effects of tau phosphorylation are site specific and the mechanisms through which it can influence aggregation may be dependent upon the modified region of tau.

Interestingly, increases in specific phosphorylated residues of tau have been developed as biomarkers measurable in CSF or plasma from AD patients, but are not observed in primary tauopathies emphasizing they may more likely reflect Aβ pathology (Therriault et al. 2023; Zetterberg 2022). Further, while increased phosphorylation of tau is observed in insoluble forms in AD, these modifications can also occur in healthy brains (Wegmann et al. 2021). Thus, while phosphorylation of tau is a feature of pathology, this does not indicate phosphorylated tau is strictly toxic, and attention must be paid to the precise modifications and the mechanistic manners in which they may influence aggregation.

Acetylation

Abnormal acetylation of tau at specific residues has been reported in AD and related tauopathies associated with aggregation (Cohen et al. 2011; Tracy et al. 2016; Min et al. 2010; Irwin et al. 2012; Wesseling et al. 2020). *In vitro* assays indicate tau acetylation can promote fibrillization (Cohen et al. 2011). Additionally, animal models with acetyl-mimetic mutants of tau show acetylation can inhibit protein turnover, increasing tau levels, (Min et al. 2010) and play a role in impaired synaptic plasticity (Tracy et al. 2016). The deacetylase silent information regulation 2 homolog 1 (SIRT1) is linked to tau pathology progression in animal models with

conditions of reduced acetylation having less tau aggregation (Min et al. 2018, 2010). Alternatively, acetylation at KXGS motifs in the MTBR of tau is inversely related to phosphorylation and reduces propensity for aggregation – highlighting both the interplay of multiple PTMs as well as the differing effects of acetylation of specific residues (Cook et al. 2014; Carlomagno et al. 2017). Acetylation also competes with ubiquitination modification of lysine residues and thus can be a key determinant of tau stability.

Ubiquitination

Ubiquitination is a critical cellular mechanism for regulating protein turnover through degradative pathways such as the ubiquitin-proteasome machinery or autophagy. In the AD brain, tau polyubiquitination is increased consistent with impairments in protein homeostasis (Abreha et al. 2018). Immunostaining of AD brain shows that NFTs of tau are ubiquitin positive, but this modification follows amino-terminal processing suggesting it is consequence of tau aggregation rather than causal (Mori et al. 1987; Iwatsubo et al. 1992; Morishima-Kawashima et al. 1993). Ubiquitination can also alter tau biochemical properties as this modification can inhibit tau fibrilization and phase separation *in vitro*. (Trivellato et al. 2023).

Other post-translational modifications

Tau is also subject to many additional post-translational modifications such as methylation, SUMOylation, glycosylation and others, though effects on disease processes are not as widely studied (Alquezar et al. 2021). Collectively, with regards to PTMs and effects on tau aggregation and pathology, they must be validated in a residue-specific manner in model systems. Further,

the complex integration of the vast number of potential PTMs of tau occurring in a cell will inform whether a given tau protein is favored to initiate or incorporate into a tau aggregate.

RNA and RNA binding proteins

Tau expression is regulated at the post-transcriptional level by RNAs and RNA binding proteins (RBPs). For example, exon 10 inclusion in *MAPT* is regulated by the serine and arginine rich splicing factor 2 (SRSF2), and loss of function of SRSF2 results in increased expression of 4R tau (Chen et al. 2014; Qian et al. 2011). miRNAs also regulate tau expression and posttranslational modifications, although whether these are through direct effects on tau, or through alteration of cellular pathways that regulate tau is unknown (Boscher et al. 2020).

Tau protein has also been observed to interact with RNAs and RBPs. RNA can be a cofactor for tau fibrillization *in vitro,* and tau aggregates in cell and mouse models contain RNA, most notably snRNAs and snoRNAs (Lester et al. 2021; Kampers et al. 1996). Characterization of tau and RNA interactions in cells has also showed particular association with tRNAs (Zhang et al. 2017). Moreover, multiple studies have reported the enrichment of RBPs in NFTs from tauopathy patient tissue and localization of RBPs in tau aggregates in model systems (Kavanagh et al. 2022). For example, U1 small nuclear ribonucleoprotein (snRNP) components were identified in tau inclusions in AD (Bai et al. 2013).

In some cases, RBPs have been proposed to affect development of tau pathology and/or toxicity. Suppressors of tau toxicity in *C. elegans* models identified several poly(A) RBPs and deadenylases including suppressor of tauopathy 2 (sut-2), polyadenylate-binding protein 2 (pabp-2) and poly(A)-specific ribonuclease (parn-2) that modulate pathological tau (Guthrie et al. 2009; Kow et al. 2021; Wheeler et al. 2019). Deletion of the mammalian homolog of sut-2 (MSUT2) in the mouse brain rescues tau aggregation and neuronal loss while overexpression exacerbates

pathology (Wheeler et al. 2019). PABP-2/PABPN1 and MSUT2 are co-depleted in AD brain sections which stratifies with earlier onset supporting a role for these RBPs in human disease (Wheeler et al. 2019). Relatedly, the loss of poly(A) deadenylase parn-2/TOE1 leads to increased tau pathology in *C. elegans* and correlates with MSUT2 expression and increased tau pathology in AD patient brain (Kow et al. 2021). These results suggest the regulation of RNAs by poly(A)-related factors is important for tau pathology, though further investigation is necessary to establish the precise molecular mechanisms.

The spliceosome component serine/arginine repetitive matrix 2 (SRRM2) colocalizes with tau inclusions in tauopathy disease tissues (McMillan et al. 2021; Lester et al. 2021). Interestingly, SRRM2 and associated nuclear speckle protein pinin (PNN) not only mislocalize to cytoplasmic tau inclusions, but also define cytoplasmic assemblies rich in polyserine motifs that are sites of tau aggregation in cellular models, discussed below (Lester et al. 2023). In support of a role in pathobiology, increased levels of polyserine exacerbates tau pathology in both cell lines and mouse models (Lester et al. 2023; Van Alstyne et al. 2024).

The stress granule RBP T-cell intracellular antigen 1 (TIA1) has also been shown to colocalize with pathogenic tau in disease (Vanderweyde et al. 2012). Stress granules are cytoplasmic assemblies of untranslating messenger ribonucleoproteins (mRNPs) that form when translation initiation is reduced (Protter and Parker 2016). TIA1-containing stress granules are proposed to facilitate tau aggregation and the reduction of TIA1 levels reduces tau pathology in a mouse model (Apicco et al. 2018). Two possible mechanisms for this effect have been proposed. First, TIA1 is proposed to directly interact with tau and increase the formation of oligomeric, and toxic, tau (Ash et al. 2021; Apicco et al. 2018; Jiang et al. 2019). Additionally, TIA1 in microglia is proposed to regulate the inflammatory response in a manner that reduces tau toxicity (Webber et al. 2024).

Stress granule RBPs have also been linked to tau aggregation through additional mechanisms. Ras GTPase-activating protein-binding protein 2 (G3BP2) - an integral component of stress granules – was shown to chaperone tau via an RNA-independent mechanism by binding to soluble forms and preventing oligomerization (Wang et al. 2023). Conversely, heterogenous nuclear ribonucleoproteinA2/B1 (hnRNPA2B1) has been proposed to promote tau pathology through mediating association with methyl-6-Adenosine (m6A) RNA species (Jiang et al. 2021). However, there are conflicting reports on whether hnRNPA2B1 colocalizes with tau aggregates in postmortem tissues (Kavanagh et al. 2024; Jiang et al. 2021). Nevertheless, a possible role for m6A RNA modifications is supported by genes promoting m6A modification being required for increased T22-antibody positive oligomeric tau in a CRISPRi based screen of iPSC-derived neurons (Samelson et al. 2023).

RIBONUCLEAR PROTEIN ASSEMBLY FORMATION AND TAU AGGREGATION

As discussed above, ribonuclear protein (RNP) assemblies, can interact with tau to influence aggregation in cells. Several RNP assemblies, such as stress granules (SGs), mitotic interchromatin granules (MIGs), and cytoplasmic speckles (CSs), have been reported to impact tau aggregation (Lester et al. 2023; Vanderweyde et al. 2012) (Figure 1.5). The exact molecular mechanisms and consequences of the interaction between tau and different RNP assemblies are not well understood.

Stress Granules

Formation

SGs are RNP assemblies which form after translation inhibition and phosphorylation of elongation initiation factor 2α (eIF2α) (Aulas et al. 2017; Protter and Parker 2016). The integrated stress response, in which different cellular stressors such as amino acid starvation, cytoplasmic

double-stranded RNA, unfolded protein, and/or heme deficiency, activates the eIF2α kinases GCN2, PKR, PERK, or HRI respectively (Pakos-Zebrucka et al. 2016). Additionally, translation inhibition through treatment with elongation inhibitors such as Patemine A (PatA) or hippuristanol also induces SG formation (Low et al. 2005; Mazroui et al. 2006).

The assembly of SGs is widely studied, and recent work from the Parker Lab has provided mechanistic insight into the interactions that drive and maintain SG assembly. SGs are formed through several weak RNA-RNA, RNA-protein, and protein-protein interactions (Ripin and Parker 2023). The Ras GTPase-activating protein-binding protein 1 (G3BP1) is a key scaffold protein for stress granule formation, as knockout of G3BP1 and G3BP2 across several cell lines ablates SG formation (Kedersha et al. 2016). G3BP1 scaffolds SGs through binding to RNA and increasing the local concentration of RNAs, facilitating RNA-RNA interactions (Parker et al. 2025). Interestingly, these RNA-RNA interactions persist with the removal of G3BP1 *in vitro* and *in cellulo* (Parker et al. 2025). Additional protein-protein interactions, such as weak interactions between intrinsically disordered regions in trans may also contribute to stress granule stability (Protter and Parker 2016).

Influences on Tau Aggregation

While tau aggregation does not occur within SGs (Lester et al. 2023), the formation of SGs has been linked to increased tau pathology (Vanderweyde et al. 2012). SG components, including TIA1 and various hnRNPs colocalize with tau aggregates *in vivo* and *in vitro*, and altering expression of these proteins also changes tau aggregation (Vanderweyde et al. 2012, 2016; Jiang et al. 2021). However, soluble and aggregated tau is excluded from G3BP1 positive SGs, yet is enriched with TIA1 positive assemblies (Piatnitskaia et al. 2019; Lester et al. 2023). One possibility is that tau aggregation alters stress granule formation. For example, the internalization of phosphomimetic tau sensitizes HEK293T cells to stress and increases TIA positive SG

formation and clearance time (Brunello et al. 2016). The impact on clearance time may be driven by changes in protein or RNA components of these stress granules. A parsimonious model is that the triggering of the integrated stress response results in an increase in hyperphosphorylated tau leading to aggregation with stress granule components prior to stress granule formation, impacting the proteome of tau aggregates and SGs (Wolozin and Ivanov 2019).

Mitotic Interchromatin Granules

Formation

MIGs were first observed in 1989, and little is known about how these assemblies form and disassemble, or their composition (Leser et al. 1989). Most research into MIG formation has been in the context of nuclear speckle assembly dynamics through the cell cycle. Several snRNPs, including U1, U2, and U4/6 become diffuse as a cell enters mitosis, however, with progression through anaphase and telophase, these snRNPs assemble into distinct granules (Ferreira et al. 1994). Upon completion of mitosis, cytoplasmic MIGs differentially release nuclear speckle components into daughter nuclei (Prasanth et al. 2003). We have observed that SRRM2 and PNN form cytoplasmic assemblies during mitosis, which we believe are MIGs (Lester et al. 2023).

Influences on Tau Aggregation

Mitotic interchromatin granules likely are not contributing to tau aggregation in neurons, as these cells are post mitotic, yet SRRM2 is observed in tau aggregates in disease (Lester et al. 2021; McMillan et al. 2021). Regardless, recent work in the Parker lab has shown that SRRM2 or PNN positive MIGs are preferred sites of tau aggregation in cycling cells (Lester et al. 2023). Neuronal cell cycle re-entry has been observed in disease and animal models (Koseoglu et al. 2019) which may contribute to neurodegeneration. In the R1.40 AD mouse model, which express

human APP with the K670 and M671Δ pathogenic mutations, neurons may re-enter the cell cycle in response to soluble oligomeric amyloid-β (Varvel et al. 2008). However, *in vitro* experiments in primary cortical neurons show that amyloid-β mediated cell cycle reentry requires tau expression (Seward et al. 2013). Whether neuronal cell-cycle reentry proceeds through mitosis, allowing for MIG formation, is unknown.

Cytoplasmic Speckles

Formation

Little is known about the assembly and composition of CSs. We have observed endogenously tagged PNN-Halo or SRRM2-Halo form cytoplasmic assemblies in the absence of stress in HEK293T cells (Lester et al. 2023). SRRM2 positive CSs have been also observed in iPSC neurons after treatment with prostaglandins or sorbitol stress (Lester et al. 2023). Increased cytoplasmic SRRM2, and possibly cytoplasmic speckle formation, has also been observed in AD mouse models and in genetic screens (Berchtold et al. 2018; Tanaka et al. 2018). For example, gene knockdown screens identified NUP153 as a regulator of SRRM2 localization, with 20% of cells exhibiting nuclear depletion and cytoplasmic assembly of SRRM2 (Berchtold et al. 2018). Others observe that loss of BANF1, ANKLE2, or PPP2CA through CRISPRi knockdown results in increased tau aggregation and cytoplasmic SRRM2 positive assemblies (Prissette et al. 2022). Additionally, SRRM2 mislocalization to the cytoplasm is observed pre-symptomatically and before amyloid plaque formation in 5xFAD mice and is mediated through ERK activity and SRRM2 phosphorylation (Tanaka et al. 2018). Thus, SRRM2 mislocalization, and possibly cytoplasmic assembly, contribute to tau aggregation and may occur in disease.

Influences on Tau Aggregation

The mislocalization of SRRM2 has been linked to increased tau pathology *in vitro* (Prissette et al. 2022; Lester et al. 2023) however the formation of cytoplasmic speckles specifically has not shown increased tau aggregation. Knockdown of PNN, a cytoplasmic speckle resident protein, results in decreased tau aggregation in HEK293T cells, however knockdown of SRRM2 has no effect. (Lester et al. 2023). In AD, neurons may encounter inflammatory cytokines secreted from disease associated microglia, which, similar to prostaglandin treatment, may result in cytoplasmic localization of SRRM2 into CSs (Odfalk et al. 2022). Further work is required to understand if SRRM2 and/or PNN mislocalization is sufficient to drive tau aggregation, or if cytoplasmic assembly of these proteins is necessary.

CHAPTER II

Polyserine-Tau Interaction Modulates Tau Fibrilization

Contribution Statement: This chapter is adapted from **Polyserine-Tau interaction modulates tau fibrilization**, authored by James Pratt, Kathleen McCann, Jeff Kuo, and Roy Parker, in submission at *Cell Reports*. JK designed and cloned polyserine variants, KM performed negative stain electron-microscopy and thioflavin-t kinetics, JP and KM performed polyserine self-assembly assays, and JP performed all other experiments. All authors edited the manuscript.

SUMMARY

Tau aggregates are the defining feature of multiple neurodegenerative diseases and contribute to the pathology of disease. However, the molecules affecting tau aggregation in cells are unclear. We previously determined that polyserine-rich domains enrich in tau aggregates, assemble into cytoplasmic puncta that can serve as sites of tau aggregation, and exacerbate tau aggregation in cells and mice. Herein, we show that polyserine domains are sufficient to define subcellular assemblies as sites of tau aggregation through localization of tau seeds. Purified polyserine spontaneously self-assembles and directly interacts with monomeric and fibrillar tau. Moreover, polyserine-tau assemblies recruit RNA, leading to faster rates of tau fibrillization *in vitro*. Using polyserine variants, we found that enrichment in tau aggregates and stimulation of tau aggregation are separable functions of polyserine, and assembly stimulates tau aggregation. Together, our results show that polyserine self-assembles and directly interacts with tau to form preferred sites of tau aggregation.

INTRODUCTION

The aggregation of tau is a hallmark of several neurodegenerative diseases, including Alzheimer's Disease (AD) (Brion et al. 1985a). Supporting a causal role for tau in disease, symptom severity in AD correlates with increased tau pathology (Hanseeuw et al. 2019). Importantly, both genetic and environmental inputs can promote tau aggregation. For example, genetic mutations in *MAPT* can result in coding variants with an increased propensity for aggregation, as in frontotemporal dementia (FTD) (Goedert and Spillantini 2000). In contrast, secondary triggering events such as repetitive head trauma or amyloid-β plaques, can increase tau aggregation in chronic traumatic encephalopathy (CTE) (McKee et al. 2015), or Alzheimer's Disease (AD) (Chung et al. 2021), respectively. While tau plays an important role in disease contexts, the intracellular mechanisms of tau aggregation, and the impact of additional proteins or other cofactors on tau aggregation, are generally unknown.

We and others have observed that tau aggregates contain other molecules, including RNA and specific RNA binding proteins (Lester et al. 2021, 2023; Ash et al. 2021; McMillan et al. 2021; Wheeler et al. 2019), which may affect tau aggregation in cells. Previously, we observed that tau aggregates enrich small structured RNAs, such as snRNAs and snoRNAs (Lester et al. 2021). Additionally, the splicing speckle proteins Serine-Argine Repetitive Matrix 2 (SRRM2) and Pinin (PNN) mislocalize to cytoplasmic tau aggregates in cell culture models, PS19 tau transgenic mice, and in human disease (Lester et al. 2021; McMillan et al. 2021), and are present in nuclear speckles that colocalize with nuclear tau aggregates in cell line and mouse models (Lester et al. 2021). SRRM2 and PNN can mislocalize into cytoplasmic tau aggregates through formation of cytoplasmic speckles (CSs), or mitotic interchromatin granules (MIGs) which act as preferred sites of tau aggregation (Lester et al. 2023).

The ability of SRRM2 and PNN to interact with, and enhance the formation of tau aggregates is based on their unique polyserine domains (Lester et al. 2023). SRRM2 contains

two C-terminal polyserine domains of 25 or 42 residues, while PNN contains a C-terminal serine rich domain with 50 of 66 residues being serine (Lester et al. 2023). These polyserine domains are both necessary and sufficient to target exogenous proteins to tau aggregates (Lester et al. 2023). In addition, three observations demonstrate these domains can affect the efficiency of tau aggregation. First, knockdown of PNN results in decreased tau aggregation in cells (Lester et al. 2023). Second, overexpression of the SRRM2 or PNN C-terminal domains, or the 42 amino acid long polyserine domain (polyserine$_{42}$), is sufficient to increase tau aggregation in HEK293T tau biosensor cells (Lester et al. 2023). Finally, polyserine$_{42}$ expression in PS19 mice exacerbates tau pathology based on increased phosphorylated tau and increased seeding capacity of brain homogenate (Van Alstyne et al. 2024). It remains unclear how polyserine domains concentrate in assemblies, if there is a direct interaction between tau and polyserine, or if polyserine is sufficient to convert other subcellular assemblies into preferred sites of tau aggregation.

To examine the physical interaction between polyserine and tau, and how those interactions affect the process of tau aggregation, we performed a series of *in cellulo* and *in vitro* experiments. We demonstrate that stress granules, a cytoplasmic assembly of RNA and proteins (Protter and Parker 2016), can be converted to a preferred site of tau aggregation through expression of a G3BP1-polyserine$_{42}$ fusion protein. We next used *in vitro* microscopy and kinetic experiments to characterize the tau-polyserine domain interaction. First, we demonstrate purified polyserine$_{42}$ forms self-assemblies. Second, we demonstrate polyserine$_{42}$ assemblies directly interact with tau monomers and seeds and can increase the rate of tau fiber formation and growth. The surface of the resulting tau fibers is decorated with polyserine assemblies. Finally, we show that the assembly of polyserine$_{42}$ is separable from enrichment in tau aggregates, and assembly correlates with effects on tau aggregation. Taken together, these observations demonstrate polyserine forms self-assemblies that can directly interact with tau to promote aggregation.

RESULTS

Polyserine$_{42}$ Converts Stress Granules into Sites of Tau Aggregation

We and others have previously observed that G3BP1 positive stress granules are not sites of tau aggregation (Lester et al. 2023; Wolozin 2012). In contrast, assemblies of overexpressed polyserine$_{42}$ and CS, which contain polyserine rich proteins, serve as preferred sites of aggregation in tau biosensor cells (Lester et al. 2023). The difference in tau aggregation between stress granules and polyserine containing assemblies could be because polyserine domains are necessary and sufficient to define a preferred site of tau aggregation, or because stress granules contain inhibitors of tau aggregation. This latter possibility is suggested by the observations that the stress granule component G3BP2 can limit tau aggregation *in vitro* and in neurons (Wang et al. 2023). To distinguish these possibilities, we examined if polyserine$_{42}$ could convert stress granules into sites of tau aggregation.

To do so, we constructed tau biosensor cell lines stably expressing either mRuby, mRuby-G3BP1[10], or mRuby-G3BP1-polyserine$_{42}$ (Figure 2.1A).

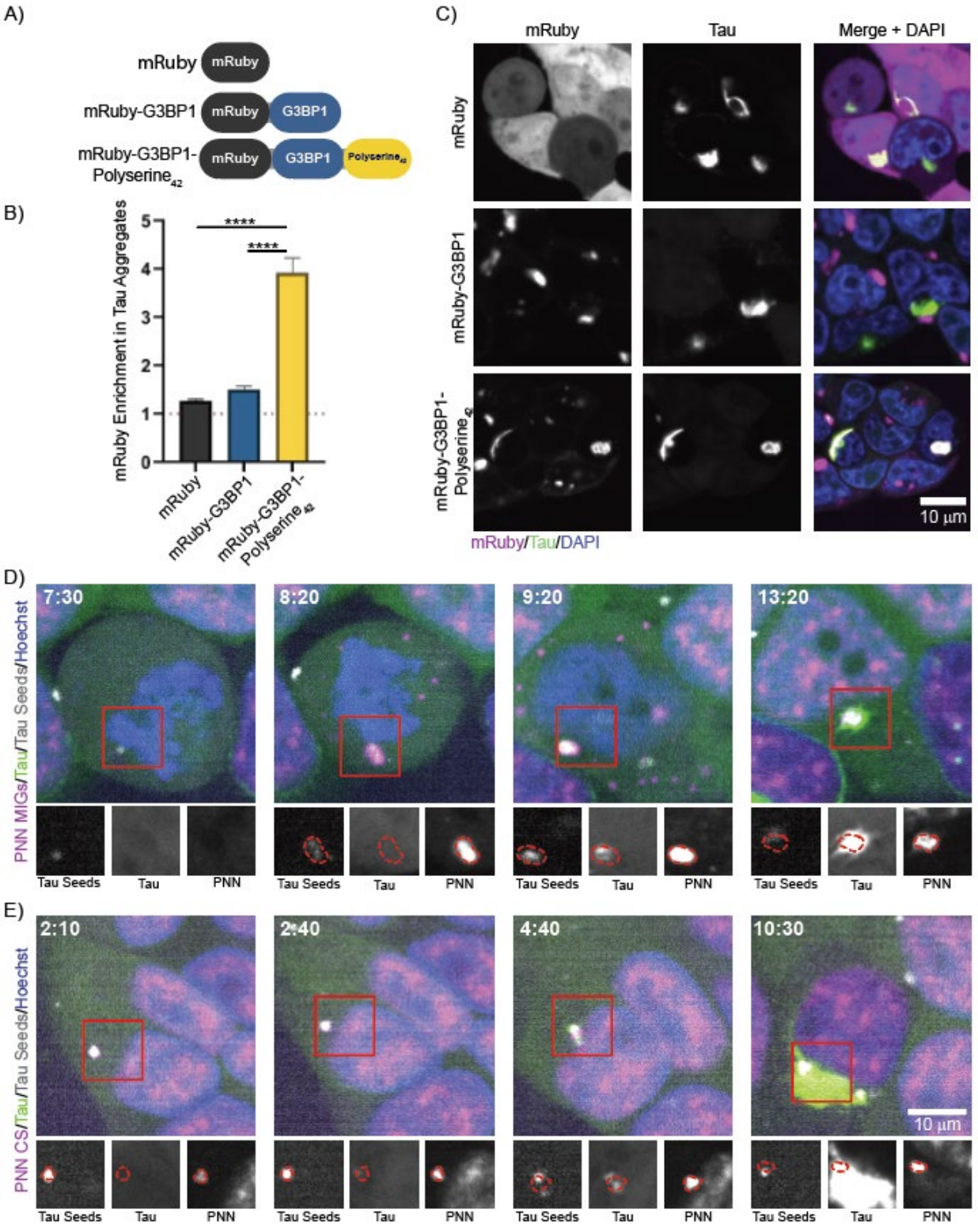
A)
mRuby
mRuby-G3BP1
mRuby-G3BP1-Polyserine42
B)
mRuby Enrichment in Tau Aggregates
****
****
mRuby
mRuby-G3BP1
mRuby-G3BP1-Polyserine42
C)
mRuby
Tau
Merge + DAPI
mRuby-G3BP1
mRuby-G3BP1-Polyserine42
10 µm
mRuby/Tau/DAPI
D)
PNN MIGs/Tau/Tau Seeds/Hoechst
7:30
8:20
9:20
13:20
Tau Seeds
Tau
PNN
E)
PNN CS/Tau/Tau Seeds/Hoechst
2:10
2:40
4:40
10:30
10 µm
Tau Seeds
Tau
PNN

Figure 2.1: Polyserine$_{42}$ Containing Assemblies Are Sites of Tau Aggregation Through Enrichment of Tau Seeds (A) Schematic of mRuby fusion proteins stably expressed in HEK293T tau biosensor cells. (B) Microscopy of HEK293T tau biosensor cells stably expressing mRuby, mRuby-G3BP1, or mRuby-G3BP1-Polyserine$_{42}$ (magenta) were transfected with brain homogenate from aged Tg2541 mice to seed tau aggregates (green) and fixed twenty-four hours after transfection, nuclei stained with DAPI (blue). (C) Quantification of mRuby enrichment in cytoplasmic tau aggregates. N = at least 164 cells from 3 biological replicates. Statistics performed with Kruskal-Wallis test with Dunn's multiple comparisons test. (****) $P < 0.0001$ (D) Stills from live cell imaging of HEK293T tau biosensor cells with endogenously tagged PNN-Halo (magenta) MIGs, transfected with fluorescent tau seeds (grey), to induce endogenous tau aggregation (green), nuclei stained with DAPI (blue). Time in hours:minutes post transfection and start of imaging. Channel breakouts from each time point in greyscale below with PNN assemblies outlined in red and superimposed to each channel. (E) Live cell imaging as performed in (D) of PNN positive CS.

The proper expression of these G3BP1 fusion proteins was verified by western blot (Figure 2.2A).

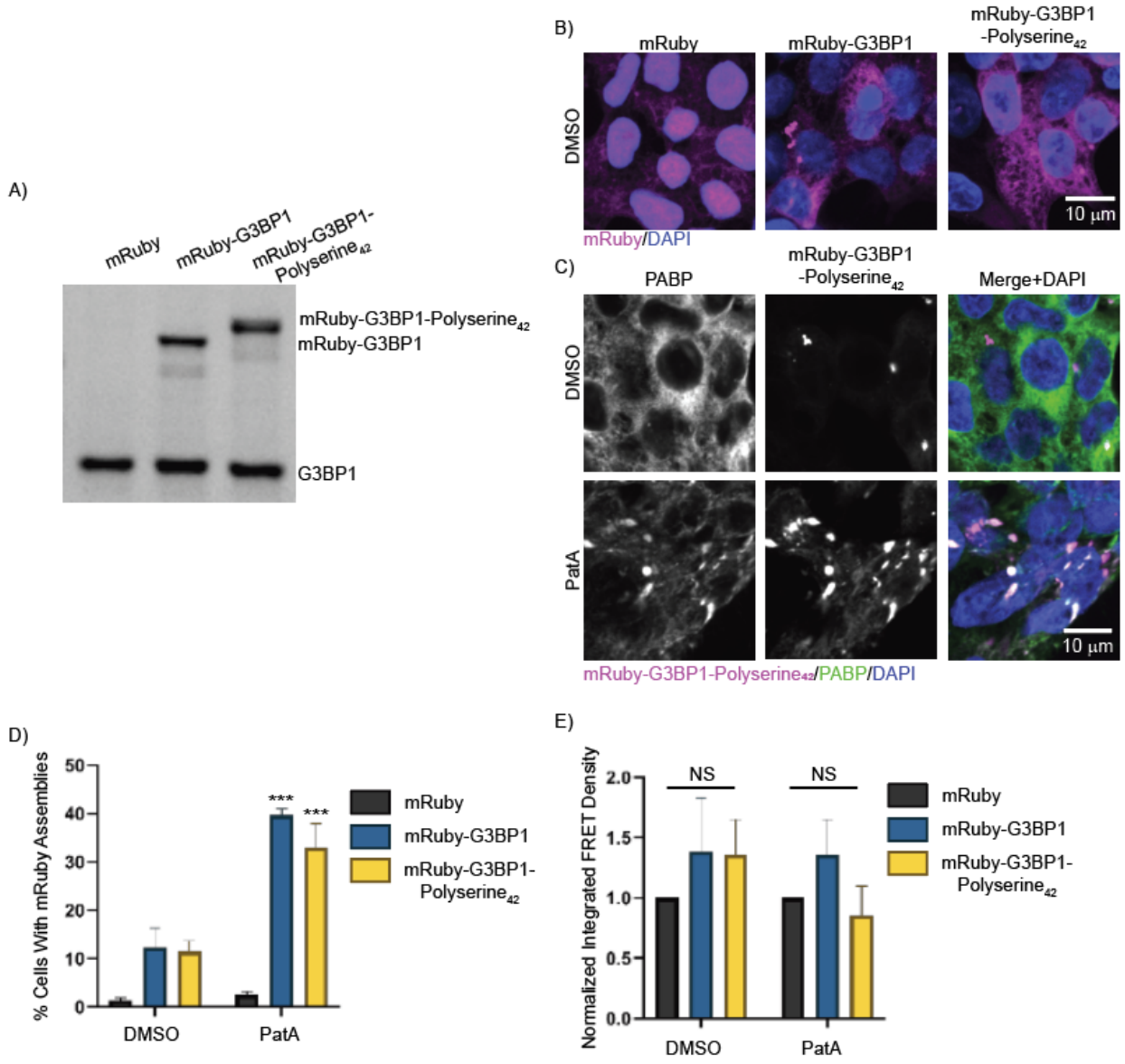

Figure 2.2: Characterization and Validation of mRuby-G3BP1-Polyserine$_{42}$ Tau Biosensor Lines (A) Western Blot stained with anti-G3BP1 conjugated to HRP from lysates prepared from HEK293T tau biosensor cells transduced with lentivirus expressing mRuby, mRuby-G3BP1, or mRuby-G3BP1-Polyserine$_{42}$. (B) Representative images of HEK293T tau biosensor cells stably expressing mRuby, mRuby-G3BP1, or mRuby-G3BP1-Polyserine$_{42}$ (magenta) fixed and nuclei stained with DAPI (blue). (C) Representative immunofluorescence images of HEK293T tau biosensor cells expressing mRuby-G3BP1-Polyserine$_{42}$ (magenta) treated with DMSO control (top) or PatA (bottom) for 12 hours. Cells were fixed and stained with anti-PABP (green), nuclei stained with DAPI (blue). (D) Quantification of percentage of cells with mRuby assemblies treated with DMSO as in (B). N = 15 images across 3 biological replicates. Statistics performed with Kruskal-Wallis test. All comparisons with DMSO are non-significant (**) $P < 0.005$. (E) Quantification of integrated FRET density (product of FRET+ cell percentage and median FRET

intensity) normalized to DMSO/PatAm Ruby control. N = 3 biological replicates. Statistics performed with Kruskal-Wallis. All comparisons are non-significant.

After seeding with brain extracts from Tg2541 mice, cells were treated with the translational inhibitor pateamine A (PatA) to induce irreversible stress granule formation (Low et al. 2005). This experiment provided several notable observations.

We observed mRuby-G3BP1 and mRuby-G3BP1-polyserine$_{42}$ assemblies form in the cytoplasm of ~10% of cells in the absence of PatA treatment and tau seeding (Figure 2.2B-D). Staining for PolyA Binding Protein (PABP), another stress granule marker, did not localize to these assemblies and showed diffuse signal in the absence of stress (Figure 2.2C). Treatment with PatA induced mRuby positive assemblies which enriched PABP in greater than 30% of cells in either G3BP1 or G3BP1-polyserine$_{42}$ expressing cell lines (Figure 2.2C and D). Therefore, the addition of polyserine$_{42}$ to G3BP1 does not block the formation of canonical stress granules. We did not observe significant differences in the amount of tau aggregation after seeding with and without treatment with PatA across the three cell lines (Figure 2.2E). Therefore, the formation of stress granules by translation inhibition does not change tau aggregation in cells.

A key result was that stress granules containing G3BP1-polyserine$_{42}$ colocalized strongly with cytoplasmic tau aggregates in PatA treated and seeded cells (Figure 2.1B and C). In contrast, we observed that tau aggregates and G3BP1 positive stress granules without polyserine$_{42}$ did not colocalize (Figure 2.1B and C), as previously reported (Lester et al. 2023; Wolozin 2012). This demonstrates that targeting polyserine domains to stress granules allows those organelles to interact with tau aggregates.

To understand if G3BP1-polyserine$_{42}$ stress granules act as sites of tau aggregation, or merge with tau aggregates after their formation, we performed live cell imaging. We found that

G3BP1 or G3BP1-polyserine$_{42}$ positive stress granules formed before tau aggregation began (Movie S1 and S2, Figure 2.3A).

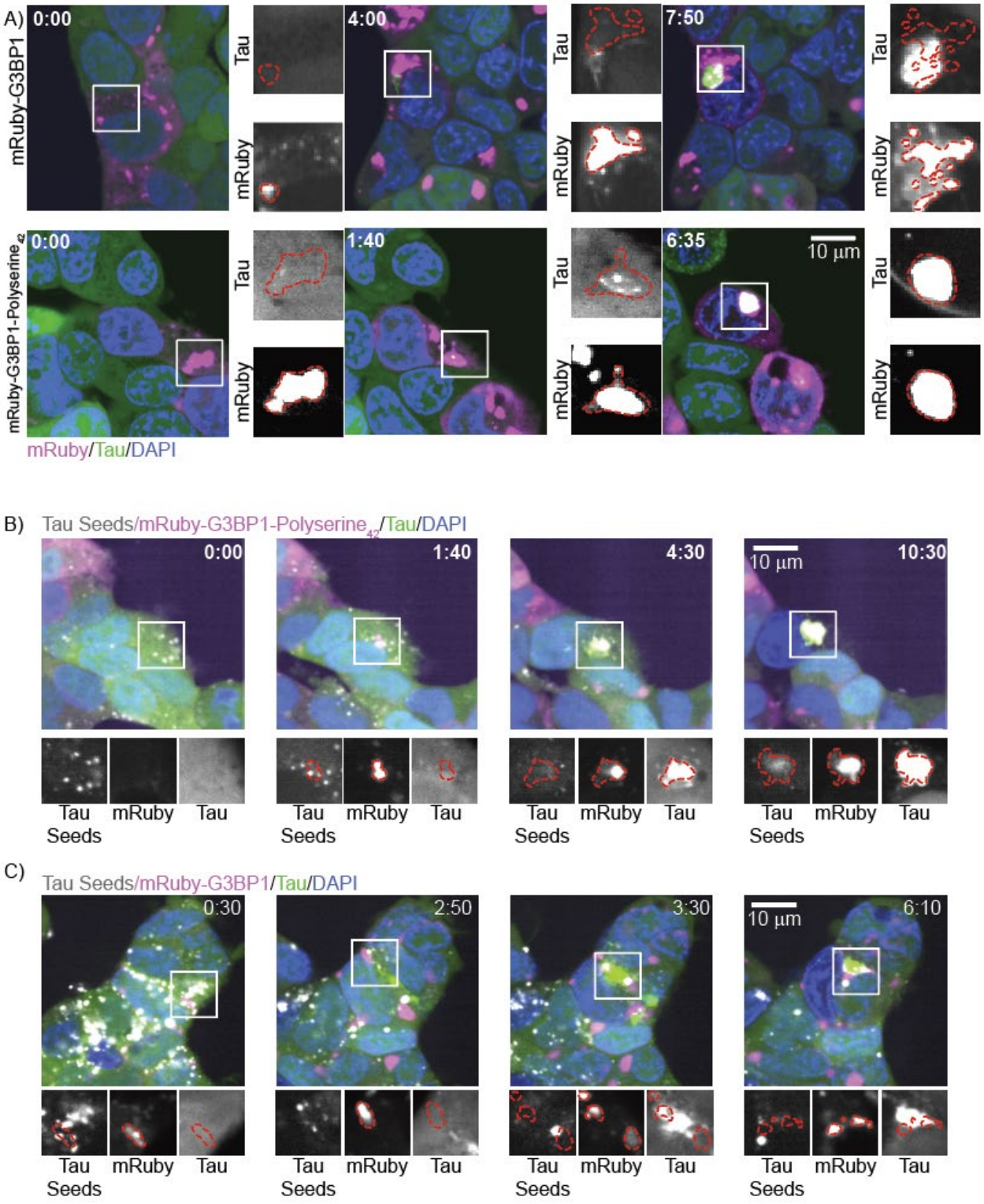

Figure 2.3: Live Cell Imaging of Tau Aggregation in mRuby-G3BP1 or mRuby-G3BP1-Polyserine$_{42}$ Expressing Tau Biosensor Cells (A) Stills from live cell imaging of HEK293T tau

biosensor cells expressing mRuby-G3BP1 (top panels, magenta) or mRuby-G3BP1-Polyserine$_{42}$ (bottom panels, magenta) transfected with tau brain homogenate from aged Tg2541 mice to induce endogenous tau aggregation (green), nuclei stained with Hoechst (blue). Time in hours:minutes post treatment with PatA and start of imaging. Channel breakouts of mRuby fluorescence and tau aggregates in gray scale with mRuby assembly perimeter in red superimposed to all channels. (B) Stills from live cell imaging of HEK293T tau biosensor cells expressing mRuby-G3BP1-polyserine$_{42}$ (magenta) transfected with fluorescent tau fibers maleimide labeled with JF594 (grey) to induce endogenous tau aggregation (green), nuclei labeled with Hoechst (blue). Time in hours:minutes post treatment with PatA and start of imaging. Channel breakouts from each time point in grayscale with mRuby assembly perimeter in red superimposed to other channels. (C) Stills from live cell imaging of HEK293T tau biosensor cells expressing mRuby-G3BP1 (magenta) transfected with fluorescent tau fibers maleimide labeled with JF49 (grey) to induce endogenous tau aggregation (green), nuclei labeled with Hoechst (blue). Time in hours:minutes post treatment with PatA and start of imaging. Channel breakouts from each time point in grayscale with mRuby assembly perimeter in red superimposed to other channels.

In cells with G3BP1 positive stress granules, tau aggregation initiated separately from stress granules (Figure 2.3A, top panels). In cells expressing G3BP1-polyserine$_{42}$, tau aggregation initiated within the stress granule and remained colocalized with G3BP1-polyserine$_{42}$ throughout imaging (Figure 2.3A, bottom panels). Thus, stress granules that contain polyserine$_{42}$ can serve as sites of tau aggregation initiation.

Taken together, this indicates that the presence of polyserine$_{42}$ is sufficient for converting stress granules into a preferred site of tau aggregation. This also demonstrates that stress granules do not contain endogenous inhibitors of tau aggregation.

Polyserine containing assemblies concentrate tau seeds

One possible mechanism by which assemblies containing polyserine domains could act as sites of tau aggregation would be to recruit nascent tau seeds as they enter the cell and then serve as a site for those seeds to grow. To examine if tau seeds interacted with polyserine domain containing assemblies, we transfected tau seeds prepared *in vitro* from fluorescently labeled tau

and followed the fate of those seeds in tau biosensor cell lines expressing SRRM2-Halo or PNN-Halo (Lester et al. 2023).

Strikingly, we observed that transfected tau seeds localized within SRRM2 positive MIGs and CSs (Movies S3 and S4, Fig 2.4A and B), and PNN positive MIGs and CSs which then led to nucleation of tau aggregate growth (Movies S5 and S6, Fig 2.1D and E).

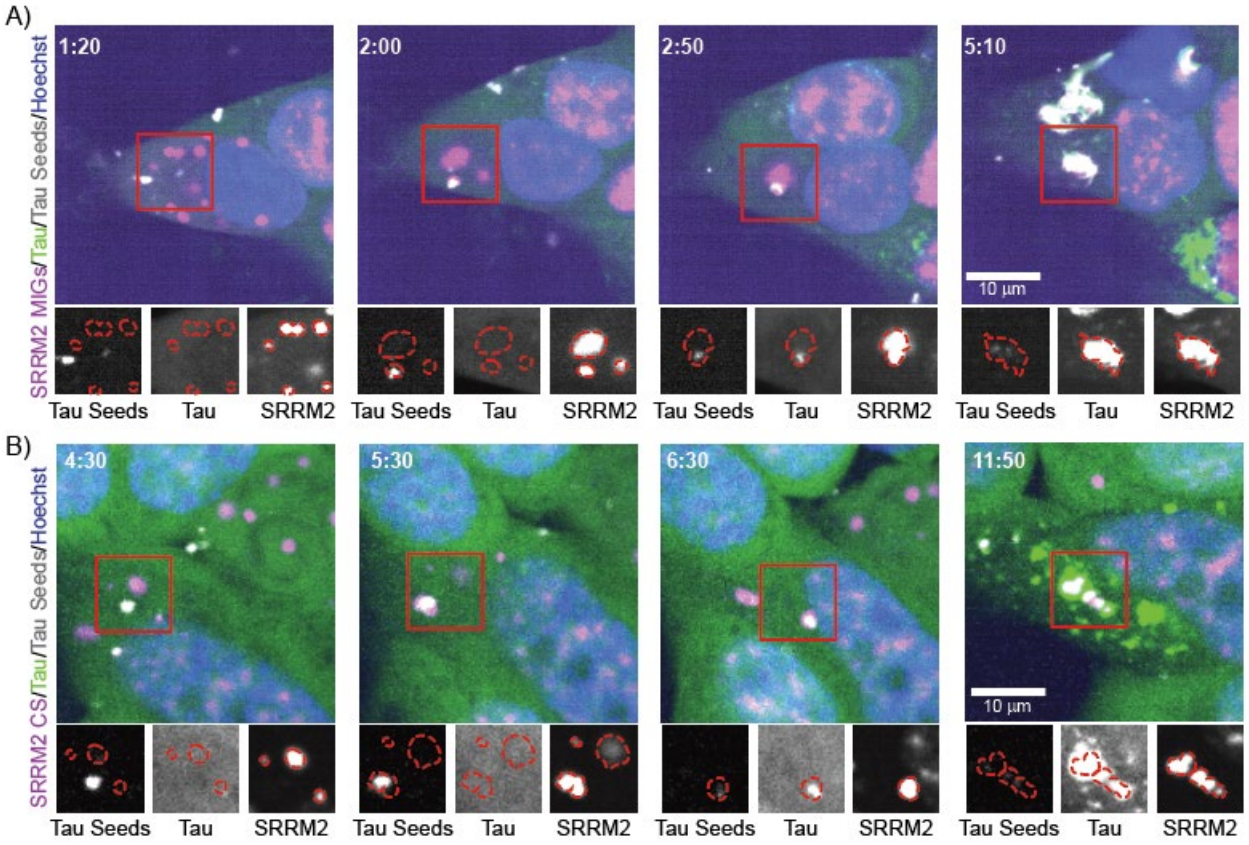

Figure 2.4: Live Cell Imaging of Tau Aggregation with Fluorescent Tau Seeds and PNN Cytoplasmic Assemblies (A) Stills from live cell imaging of HEK293T tau biosensor cells with endogenously tagged full length SRRM2-Halo labeled with JF549 (magenta) MIGs transfected with fluorescent tau seeds maleimide labeled with JF646 (grey) to induce endogenous tau aggregation (green), nuclei labeled with Hoechst (blue). Time in hours:minutes after transfection of tau seeds and start of imaging. Channel breakouts in grayscale below each time point with SRRM2 assembly perimeter in red superimposed to other channels. (B) Stills from live cell imaging of cells as in (A) of SRRM2-Halo positive CSs.

Similarly, we observed fluorescent tau seeds localized in stress granules with G3BP1-polyserine$_{42}$ (Movie S7, Figure 2.3B) but not in wild-type stress granules (Movie S8, Figure 2.3C). These observations support that polyserine containing assemblies serve as sites of tau aggregation, at least in part, by localizing tau seeds.

Polyserine$_{42}$ Self-Assembles In Vitro

Our previous observations that polyserine$_{42}$ overexpression forms cytoplasmic assemblies (Lester et al. 2023) demonstrated that polyserine domains can promote the assembly of non-membrane bound organelles in cells. To determine if this was driven by possible self-assembly properties of polyserine, we purified and examined the properties of a 42 amino acid long polyserine domain, as found in the C-terminus of SRRM2 (Lester et al. 2023). We purified polyserine$_{42}$ with a TEV-cleavable, N-terminal SUMO tag for solubility, and a C-terminal Halo tag to facilitate visualization. As a control, we purified Halo with a TEV-cleavable, N-terminal SUMO tag (Figure 2.5A).

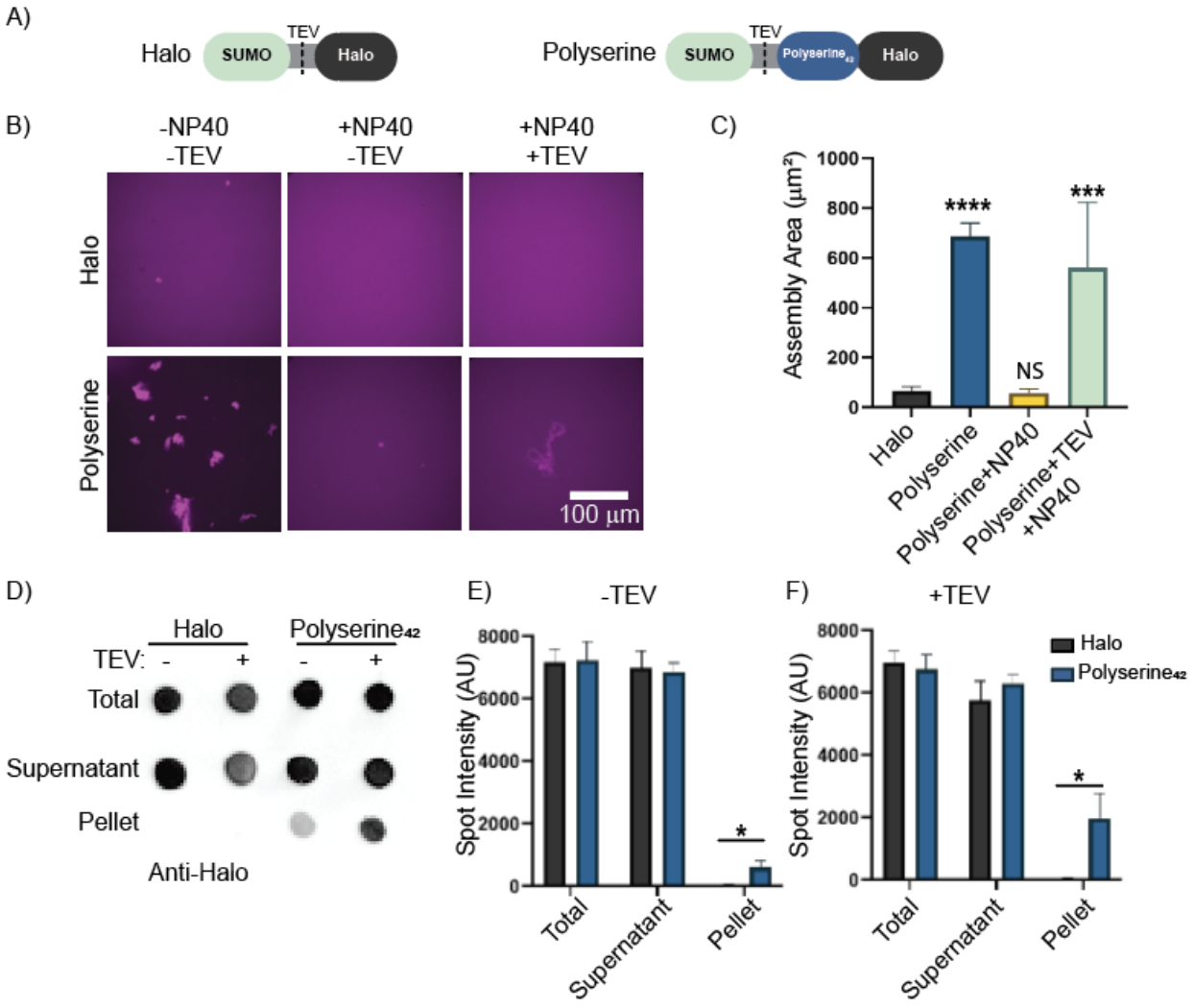

Figure 2.5: Polyserine$_{42}$ Self-Assembles *in vitro* (A) Schematic of recombinant SUMO(TEV)-Halo and SUMO(TEV)Polyserine$_{42}$-Halo constructs. (B) Representative images of Halo or Polyserine$_{42}$-Halo labeled with Janelia-Fluor 646 Halo Ligand purified without detergent or TEV protease treatment (left), with 0.1% NP40 (middle), and with both 0.1% NP40 and TEV protease treatment (right). (C) Quantification of assembly size. N= at least 35 assemblies across 3 biological replicates, Statistics were performed with Kruskal-Wallis with Dunn's Multiple Comparisons test. (***) P = 0.006 (****) P < 0.0001. (D) Representative dot blot of Halo or Polyserine$_{42}$-Halo stained with Anti-Halo from ultracentrifugation pelleting experiments performed in 0.1% NP40 with and without TEV protease treatment. (E) Quantification of dot intensity from N = 3 biological replicates of dot blot as in (D) without TEV treatment. Statistics performed with Mann-Whitney U test across Halo (Black) or Polyserine$_{42}$-Halo (Blue) from Total, Supernatant, or Pellet fractions (*) P < 0.005 (F) Quantification of dot intensity from N = 3 biological replicates of dot blot as in (D) with TEV treatment. Statistics performed with Mann-Whitney U test across Halo (Black) or Polyserine$_{42}$-Halo (Blue) from Total, Supernatant, or Pellet fractions (*) P < 0.005.

To monitor assembly by confocal microscopy we labeled polyserine$_{42}$-Halo and Halo with a Janelia Fluor 646-Halo ligand.

Following purification, we observed polyserine$_{42}$ rapidly and spontaneously self-assembles *in vitro*. Polyserine$_{42}$ forms large, non-spherical assemblies, while the halo control only formed rare, much smaller, assemblies (Figure 2.5B and C). When purified in the presence of 0.1% NP-40, polyserine$_{42}$ still formed assemblies, suggesting they are partially resistant to solubilization with detergent (Figure 2.5B and C). A fraction of purified polyserine$_{42}$ pellets when subjected to ultracentrifugation, providing further evidence for polyserine$_{42}$ assembly (Figure 2.5D-F). Removal of the SUMO solubility tag through TEV cleavage increases the size of polyserine$_{42}$ assemblies purified in detergent, and the amount of pelleted polyserine$_{42}$ (Figure 2.5B-F). Thus, self-assembly is an intrinsic feature of polyserine domains.

Polyserine$_{42}$ assemblies directly interact with monomeric and seed competent tau

Polyserine$_{42}$ assemblies in cells are sites of tau aggregation (Lester et al. 2023). Moreover, we observed that tau seeds could be localized to polyserine assemblies such as MIGs, CSs, and stress granules tagged with polyserine$_{42}$. This suggests several possible manners by which polyserine$_{42}$ might interact with tau and affect aggregation. First, polyserine$_{42}$ might form a structure and/or organization that specifically binds tau as a monomer or fiber. Second, polyserine$_{42}$ assemblies could bind proteins promiscuously, through a network of hydrogen bond donors and acceptors. To understand if polyserine$_{42}$ assemblies are directly interacting with tau or tau seeds, we asked if tau monomers or tau seeds could associate with self-assembled polyserine$_{42}$.

We purified full length 2N4R P301S tau with a single cysteine to allow for direct observation of tau via maleimide labeling with fluorescent dyes (Figure 2.6A).

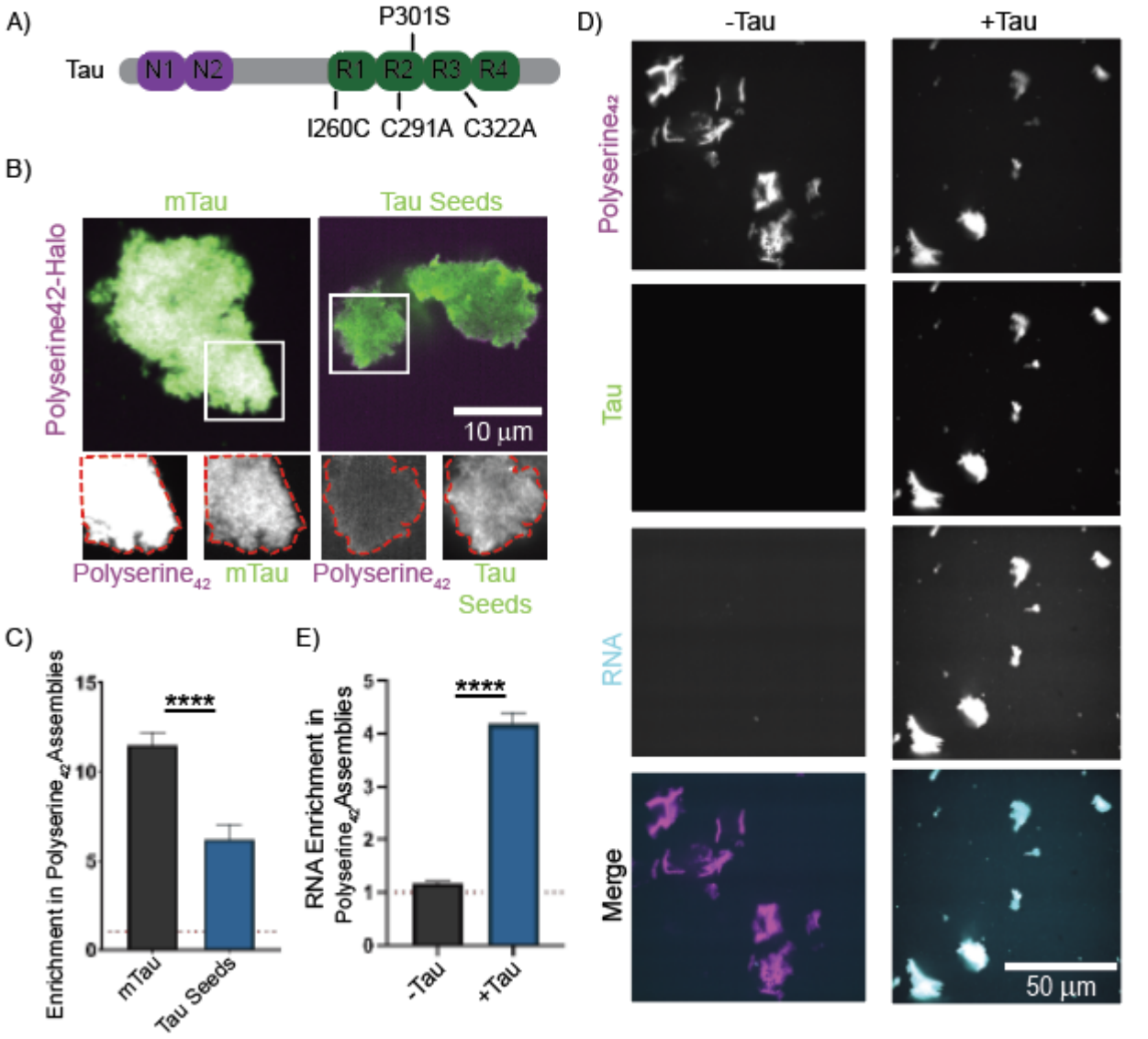

Figure 2.6: Polyserine$_{42}$ Interacts Directly with Tau Monomers and Seeds (A) Schematic of recombinant tau construct used. (B) Representative images of tau monomers (mTau) maleimide labeled with JF-646, tau seeds prepared from mTau maleimide labeled with JF-646 incubated with shaking with polyU RNA (green) mixed with Polyserine$_{42}$-Halo labeled with JF-549. Channel breakouts shown below each image in grayscale with polyserine assembly perimeter in red superimposed to other channels. (C) Quantification of protein enrichment in Polyserine$_{42}$-Halo assemblies as in (B). Statistics performed with one-way Kruskal-Wallis test with Dunn's multiple comparisons test. (***) $P < 0.005$ (****) $P < 0.0001$. (D) Representative images of Polyserine$_{42}$-Halo assemblies (magenta) incubated with fluorescent polyU RNA (cyan) with and without tau monomers (green). Channel breakouts in grayscale. (E) Quantification of RNA enrichment in Polyserine$_{42}$-Halo assemblies with and without tau monomers as in (D). Statistics performed with Mann-Whitney U test. (****) $P < 0.0001$

We mixed monomeric tau with polyserine$_{42}$-Halo assemblies or Halo alone and performed confocal microscopy to monitor potential tau and polyserine$_{42}$ interactions. Tau does not alter the polyserine$_{42}$ self-assembly in vitro (Figure 2.7A) and is not required for polyserine$_{42}$ assembly in WT HEK293 cells (Figure 2.7B).

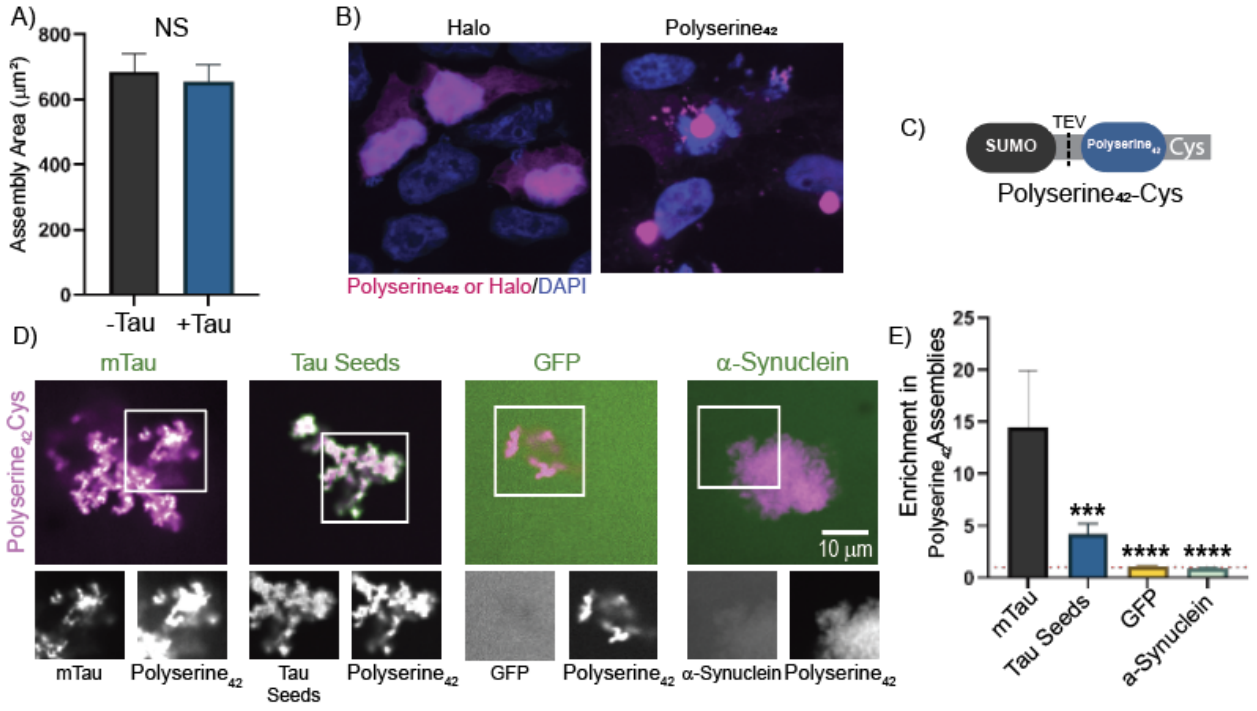

Figure 2.7: Polyserine Protein Interaction Specificity (A) Quantification of assembly area of Polyserine$_{42}$-Halo with and without incubation with full length tau monomers. N = at least 807 assemblies across 3 biological replicates. Statistics performed with Kruskal-Wallis test with Dunn's multiple comparisons test. Comparison is nonsignificant. (B) Representative images of wildtype HEK293T cells transfected with a plasmid expressing Polyserine$_{42}$-Halo or Halo labeled with JF646 (magenta) for 48 hours. Cells were fixed and nuclei stained with DAPI (blue). (C) Schematic of recombinant polyserine$_{42}$-Cys. (D) Representative images of SUMO-Polyserine$_{42}$-Halo labeled with JF549 mixed with tau monomers maleimide labeled with JF646, GFP, GFP+30, or GFP-30 (green) Channel breakouts in grayscale below each image with polyserine assembly perimeter in red superimposed across channels. (E) Quantification of protein enrichment in Polyserine$_{42}$ assemblies. N = at least 10 images across 3 biological replicates. Statistics performed with Kruskal-Wallis test compared to tau monomers. (***) $P < 0.001$ (****) $P < 0.0001$ (E) Representative images of Polyserine$_{42}$-cys maleimide labeled with JF646 (magenta) mixed with GFP+30 or GFP-30 (green). Channel breakouts in gray scale below each image. (F) Quantification of enrichment of tau monomers, tau seeds, GFP, α-synuclein (reproduced from figure 3) GFP+30 and GFP-30 in Polyserine$_{42}$ assemblies. N = at least 10 images across 3 biological replicates. Statistics performed with Kruskal-Wallis test compared to tau monomers. (***) $P < 0.001$ (****) $P < 0.0001$

Importantly, we observe that polyserine$_{42}$-Halo assemblies directly interact with tau monomers (Figure 2.6B and C). To rule out effects from the SUMO or Halo tags, we also purified polyserine$_{42}$ with a C-terminal cysteine to allow for maleimide labeling, and a TEV-cleavable N-terminal SUMO tag for solubility (Figure 2.7C) We observe polyserine$_{42}$-Cys assemblies also interact with tau monomers directly (Fig 2.7D and E). Interestingly, polyserine$_{42}$-cys assemblies did not interact with GFP or α-synuclein (Figure 2.7D and E). Therefore, polyserine$_{42}$ directly interacts with tau monomers with some degree of specificity.

Since we observed tau seeds interacting with polyserine domain containing assemblies in cells (Figure 2.1C), we also examined if tau seeds prepared by sonication of fluorescently labeled tau fibers enriched in polyserine$_{42}$ assemblies *in vitro*. We observed tau seeds could associate with polyserine$_{42}$-Halo and polyserine$_{42}$-Cys assemblies, although to a lesser degree than tau monomers (Figure 2.6B and C, 2.7D and E). This suggests that the recruitment of tau seeds into polyserine$_{42}$ assemblies in cells could occur through direct interaction.

We also examined if polyserine$_{42}$ assemblies enrich RNA, a co-factor sufficient for inducing tau fiber formation (Kampers et al. 1996). We mixed polyserine$_{42}$-Halo assemblies with fluorescently labeled polyU RNA. We observed polyserine$_{42}$-Halo assemblies do not enrich polyU RNA (Figure 2.6D and E). However, in the presence of tau we observed that tau, RNA, and polyserine$_{42}$-Halo co-assemble (Figure 2.6D and E). Therefore, polyserine$_{42}$ assemblies enrich RNA in a tau dependent manner.

Polyserine$_{42}$ Increases the Rate of Tau Fiber Formation and Growth

Since polyserine$_{42}$ can interact with tau, and thereby potentially either alter the folding of tau and/or create a high local concentration of both tau and RNA, it may directly increase rates of tau aggregation. To measure the rate of tau fiber formation and growth we used an *in vitro*

thioflavin-t (ThT) kinetics assay. We mixed monomeric 2N4R P301S tau with polyU RNA, which is sufficient to induce tau fibrillization (Figure 2.8A yellow curve), with polyserine$_{42}$ (Figure 2.8A black curve) or the halo control (Figure 2.8A blue curve) and measured the increase in bound ThT fluorescence over time.

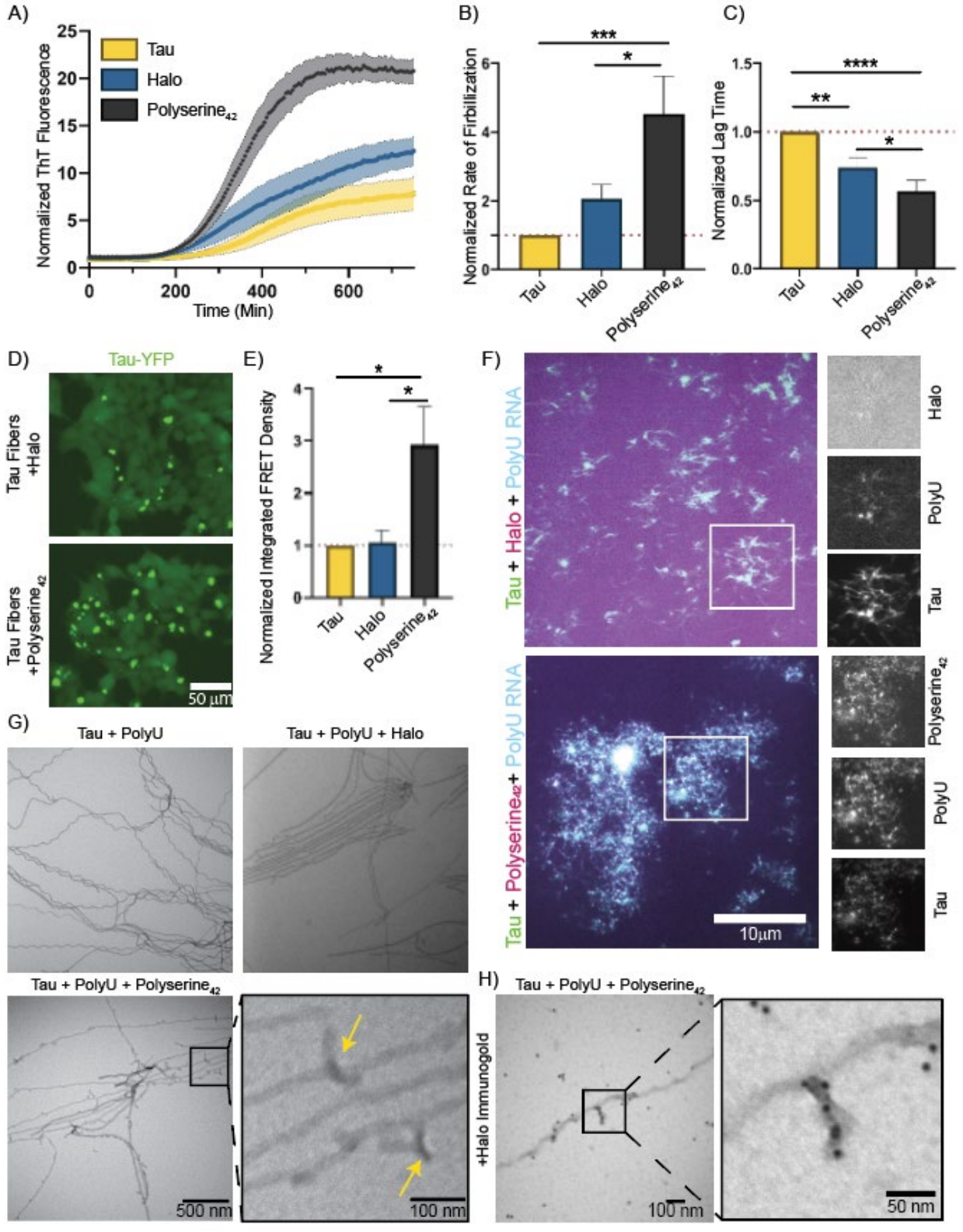
A)
Normalized ThT Fluorescence
Time (Min)
Tau
Halo
Polyserine42
B)
Normalized Rate of Firbillization
C)
Normalized Lag Time
D)
Tau-YFP
Tau Fibers +Halo
Tau Fibers +Polyserine42
50 µm
E)
Normalized Integrated FRET Density
F)
Tau + Halo + PolyU RNA
Tau + Polyserine42 + PolyU RNA
10µm
Halo
PolyU
Tau
Polyserine42
G)
Tau + PolyU
Tau + PolyU + Halo
Tau + PolyU + Polyserine42
500 nm
100 nm
H)
Tau + PolyU + Polyserine42
+Halo Immunogold
100 nm
50 nm

Figure 2.8: Polyserine$_{42}$ Increases the Rate of Tau Fiber Formation and Alters Tau Fiber Ultrastructure (A) Monomeric tau was incubated with PolyU RNA, with and without Halo or Polyserine$_{42}$-Halo and thioflavin-t (ThT). ThT fluorescence was measured every 5 minutes for 24 hours, X-axis truncated to show first 800 minutes. Fluorescence normalized to first time point across each condition. N = 9 technical replicates across 3 biological replicates. (B) Quantification of the rate of fibrilization of tau derived from the slope of the linear region of the curves in (A). N = 9 technical replicates across 3 biological replicates. Statistics performed with Kruskal-Wallis test. (*) $P < 0.05$ (***) $P < 0.001$ (C) Quantification of the lag time derived from the x-intercept of an extrapolation of the linear region of curves in (A). Statistics performed with Kruskal-Wallis test. (*) $P < 0.05$ (**) $P< 0.005$, (***) $P < 0.001$ (D) Representative images of HEK293T tau biosensor cells transfected with tau fibers prepared with monomeric tau, polyU RNA, and Halo (top) or with Polyserine$_{42}$-Halo (bottom) to seed tau aggregates (green). (E) Quantification of integrated FRET density (product of FRET+ percentage and median fluorescence intensity) of HEK293T tau biosensor cells transfected with tau fibers prepared with polyU RNA with and without Halo or Polyserine$_{42}$-Halo normalized to cells transfected with tau fibers prepared without Halo or Polyserine$_{42}$-Halo). N = 3 biological replicates. Statistics performed with Kruskal-Wallis test. (*) $P < 0.05$. (F) Representative images of tau fibers prepared with tau monomers (green), FITC-fluorescent polyU RNA (cyan), and Polyserine$_{42}$-Halo or Halo labeled with JF646. Channel breakouts and zooms shown in gray scale. (G) Representative negative stain electron microscopy images of tau fibers prepared as in F. Yellow arrows show additional densities present in Polyserine$_{42}$-Halo containing tau fiber preps. (H) Representative image of immunogold negative stain electron microscopy of tau fibers prepared as in F stained with anti-halo and secondary antibody conjugated with gold nanoparticles, zoom and inset shows a Polyserine$_{42}$-Halo assembly on the surface of a tau fiber.

We then determined the fibrilization growth rate and lag time by extracting the slope and extrapolated x-intercept, respectively, of the linear region of the resulting curves.

Importantly, we observed that polyserine$_{42}$ significantly decreases the lag time and increases the growth rate compared to halo alone, which had a small effect compared to no addition of protein (Figure 2.8A-C black bars). Halo may exert this small effect on tau fibrilization rates through electrostatic interactions with tau, as the Halo tag is negatively charged, and tau is positively charged. Nevertheless, this suggests that polyserine$_{42}$ can increase tau fibrillization, potentially by increasing the rate of formation of initial seeding competent tau species, and the rate of growth of those seeds.

To examine if polyserine$_{42}$ was increasing the conversion of tau into fibrillar species by an orthogonal assay, we asked if polyserine$_{42}$ increases the amount of seeding competent tau following *in vitro* fibrillization. In this experiment, we transfected tau fibrilization reactions after 24 hours of incubation with or without polyserine$_{42}$, or Halo into HEK293T tau biosensor cells(Holmes et al. 2014). The HEK293T tau biosensor cells express cyan fluorescent protein (CFP) or yellow fluorescent protein (YFP) tagged forms of the microtubule binding domain of tau with a P301S pathogenic mutation that forms FRET (Förster Resonance Energy Transfer) positive tau aggregates after transfection of exogenous tau seeds(Holmes et al. 2014). In agreement with the increased rate of tau fiber formation and growth, we found that the presence of polyserine$_{42}$ results in an increase in the amount of seeding competent tau as compared to Halo alone (Figure 2.8D and E). This provides additional evidence that polyserine$_{42}$ increases the formation of fibrillar, seeding competent tau.

Polyserine$_{42}$ Incorporates into Growing Tau Aggregates and Changes Tau Fiber Ultrastructure

After observing that polyserine$_{42}$ directly increases the rate of formation and growth of tau fibers, we asked if the resulting fiber structures and composition are altered. Confocal and negative stain electron microscopy were performed to determine the composition and ultrastructure, respectively, of tau fibers. We prepared tau fibers as described previously and imaged fibers after 24 hours of fibrilization.

With confocal microscopy we found that tau fibers prepared in the presence of polyserine$_{42}$ show colocalization of polyserine$_{42}$, tau, and polyU RNA (Figure 2.8F). Tau fibers prepared in the presence of halo alone show diffuse halo signal, while tau and polyU RNA fluorescence is colocalized (Figure 2.8F).

Negative stain electron microscopy of tau-RNA fibers showed polyserine$_{42}$ can change tau fiber ultrastructure. Tau fibers made in the presence of polyserine$_{42}$ contain additional densities decorating the fiber (Figure 2.8G, yellow arrows) which are not observed with tau fibers prepared with Halo, or no additional protein. To identify these unique densities, we performed immunogold labeling against the Halo tag. We observed the enrichment of gold-nanoparticle densities on the extra-densities observed with tau-polyserine$_{42}$ fibers (Figure 2.8H). We did not observe staining throughout the tau fiber, indicating that polyserine$_{42}$ may interact with the surface of fibers, as opposed to incorporating into growing tau fibers. Taken together, this suggests that polyserine$_{42}$ can interact with and possibly alter the form of growing tau fibers.

Polyserine-tau interaction is separable from increasing tau aggregation.

The results above show polyserine$_{42}$ self-assembles, localizes to tau aggregates, and increases tau fibrillization. In principle, these effects could all be due to one biochemical property of polyserine$_{42}$ or might reflect different functions. To address the possible overlap of these functions, we created variants of polyserine$_{42}$ and examined their ability to localize to tau aggregates, affect the degree of tau aggregation, and form intracellular assemblies in HEK293T tau biosensor (Holmes et al. 2014) cells. We created variants where a fraction of serine residues was substituted with negatively charged aspartic acid, positively charged lysine, or neutral threonine residues without altering peptide length (Figure 2.9A).

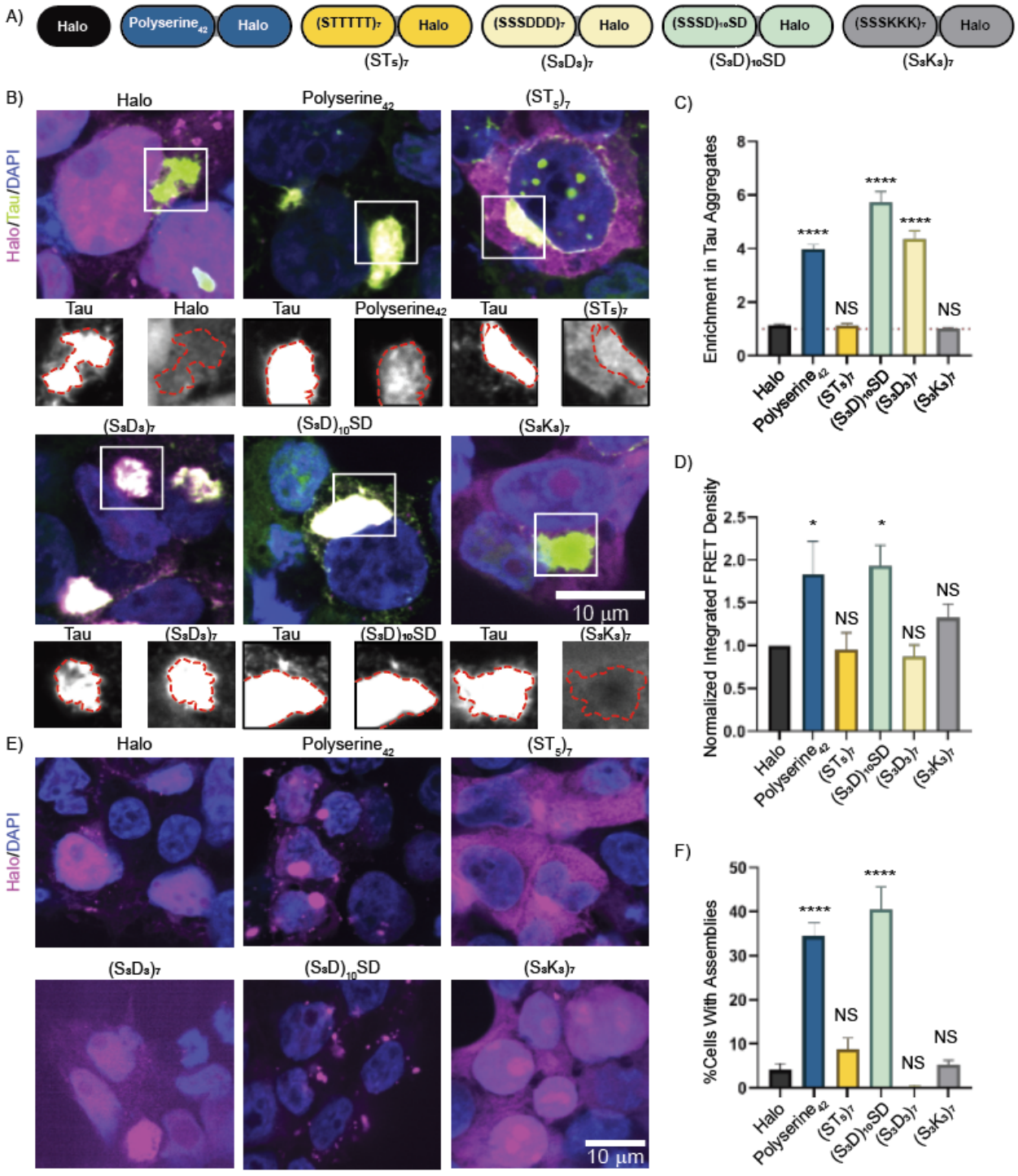

Figure 2.9: Analysis of Polyserine$_{42}$ Variants (A) Schematic of Polyserine$_{42}$-Halo variants used. (B) Representative images of HEK293T tau biosensor cells transfected with plasmids expressing Halo, Polyserine$_{42}$-Halo, or polyserine$_{42}$-Halo variants labeled with JF646 halo-ligand (magenta) for 24 hours, then transfected with tau brain homogenate from aged Tg2541 mice to induce endogenous tau aggregation (green), and fixed after 24 hours, nuclei stained with DAPI (blue). Channel breakouts show tau aggregate perimeter in red superimposed to Halo/ Polyserine$_{42}$-Halo

/Polyserine$_{42}$-Halo variant channels. (C) Quantification of Halo/ Polyserine$_{42}$-Halo /Polyserine$_{42}$-Halo variants enrichment in cytoplasmic tau aggregates. N = at least 129 cells with tau aggregates and Halo/ Polyserine$_{42}$-Halo/Polyserine$_{42}$-Halo variant expression across 3 biological replicates. Statistics performed with Kruskal Wallis test with Dunn's multiple comparisons test compared to Halo enrichment. (*) $P < 0.05$ (****) $P < 0.0001$. (D) Quantification of integrated FRET density (product of FRET+ percentage and median FRET intensity) of top 10% Halo expressing cells normalized to Halo. N = 6 biological replicates. Statistics performed with Kruskal-Wallis test compared to Halo. (*) $P < 0.05$. (E) Representative images of Halo/ Polyserine$_{42}$-Halo/Polyserine$_{42}$-Halo variants (magenta) expressed in Wild Type HEK293T cells for 48 hours, and fixed, nuclei stained with DAPI (blue). (F) Quantification of percent cells expressing Halo/ Polyserine$_{42}$-Halo/ Polyserine$_{42}$-Halo variants with at least one Halo/ Polyserine$_{42}$-Halo/Polyserine$_{42}$-Halo variant assembly. N = 15 images across 3 biological replicates. Statistics performed with Kruskal-Wallis test. (****) $P < 0.0001$.

We began by examining the ability of polyserine$_{42}$ variants to localize to tau aggregates in cells following transfection. First, we observed the replacement of some serine residues with aspartic acids did not alter recruitment into tau aggregates, as constructs with 50% or 25% of the serine residues replaced by aspartic acids $(S_3D_3)_7$, or $(S_3D)_{10}SD$, respectively, still enriched with tau aggregates (Figure 2.9B and C). In contrast, polyserine domains with 50% substitution with lysine $(S_3K_3)_{7,}$ or a threonine rich variant, $(ST_5)_7$, failed to colocalize with tau aggregates (Figure 2.9B and C).

The observation that negatively charged amino acids could substitute serine raised the possibility serine phosphorylation may mediate polyserine interactions with tau aggregates in cells. However, three observations suggest this is not the case. First, the substitution of serine with threonine ($(ST_5)_7$), which are often substrates for shared serine/threonine kinases, led to a construct that abolished enrichment with tau aggregates (Figure 2.9B and C). Second, phos-tag analysis (Kinoshita et al. 2009) of overexpressed polyserine$_{42}$ did not show a substantial shift in molecular weight, indicating no phosphorylation (Figure 2.10A).

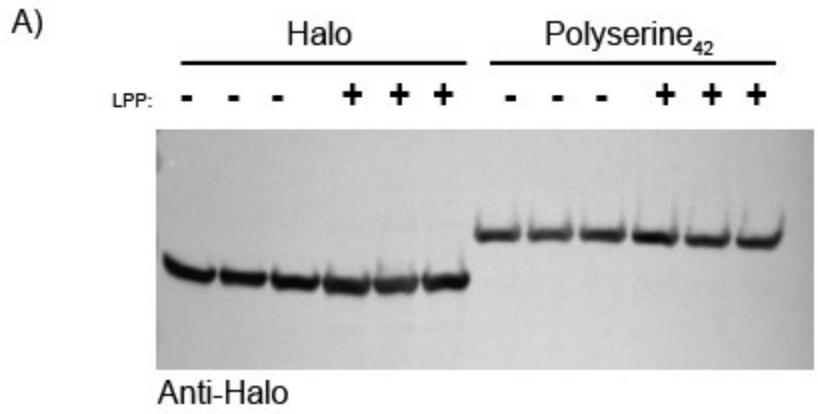

Figure 2.10: Phos-Tag Analysis of Halo or Polyserine$_{42}$-Halo From HEK293T Cells (A) Plasmids expressing Halo or Polyserine$_{42}$-Halo were transfected into WT HEK293T cells. Cells were harvested after 48 hours, lysed with and without phosphatase inhibitor and treated with or without lambda-protein-phosphatase (LPP). Lysates were loaded onto a PhosTag SDS-PAGE gel, transferred to a nitrocellulose membrane which was probed with anti-Halo.

Finally, we note that recombinant polyserine$_{42}$, which is not phosphorylated, can interact with tau *in vitro* (Figure 2.6) demonstrating phosphorylation is not required for polyserine$_{42}$-tau interaction.

Next, we asked how these variants altered tau aggregation in cells using flow cytometry (Lester et al. 2023; Holmes et al. 2014). We observed that one of these variants retained the ability to increase tau fibrillization. Specifically, we observed that, like polyserine$_{42}$, $(S_3D)_{10}SD$ increased tau aggregation (Figure 2.9D). In contrast, $(ST_5)_7$, and $(S_3K_3)_7$, which do not enrich in tau aggregates, also do not increase tau aggregation (Fig 5B-E). Interestingly, $(S_3D_3)_7$, which enriches with tau aggregates, does not increase tau aggregation (Figure 2.9B-D). This demonstrates that the interaction of polyserine domains with tau aggregates can be separated from their ability to promote tau aggregation.

Interestingly, we observed a correlation between the ability for a variant to form assemblies with its ability to increase tau aggregation. Specifically, we observed that polyserine$_{42}$ and $(S_3D)_{10}SD$, both of which increase tau aggregation, formed intracellular assemblies (Figure 2.9E

and F). In contrast, $(ST_5)_7$, $(S_3K_3)_7$, and $(S_3D_3)_7$ all failed to form intracellular assemblies and to promote tau aggregation (Figure 2.9E and F).

Polyserine$_{42}$ Self-Assembly Stimulates Tau Aggregation

To more directly test the role of polyserine$_{42}$ assembly driving the stimulation of tau aggregation, we overexpressed a maltose binding protein (MBP)-polyserine$_{42}$-Halo construct in tau biosensor cells (Holmes et al. 2014) to reduce polyserine$_{42}$ assembly, as MBP has been used to increase solubility of recombinant proteins for structural biology (Kapust and Waugh 1999).

First, we ensured that MBP fusion reduced polyserine$_{42}$ assembly but retained enrichment in tau aggregates. We found that MBP-polyserine$_{42}$-halo expression reduced the fraction of cells with assemblies to levels similar to MBP-Halo expression alone (Figure 2.11A and B).

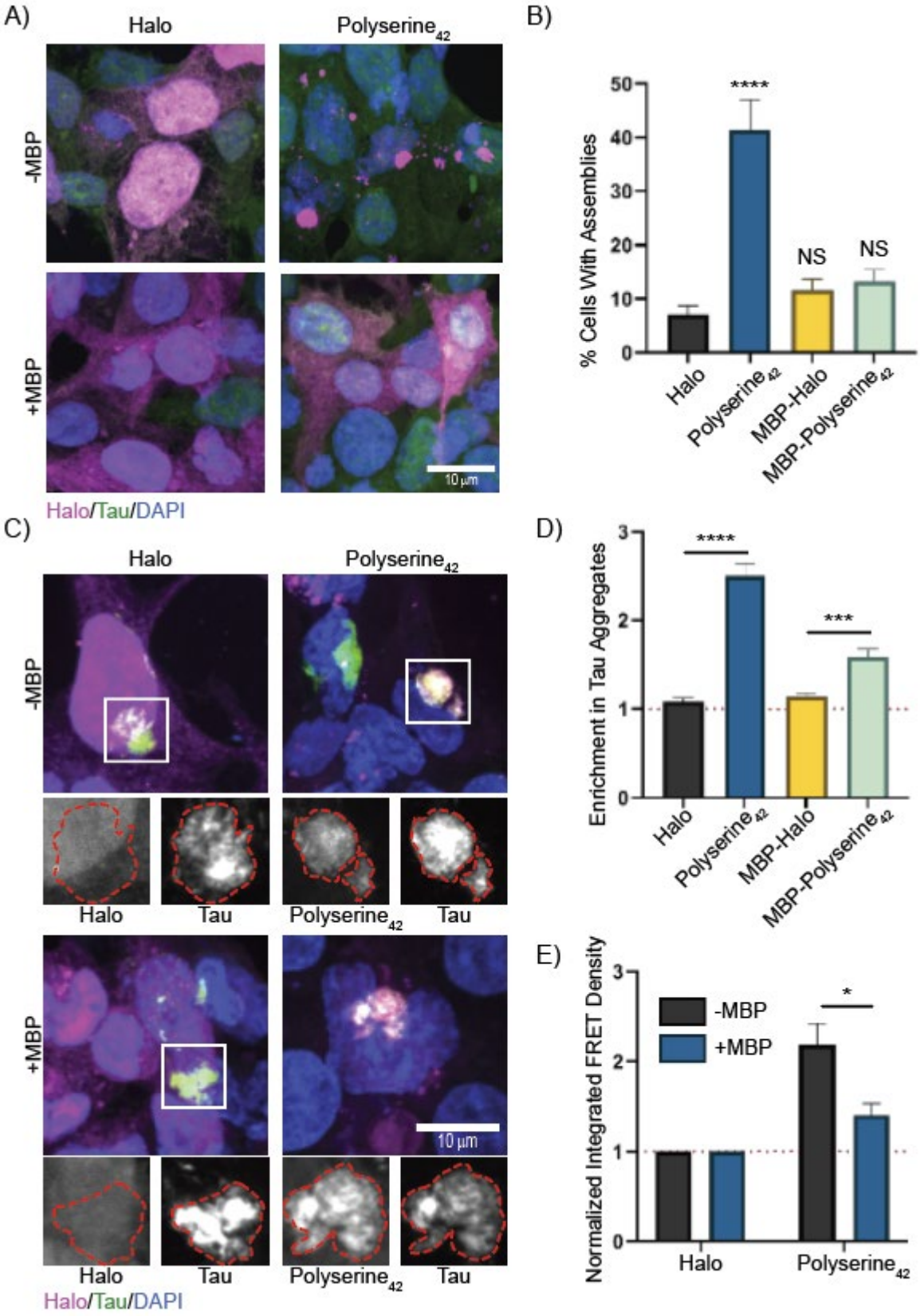
A)
Halo
Polyserine42
-MBP
+MBP
10 µm
Halo/Tau/DAPI
B)
% Cells With Assemblies
50
40
30
20
10
0
****
NS
NS
Halo
Polyserine42
MBP-Halo
MBP-Polyserine42
C)
Halo
Polyserine42
-MBP
+MBP
Halo
Tau
Polyserine42
Tau
10 µm
Halo/Tau/DAPI
D)
Enrichment in Tau Aggregates
3
2
1
0
****
***
Halo
Polyserine42
MBP-Halo
MBP-Polyserine42
E)
Normalized Integrated FRET Density
3
2
1
0
-MBP
+MBP
*
Halo
Polyserine42

Figure 2.11: MBP-Polyserine$_{42}$ Fusion Protein Blocks Polyserine Assembly and Stimulation of Tau Aggregation (A) Representative images of HEK293T tau biosensor cells transfected with plasmids expressing Halo, Polyserine$_{42}$-Halo, MBP-Halo, or MBP-Polyserine$_{42}$-Halo labeled with JF646 (magenta) for 48 hours, tau-YFP (green), and nuclei stained with DAPI (blue). (B) Quantification of percentage of cells expressing Halo tagged constructs with Halo assemblies. N = 15 images across 3 biological replicates. Statistics performed with Kruskal-Wallis test compared to Halo. (****) P < 0.0001 (C) Representative images of HEK293T tau biosensor cells transfected with plasmids expressing Halo, Polyserine$_{42}$-Halo, MBP-Halo, or MBP-Polyserine$_{42}$-Halo labeled with JF646 (magenta) for 24 hours, transfected with tau brain homogenate from aged Tg2541 mice to induce endogenous tau aggregation (green), cells were fixed 24 hours later and nuclei stained with DAPI (blue). Channel breakouts for Halo, Polyserine$_{42}$-Halo, MBP-Halo, or MBP-Polyserine$_{42}$-Halo and tau shown below with tau aggregate perimeter in red superimposed across channels. (D) Quantification of enrichment of Halo, Polyserine$_{42}$-Halo, MBP-Halo, or MBP-Polyserine$_{42}$-Halo in tau aggregates as in (C). N = at least 109 cells with Halo, Polyserine$_{42}$-Halo, MBP-Halo, or MBP-Polyserine$_{42}$-Halo expression and tau aggregates across 3 biological replicates. Statistics performed with Kruskal-Wallis test. (***) P = 0.0001 (****) P < 0.0001.

Second, we confirmed that MBP-polyserine$_{42}$ enriches with tau aggregates (Figure 2.11C and D).

We next tested if this separation of functions altered tau aggregation. We found that addition of MBP reduced polyserine$_{42}$ effects on promoting tau aggregation (Figure 2.11D). Therefore, polyserine$_{42}$ self-assembly positively correlates with increased tau aggregation, and that self-assembly and targeting to tau aggregates are separable functions.

DISCUSSION

In this study we demonstrate that polyserine$_{42}$ spontaneously self assembles. The key observation is that purified polyserine spontaneously forms microscopically visible assemblies large enough to pellet via ultracentrifugation (Figure 2.5). While the specific structure of these polyserine assemblies is unknown, it may form complex coiled-coil structures similar to serine repeats of shorter lengths (Lilliu et al. 2018). Additionally, the self-assembly of polyserine provides a molecular understanding of polyserine assemblies that form upon overexpression in cells and mice (Lester et al. 2023; Van Alstyne et al. 2024). Polyserine assemblies are also observed in spinocerebellar ataxia type 8 (SCA8) and Huntington's Disease (HD), produced by RAN

translation, and may form through similar self-assembly mechanisms (Ayhan et al. 2018; Davies and Rubinsztein 2006). An interesting possibility is that polyserine domain self-assembly may promote the assembly of nuclear speckles, as SRRM2 is essential for nuclear speckle formation (Lester et al. 2023; Ilik et al. 2020).

Our data supports a hypothesis that polyserine assembly is required to stimulate tau aggregation. Importantly, blocking polyserine assembly via expression of an MBP-polyserine fusion protein also reduces stimulation of tau aggregation (Figure 2.11). Taken together with our findings that polyserine variants which do not assemble also do not increase tau aggregation (Figure 2.9), we conclude that assembly drives the stimulation of tau aggregation. This may also explain the observation that polyserine puncta and tau aggregation are observed in some cases of SCA8 and HD (Gratuze et al. 2016; Yonenobu et al. 2023). Further study is required to understand if pathological polyserine assembly directly induces tau aggregation in these diseases.

Polyserine assemblies increase tau aggregation which can occur through direct interaction with tau. We previously observed that overexpression of polyserine$_{42}$ increases tau aggregation in HEK293T tau biosensor cells and pathology in PS19 mice (Lester et al. 2023; Van Alstyne et al. 2024). Here, we provide evidence that this increased aggregation can occur due to direct interaction between polyserine assemblies, tau monomers and other cofactors sufficient to induce tau aggregation (Figure 2.6). Additionally, polyserine containing assemblies can localize tau seeds, creating preferred sites for tau aggregation (Figure 2.1). Thus, polyserine expression and assembly may exacerbate tau pathology by creating a complex network with tau seeds which promotes subsequent aggregation.

Polyserine assemblies may interact with tau and increase tau aggregation in multiple ways. In one manner, polyserine assemblies enrich tau monomers and cofactors, such as RNA, sufficient for fibrilization in a high local concentration (Figure 2.6). This higher concentration of tau and RNA may then lead to faster fiber formation and growth (Figure 2.8). Alternatively, polyserine may interact with tau monomers and bias the folding of tau into an aggregate prone form. Finally, polyserine assemblies may increase tau aggregation by enriching seeding competent oligomers or fibers with tau monomers, thus increasing the rate of fiber growth independent of additional cofactors.

In conclusion, we hypothesize that polyserine domains self-assemble, which increases the local concentration of tau monomers and fibers through direct interactions, resulting in increased rates of tau aggregate formation (Figure 2.12).

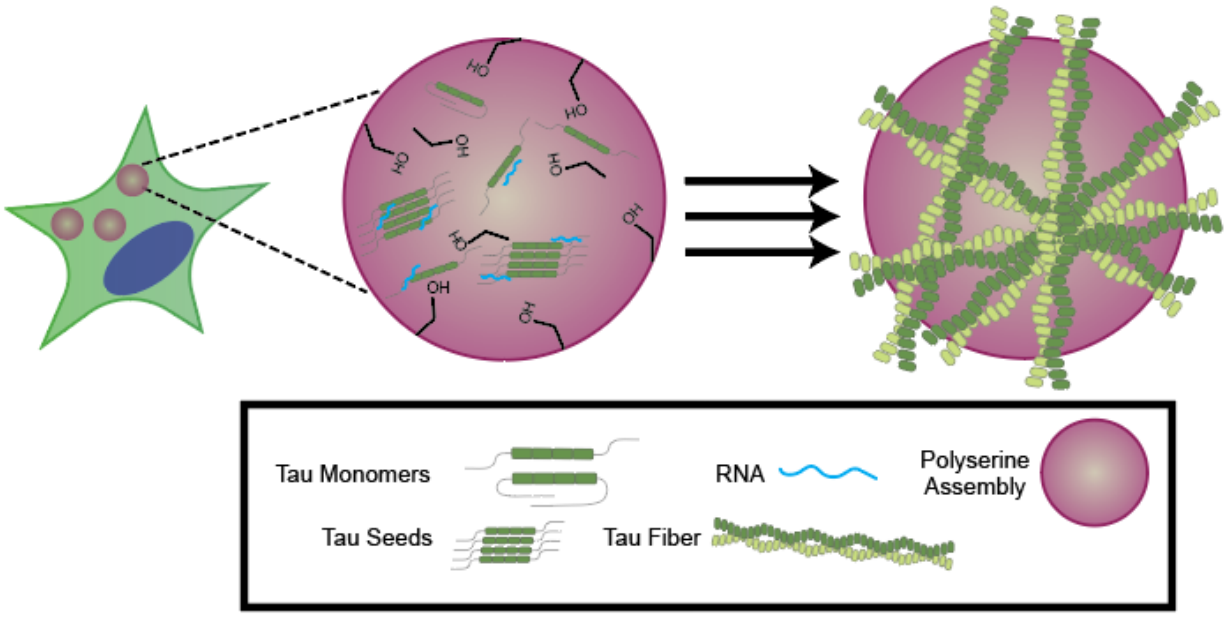

Figure 2.12: Polyserine$_{42}$ Assemblies are Preferred Sites of Tau Aggregation Through Enrichment of Tau Seeds Stimulating Tau Aggregation. (A) Model showing a possible mechanism in which polyserine containing assemblies enrich tau monomers, RNA, and tau seeds to create preferred sites of tau aggregation, which in turn stimulates tau aggregation. Tau seeds can enrich in cytoplasmic polyserine containing assemblies where they interact with endogenous tau, and possibly other cellular cofactors to grow a tau aggregate.

METHODS

Cell culture and tau aggregate seeding of HEK293T cells

HEK293T tau biosensor cells (Holmes et al. 2014) stably expressing the 4R repeat domain of tau (K18) with the P301S mutation were purchased from ATCC (CRL-3275). Cells were plated at 1.25 X 10^5 cells/mL in 500 uL of DMEM supplemented with 10% FBS and 0.2% penicillin-streptomycin on poly-D-lysine coated glass coverslips for immunofluorescence and microscopy, or directly in a 24-well cell culture treated plate (Corning 2536) for flow cytometry. Cells were allowed to grow overnight at 37 ºC and 5% CO_2. The next day, plasmids were transfected using lipofectamine 3000 following manufacturers protocol. For cells expressing Halo tagged constructs, Janelia Fluor 646 (Promega) was added for downstream imaging, or TMRDirect Ligand (Promega) was added for downstream flow cytometry. The next day, cells were transfected with lipofectamine 3000 with 0.25 uL of 1 mg/mL clarified brain homogenate from Tg2541 mice per well. 24 hours later, cells were either fixed for immunofluorescence and imaging or were processed for flow cytometry (see below).

Clarification of brain homogenate for tau aggregate seeding in HEK293T tau biosensor cells

As previously described(Lester et al. 2021), 10% brain homogenate from Tg2541 mice was centrifuged at 500 x g for 5 minutes. The supernatant was collected and centrifuged again at 1000 x g for 5 minutes. The supernatant was collected, protein concentration determined with a bicinchoninic acid assay (BCA) and diluted with PBS to 1 mg/mL. Aliquots were stored at -80C for downstream transfection.

Generation of cell lines

For production of mRuby-G3BP1-polyserine$_{42}$ expressing HEK293T tau biosensor lines, construct encoding mRuby-G3BP1-polyserine$_{42}$ was cloned into a pLenti EF1 vector. Wildtype HEK293T cells were transfected using Lipofectamine 3000 with pLenti plasmids and lentiviral packaging plasmids (Gag-pol (Addgene #14887), VSV-G (Addgene #8454), rSV-REV (Addgene #12253). Lentivirus was collected 48 hours later and was added to HEK293T tau biosensor cells described previously(Holmes et al. 2014). Transduced cells were selected with blasticidin (2 µg/mL).

Immunofluorescence and Fixed Cell Imaging

As described above, cells plated and prepared on poly-D-lysine coated coverslips were fixed with 4% paraformaldehyde for 15 minutes. Cells were washed once with 1xPBS, permeabilized with 0.5% TritonX for 10 minutes, washed three times with 1x PBS, and blocked with 5% BSA in PBS for 1 hour at room temperature. Primary antibodies were added in blocking buffer for two hours at room temperature (Rabbit anti-PolyA Binding Protein (abcam 21060 1:500 in TBS-T)). Cells were washed three times with 1x PBS. Secondary antibody (Anti-Rabbit-AlexaFluor 549 (abcam150092 1:1000 in TBS-T)) solution in blocking buffer with 1x DAPI was added to cells for 1 hour. Cells were washed three times with 1x PBS and mounted using ProLong Glass Antifade Mountant.

For monitoring enrichment of stress granules with tau aggregates, cells were plated as described above. Twenty-four hours after plating, cells were transfected with tau brain homogenate (described above) and seven hours later treated with 50 nM PatA. Twelve hours later, cells were fixed and mounted as described above.

For monitoring enrichment of polyserine and polyserine variants with tau aggregates, cells were plated as described above. Twenty-four hours after plating, cells were transfected with plasmids encoding Halo tagged constructs alongside JF646 Halo-ligand (Promega). Twenty-four hours after transfection, tau aggregates were induced as described above. Twenty-four hours after tau brain homogenate transfection, cells were fixed and mounted as described above.

Live Cell Imaging

For analysis of tau aggregation in the context of stress granules with and without polyserine, cells were plated on 24 well poly-D-lysine glass bottom plates with #1.5 cover glass at 0.2 x 10^6 cells/mL. Cells were allowed to grow overnight at 37 ºC and 5% CO_2. Tau aggregation was induced 24 hours later with brain homogenate from Tg2541 mice as described above, seven hours later, stress granules were induced with 50 nM PatA and nuclei were stained with Hoechst. Images were collected every 10 minutes for 16 hours.

For live cell imaging of tau seeds, cells were plated as described above. For localization with SRRM2 or PNN, JF549 was added alongside initial plating. Cells were allowed to grow overnight at 37 ºC and 5% CO_2. Fluorescent tau fibers were prepared (see below) pelleted and 100K x g for 30 minutes, washed once in 1xPBS, pelleted again at 100K x g for 30 minutes and resuspended in 1xPBS. Tau fiber pellets were then sonicated just prior to transfection (performed identically to transfection of tau brain homogenate from Tg2541 mice). For localization to stress granules, cells were treated with 50 nM PatA 7 hours after tau fiber transfection alongside nuclei staining with Hoechst just prior to imaging. For localization to SRRM2 or PNN assemblies, tau fiber transfection occurred alongside nuclei staining with Hoechst just prior to imaging. Images were collected every 10 minutes for 16 hours.

Cloning of polyserine expression plasmids

To express polyserine variants in HEK293T tau biosensor cells(Holmes et al. 2014) custom gBlocks were ordered from Twist Bioscience and cloned into pCDNA3.1-Halo plasmids under a CMV promoter using In-Fusion cloning. Bacterial expression plasmids were produced using custom gBlocks ordered from Twist Bioscience or IDT which were cloned into pET28 vectors using In-Fusion cloning.

Protein expression and purification

pET28 plasmids expressing SUMO-Polyserine$_{42}$-Halo, SUMO-Halo, SUMO-Polyserine$_{42}$-Cys, SUMO-Cys, and pET29 2N4R P301S single cysteine (See Fig 3A) were transformed into Rosetta2(DE3)pLysS *E. coli* and grown in LB media supplemented with kanamycin and chloramphenicol. One liter LB cultures were inoculated with overnight cultures, incubated with shaking at 37 ºC until O.D$_{600}$ >= 0.4, and protein expression was induced with 0.2 mM IPTG (polyserine constructs), or 0.5 mM IPTG (Halo and SUMO-Cys constructs), or 0.4 mM IPTG (tau constructs) for 4 hours at 37°C. Bacteria was pelleted and stored at -80 ºC.

All SUMO tagged constructs were purified using Ni-NTA columns. Cell pellets were resuspended in Lysis Buffer (50 mM MOPS pH 7.0, 300 mM NaCl, 30 mM imidazole, 1 mM DTT, supplemented with Ultra EDTA-free protease inhibitors and 0.1 mM AEBSF) and lysed with sonication. Cell lysate was clarified with centrifugation and filtered through a 0.2 µm pore filter. For downstream imaging with halo-ligands, JF594 or JF646 was added to clarified lysate and nutated at room temperature for 30 minutes. Labeled protein lysate was added to equilibrated Ni-NTA, washed with 5 column volumes (CV) of lysis buffer, 10 CV of lysis buffer with 500 mM NaCl, and finally 10 CV of lysis buffer with 1M NaCl. Six CV of Elution buffer (50 mM MOPS pH 7.0, 200

mM NaCl, 300 mM imidazole, 1 mM DTT, supplemented with Ultra EDTA-free protease inhibitor (Sigma) and 0.1 mM AEBSF) was added and incubated with resin for 30 minutes. Elution buffer was collected and concentrated before overnight dialysis into storage buffer (50 mM MOPS pH 7.0, 100 mM NaCl, 1 mM DTT). For maleimide labeling, proteins were purified as described above, but with 1 mM TCEP instead of DTT in all buffers. For maleimide labeling, concentrated, purified protein was incubated with 3 molar excess of maleimide dye for 2 hours at room temperature. Excess dye was removed with overnight dialysis into storage buffer as described above.

Full length tau constructs were purified over three columns, Ni-NTA, SP cation exchange, and S200 size exclusion. Clarified cell lysates were prepared as described above in Tau Lysis Buffer (50 mM Tris pH 7.4, 300 mM NaCl, 30 mM imidazole, 1 mM DTT, supplemented with Ultra EDTA-free protease inhibitor (Sigma)). Lysate was added to equilibrated Ni-NTA, washed with 5 CV of Tau Lysis Buffer, 10 CV Tau wash buffer supplemented with 500 mM NaCl, 10 CV Tau wash buffer with 1 M NaCl, and eluted in Tau elution buffer (50 mM Tris pH 7.4, 100 mM NaCl, 300 mM imidazole, 1 mM DTT). Eluted protein was dialyzed overnight into Buffer A (50 mM MES pH 6.00, 150 mM NaCl, 1 mM DTT). Protein was loaded into a superloop on an AKTA Pure 25 M and passed through a pre-equilibrated SP cation exchange column. Protein was eluted with a gradient of Buffer B (Buffer A with 1 M NaCl) and fractions collected. Protein containing fractions were pooled, concentrated to 1 mL and loaded onto an S200 size exclusion column. Protein was eluted in storage buffer (1x PBS pH 7.4, 1 mM TCEP (for maleimide labeling) or 1 mM DTT (for fibrilization reactions). Protein containing fractions were pooled and concentrated to 50 μM and stored at 4 ºC.

Microscopy Colocalization

Colocalization assays were performed in 1xPBS with 3 μM polyserine or halo proteins and 5 μM of experimental proteins. Protein mixture was brought up to 50 μL in Bio-One CELLview slides (Greiner) and immediately imaged. Imaging was performed on a Nikon spinning disk confocal microscope at 60x magnification.

In vitro polyserine assembly

To assess assembly formation, 20 μM purified SUMO-Halo and SUMO-polyserine$_{42}$-Halo were incubated with TEV for 24 hours at room temperature in storage buffer. Reactions were either subjected to ultracentrifugation for dot blots, or microscopic examination. For ultracentrifugation analysis, reactions were pelleted at 100K x g for 1 hour, supernatant kept, and pellet washed with dialysis buffer, and pelleted again at 100K x g for 30 minutes. 1 μL of total, supernatant, and pellet fractions were spotted onto nitrocellulose and blotted with anti-HaloTag pAb (Promega). For microscopic examination, reactions were transferred to Bio-One CELLview slides (Greiner) and imaged at 60x magnification on a Nikon spinning disk confocal microscope.

Preparation of Recombinant Tau Fibers

Tau fibers were prepared using JF646-maleimide labeled tau monomers purified and stored in TCEP as described above. For fibrilization, 5 μM tau monomers were incubated with 40 ng polyU RNA in 1xPBS pH 7.4 and freshly prepared 1 mM DTT for 24 hours with shaking at 37 ºC. Reactions were done in separate 50 μL reactions and pooled after incubation. Tau fibers were separated from soluble tau species via ultracentrifugation. Pooled tau fiber reactions were centrifuged at 100K xg for 30 minutes, the supernatant removed, and the pellet resuspended in equal volumes of 1x PBS pH 7.4. The resuspended pellet was centrifuged at 100K xg for 30

minutes, the supernatant removed, and the pellet resuspended in 1x PBS pH 7.4. The resuspended pellet was sonicated and immediately used in downstream experiments.

Preparation of Fluorescent RNA

Fluorescent polyU RNA homopolymers were prepared using poly-uridylic acid (Millipore Sigma) and the Label IT® Nucleic Acid Fluorescein Labeling Kit (Mirus Bio) according to manufacturers protocol. Fluorescent RNA was labeled on the day of recombinant tau fiber reactions.

Thioflavin-T kinetics assays

To assess fibrilization kinetics, 5 μM unlabeled 2N4R tau purified and stored in 1 mM DTT was mixed with 40 ng polyU RNA, 3 μM SUMO-polyserine$_{42}$-Halo or SUMO-Halo, and 20 μM thioflavin T in 1x PBS pH 7.4 supplemented with freshly prepared 1 mM DTT. Reactions were prepared in 175 uL master mix and 50 μl was aliquoted into three wells of a 96 well #1.5 cover glass bottom plate (Greiner). Negative controls without tau, with and without RNA, and with and without additional proteins were also prepared in triplicate. Thioflavin T fluorescence was measured every 5 minutes for 24 hours on a BMG CLARIOstar plate reader using 446 nm excitation and 482 nm emission, incubating at 37°C and shaking at 300 RPM for 30 seconds prior to each measurement. The linear ranges of the produced curves were extracted, and a line was fitted to determine the slope (rate of fiber growth) and X-intercept (lag time).

Immunogold labeling and TEM

For TEM, tau fibers were made by incubating 5 μM monomeric 2N4R P301S Tau, 40 ng PolyU RNA, 1 mM DTT, with and without 3 μM SUMO-polyserine$_{42}$-Halo or SUMO-Halo, in 1x PBS pH 7.4 for 24 hours at 37°C while shaking at 300 RPM. Tau fibrilization samples were diluted 1:5 and 5 μl of each were adsorbed on a carbon-coated copper grids (300 mesh, Electron Microscopy Sciences) for 1 min. Excess sample was wicked off and grids were incubated with 5 μl 2% uranyl-acetate (UA) for 30 seconds. Excess UA was wicked off and grids were allowed to dry.

For immunogold labeling, 10 μl of diluted tau fibrilization samples (See above) were adsorbed on carbon-coated nickel grids (300 mesh, Electron Microscopy Sciences) for 10 minutes. Excess fibrils were removed by placing the grids on three successive drops of fresh 1x PBS without drying. Grids were blocked in 1% BSA in PBS for 60 min and subsequently incubated with primary anti-Halo antibody (anti-HaloTag pAb (Promega)) diluted 1:100 in 1% BSA in PBS) for 60 min. The grids were washed on five successive drops of fresh 1x PBS without drying and incubated with gold-labeled secondary antibody (10 nm-Gold goat anti-rabbit IGG (Ted Pella) diluted 1:50 in 1% BSA) for 60 min. Grids were washed again on five successive drops of fresh 1x PBS and samples were negatively stained by incubating in 5 μl 2% UA for 30 seconds. TEM was performed with a FEI Tecnai T12 spirit equipped with an AMT CCD camera.

SDS-PAGE and Western Blotting

For analysis of proper expression of mRuby-G3BP1 and mRuby-G3BP1-Polyserine$_{42}$, cells were grown in 6 well plates to 80% confluence. Cells were harvested in 1x PBS and pelleted at 300 xg for 8 minutes. The cell pellet was resuspended in lysis buffer (10 mM Tris pH 7.4, 2.5

mM $MgCl_2$, 100 mM NaCl supplemented with PhosStop (Sigma) and Ultra Complete Protease Inhibitor (Sigma)). Cells were lysed via pipetting through a 26g needle 10 times. Lysate was clarified via centrifugation at 10K xg for 15 minutes at 4 ºC. Supernatant was collected and stored at -80.

Cell lysate protein concentration was measured with Bradford assay and normalized to the lowest protein concentration. Lysate mixed with 4X SDS-Loading dye and boiled for 5 minutes prior to loading on a NuPAGE 4-12% Bis-Tris mini gel (Invitrogen). Protein was transferred to nitrocellulose membrane which was then blocked with 5% BSA in TBS-T. The blocked membrane was incubated with primary antibody solution diluted in 5% BSA in TBS-T overnight at room temperature, washed 3 times with TBS-T, and incubated with secondary antibody solution for one hour followed by 3 washes with TBS-T. Blot was developed with Clarity Western ECL Substrate (BioRad).

Flow Cytometry

Flow cytometry was used to determine the fraction of cells with tau aggregates as described previously(Lester et al. 2023). Briefly, HEK293T tau biosensor cells(Holmes et al. 2014) were plated at 0.125 x 10^6 cells/mL in 500 µL in a 24 well plate. For halo expression, 24 hours after plating, plasmids expressing halo tagged constructs were transfected with lipofectamine 3000 following manufacturers protocol. At the time of transfection, 200 nM of TMRDirect halo-ligand was added. Twenty-four hours after transfection, tau aggregates were induced as described above using 0.5 ng/µL of tau brain homogenate. Twenty-four hours after transfection of tau brain homogenate, cells were trypsinized, washed with PBS and filtered with 50 µm nylon mesh filters prior to analysis. Sorting was performed on BD FACSCelesta™ Cell Analyzer with the following filter sets: 561-585 (Halo expression), 405-450 (CFP), and 405-525 (FRET). Analysis

was performed using FlowJo. Gating was performed sequentially, first gating for cells, single cells, then Halo expression for top 10% expressing cells, and finally, gated for FRET+ cells. The FRET+ gate was set using a mock transfected well with 1% as previously detailed(Holmes et al. 2014). The integrated FRET density was determined as a product of the median FRET intensity and the percentage of FRET+ cells.

For analysis of expression of G3BP1 and G3BP1-Polyserine$_{42}$ with and without stress, cells were plated at the same density. Cells were transfected with tau brain homogenate 24 hours after plating as described above. Seven hours after transfection of tau brain homogenate, cells were treated with 50 nM PatA. Twelve hours after PatA treatment, cells were then processed and analyzed as described above.

Quantification and statistical analysis

Information on statistical analysis and software used can be found in this section and in the Key resources table. Statistical details of expriments are included in the figure captions (including statistical tests used, value of n, what n represents). All error bars reported are SEM. All statistical analyses were performed using GraphPad-Prism 10.

Image Analysis

All image analysis was performed with Cell Profiler version 4.2.8.

To measure the fraction of cells with mRuby or Halo positive assemblies, as well as the enrichment of mRuby or Halo fluorescence in tau aggregates, the same pipeline was used. Briefly, cell nuclei and cytoplasm were segmented and filtered for Halo or mRuby expressing cells. This

population of cells was then further filtered for cells with and without tau aggregates, or with and without mRuby or Halo assemblies. For enrichment of Halo or mRuby, the mean intensity was determined inside tau aggregates, and from the remainder of the cytoplasm on a single cell basis. Enrichment was determined as the mean intensity of Halo or mRuby inside tau aggregates divided by the mean intensity of Halo or mRuby in the remainder of the cytoplasm.

To determine the enrichment of proteins in polyserine assemblies, fields of view were segmented for polyserine assemblies, these assemblies were then merged as one object per field of view. The mean intensity of the additional proteins was then measured in and outside polyserine assemblies, and enrichment was determined with the same method described above. This pipeline was also used to measure the area of polyserine assemblies on a per assembly basis.

CHAPTER III

Could SARS-CoV-2 Cause Tauopathy?

This section is adapted from **Could SARS-CoV-2 Cause Tauopathy?** Authored by James Pratt, Evan Lester, and Roy Parker, published in *The Lancet Neurology* in 2021 (PMID: 34146504) (Pratt et al. 2021).

SUMMARY

The ongoing COVID-19 pandemic has unexpected consequences. We consider the possibility that a fraction of COVID-19 infected individuals will develop a neurodegenerative disease and associated aggregation of tau protein, referred to as a tauopathy, as a consequence of SARS-CoV-2 infection. This hypothesis is based on the observations that some COVID-19 infected individuals have neurological effects including neuroinflammation, that neuroinflammation can promote tauopathy, and that other infectious diseases can trigger tauopathies in a subset of infected individuals.

At the time of this publication, Sars-CoV-2 has infected 124 million people globally and continues to spread worldwide. Although SARS-CoV-2 is classified as a respiratory virus, some infected individuals show neurological symptoms. Recently, a large cohort study on neurologic sequelae of COVID-19 found that 33.62% of COVID-19 patients received a psychiatric or neurological diagnosis within sixth months of COVID-19 infection (Zubair et al. 2020). Some of these diagnoses are indicative of acute and sub-acute changes to the central nervous system (CNS). While we do not yet know the long-term consequences of these changes, viral infection in a subset of patients may promote chronic neuroinflammation and, over a period of years, lead to tau aggregation and neurodegeneration.

Tauopathies are a large class of neurodegenerative disease (encompassing more than 20 different diseases) and are characterized by their shared deposition of insoluble, aggregated tau in neurons and occasionally glial cells. Tauopathies are classified as either primary tauopathies, in which tau is thought to be the driver of disease, or secondary tauopathies, in which tau aggregation is downstream of another insult. Secondary tauopathies can have far ranging causes from extracellular accumulation of **β**-amyloid in Alzheimer's disease to repetitive head trauma in chronic traumatic encephalopathy. While the exact mechanism for how these diverse insults lead to tau aggregation and neurodegeneration is still poorly understood, many of these secondary tauopathies share an association with neuroinflammation (Heneka et al. 2020). In particular, activation of the NLRP3 inflammasome can promote tau hyperphosphorylation and tau neurofibrillary tangle (NFT) formation (Heneka et al. 2020). NLRP3 activation in microglia induces tau mis-localization to the soma in neighboring neurons and is an early sign of Alzheimer's Disease (Heneka et al. 2020). The association between neuroinflammation and tauopathies raises the possibility that neuroinflammation, and activation of the NLRP3 inflammasome, triggered during some COVID infections may promote downstream tau aggregation and neurodegeneration.

Evidence suggests that SARS-CoV-2 can impact the central nervous system (CNS) in at least two manners (Fig. 1). First, SARS-CoV-2 viruses may be able to cross the blood brain barrier (BBB) and directly infect neurons and/or the surrounding vasculature. This CNS infection could be through infection of the vascular endothelium, invasion via olfactory nerve, or leukocyte migration across the BBB (Zubair et al. 2020). Additionally, SARS-CoV-2 has been identified in brain microvascular endothelial cells, which indicates possible disruption of the BBB and supporting vasculature (Zubair et al. 2020). Once inside cells, SARS-CoV-2 can directly activate the NLRP3 inflammasome (via ORF3a protein) (Heneka et al. 2020) and induce tau mis-localization (Ramani et al. 2020). Additionally, increased tau concentration in the cerebrospinal fluid (CSF) has been observed following SARS-CoV-2 induced encephalopathy (Virhammar et al. 2021).

A second possible way for SARS-CoV-2 to impact the CNS is through inducing a widespread systemic inflammatory response that can trigger neuroinflammation. For example, cytokines released in systemic inflammation activate neuroinflammatory glial cells through multiple mechanisms, including disruption of the BBB (Sisniega and Reynolds 2021). The increase in cytokine levels during SARS-CoV-2 infection, including IL-18 and IL-1$\boldsymbol{\beta}$, can also lead to activation of the NLRP3 inflammasome (Heneka et al. 2020).

While no specific virus directly causes tauopathy, it is likely that accumulated exposures to pathogens that contribute to neuroinflammation may increase risk of tauopathy development over time. For example, two tauopathies, subacute sclerosing panencephalitis (SSPE) and postencephalitic parkinsonism (PEP), have been suggested to be triggered by viral infections (Garg et al. 2019; Buée-Scherrer et al. 1997) (Figure 3.1).

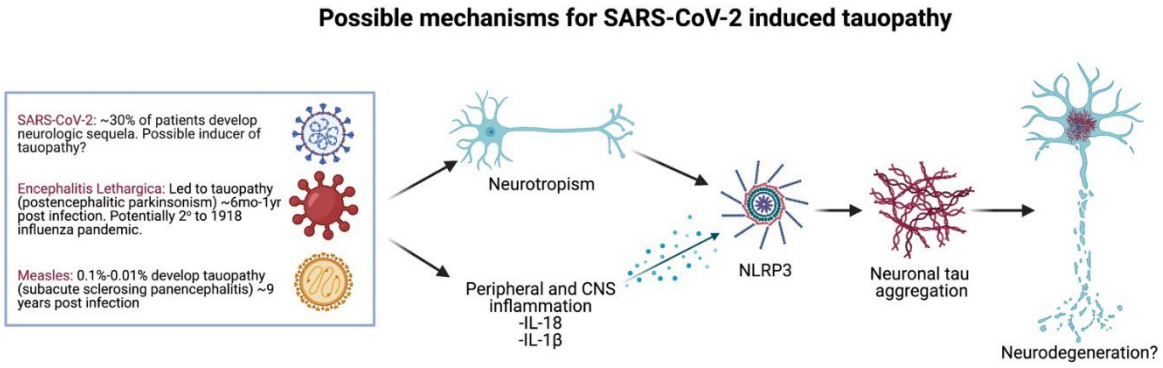

Figure 3.1: Possible Mechanisms for SARS-CoV-2 Induced Tauopathy Previous viral pandemics have shown different mechanisms for viral induced tauopathy. Encephalitis Lethargica, following the 1918 influenza pandemic, or Subacute Sclerosing Panencephalitis, a sequelae to Measels, are both tauopathies. From these viruses, we can infer than severe infection with SARS-CoV-2 can lead to peripheral or central nervous system infection leading to increased secretion of pro-inflammatory cytokines. Alternatively, SARS-CoV-2 can infect neurons directly, both resulting in NLRP3 inflammasome activation and tau aggregation. This tau aggregation may then lead to neurodegeneration.

SSPE and PEP share hallmarks of hyperphosphorylated tau, NFT formation, and neurodegeneration (Garg et al. 2019; Buée-Scherrer et al. 1997). In the case of SSPE, a slow acting mutant measles virus enters the CNS, and in some cases is observed in neurons and glial cells that contain tau NFTs (Garg et al. 2019). The virus that induced PEP has not been determined however PEP is thought to be a long-term sequela to the viral encephalitis lethargica (EL) pandemic between 1917-1928 (Buée-Scherrer et al. 1997). Both SSPE and PEP had delayed onsets compared to their respective associated viral infection. SSPE on average is diagnosed ~9.7 years post measles onset, while PEP onset was generally 1-5 years after acute phase EL (Hoffman and Vilensky 2017) If COVID-19 infection leads to tauopathy in a similar manner as PEP and SSPE, one anticipates onset from 1 to 10 years post COVID-19 infection.

If COVID-19 can promote tauopathy, it would be expected to only be in a small fraction of the large number of individuals infected with SARS-CoV-2. For comparison, only 0.01-0.1% of measles infections lead to SSPE (Garg et al. 2019). If a COVID-19 induced tauopathy develops

at a similar rate as SSPE, one anticipates ~10,000-100,000 cases of COVID-19 induced tauopathy for every 100 million SARS-CoV-2 infected individuals (a rough estimate of cumulative infections in the United States to date). Uncertainty is increased here as the fraction of SARS-CoV-2 infected individuals with substantial neuroinflammation, and therefore potentially at higher risk for secondary tauopathy, is unknown. It is also important to note that no direct causal link between COVID-19 and later neurologic or psychiatric complications has been determined, and some complications, including anxiety disorders, may be due to the stress and trauma that are a result of social factors like isolation and current treatment options such as intubation (Zubair et al. 2020).

The potential of a COVID induced tauopathy suggests possible actions. First, it would be of interest to perform long term studies, or monitor centralized health records, for increases in early onset neurological dysfunction in COVID survivors, particularly those who showed acute or sub-acute neurological symptoms. Such studies should persist for at least decade given the average time for SSPE onset is ~9.7 years and focus on relatively young individuals (30-40 years old) to reduce the fraction of individuals that will develop typical age related tauopathies. Second, it would be of interest to examine COVID survivors for abnormal tau modifications, as can be assessed in blood or CSF tests, or tau aggregation, which can be examined experimentally using tau targeting PET tracers. While further research into the long-term effects of SARS-CoV-2 infection is required, it is worth considering the possibility that, in some individuals, COVID-19 may induce tauopathy in the next decade.

CHAPTER IV

Discussion and Future Directions

Herein we reviewed tauopathies, tau misfolding and aggregation, how intracellular interaction with polyserine-containing assemblies exacerbates tau aggregation in cells, and finally, how the SARS-CoV-2 pandemic may result in increased diagnoses of tauopathies through neuroinflammation. This work presents two major themes. The first is the formation of cytoplasmic polyserine-containing assemblies exacerbate tau aggregation through direct interactions. The second, is that neuroinflammation, triggered through viral infection, may increase tau aggregation. Understanding the order of events in cytoplasmic speckle formation, neuroinflammation and tau aggregation, is imperative towards understanding the pathways for developing tau pathology.

The mechanism of SRRM2 mislocalization into cytoplasmic assemblies, which act as preferred sites of tau aggregation, is unknown. There are at least two possible mechanisms for SRRM2 mislocalization. The first is that intracellular stresses, including tau oligomerization, results in nuclear envelope disruption and subsequent nuclear speckle protein mislocalization. Alternatively, the neuronal microenvironment, or the complex mixture of glial cell types, protein aggregates such as amyloid-β plaques, and/or pro-inflammatory signals, such as prostaglandins or cytokines, converge on neurons to trigger SRRM2 mislocalization through intercellular signaling cascades.

Nuclear speckle protein mislocalization may be driven by nuclear envelope disruption. In the simplest experiment, knockdown of NUP153, BANF1, or ANKLE2, proteins involved in nuclear envelope integrity and assembly, results in SRRM2 positive cytoplasmic assemblies (Berchtold et al. 2018; Prissette et al. 2022). Additionally, tau oligomers have been observed to disrupt the nuclear envelope via direct binding to nuclear lamin (Jiang and Wolozin 2021), or disruption of nuclear pores (Sun et al. 2024).

SRRM2 mislocalization may be driven by extracellular or intercellular triggers. Several lines of evidence support this model. First, SRRM2 localizes to the cytoplasm in 5xFAD mice before amyloid-β plaque formation via signaling through ERK (Tanaka et al. 2018). Second, the pro-inflammatory chemokine CCL3, secreted from activated microglia, stimulates neurodegeneration through CCR5 mediated inhibition of autophagy, exacerbating tau pathology *in vivo* (Festa et al. 2023). Additionally, CCR5 activation with CCL3 results in increased ERK signaling *in vitro* (Kodama et al. 2020), which may cause increased cytoplasmic SRRM2.

With these two models in mind, it is important to understand the cause or consequence relationship between cytoplasmic SRRM2 assemblies and tau aggregation. First, we must understand if neuroinflammation triggers SRRM2 mislocalization independent of tau oligomerization and aggregation, as this may be a key step in *de novo* tau aggregation. Next, understanding if seeding competent tau species are sufficient to induce nuclear envelope disruption and mislocalization of SRRM2 or PNN into CSs will provide insight into specific toxicities of tau.

We posited early that SARS-CoV-2 infection may result in the development of a secondary tauopathy. As we have progressed through the pandemic, the development of Long COVID in a subset of patients has become a growing problem. New research in the last few years has provided insight into how SARS-CoV-2 contributes to the development of tau pathology and neurodegeneration, which may underpin Long COVID. Cognitive impairment in patients with severe COVID-19 correlated with increased activation of signaling cascades upregulated in AD (Reiken et al. 2022). Activation of these signaling cascades from SARS-CoV-2 infection results in increased hyperphosphorylated tau *in vitro* (Di Primio et al. 2023). Increased phosphorylated tau has been observed in patients that have recovered from acute SARS-CoV-2 infection, correlating with prolonged activation of microglia and neuroinflammation in the hippocampus in the absence of direct viral infection (Qi et al. 2024). Finally, patients that developed severe COVID-19 show

increased levels of phosphorylated tau in the blood, a biomarker of neurodegeneration (Jaiswal et al. 2025). While the exact impact of COVID-19 on tau aggregation is unknown, there is a clear link between severe infection and development of tau pathology.

As our population grows older on average, and we learn more about the impact of the SARS-CoV-2 pandemic, the diagnosis and development of tauopathies and other neurodegenerative diseases will continue to increase. Therefore, it is even more paramount that we understand the mechanisms of *de novo* tau aggregation, pathological spread, and gain of function toxicities of tau in disease. This work provides insight into a new mechanism of *de novo* tau aggregation, and further work understanding the cause and consequence of nuclear speckle protein mislocalization in disease may create a new target for treatment of tauopathies.

BIBLIOGRAPHY

Abreha MH, Dammer EB, Ping L, Zhang T, Duong DM, Gearing M, Lah JJ, Levey AI, Seyfried NT. 2018. Quantitative Analysis of the Brain Ubiquitylome in Alzheimer's Disease. *Proteomics* **18**: e1800108. https://www.ncbi.nlm.nih.gov/pmc/articles/PMC6283072/ (Accessed November 30, 2024).

Alberti S, Dormann D. 2019. Liquid–Liquid Phase Separation in Disease. *Annu Rev Genet* **53**: 171–194.

Alosco ML, Mian AZ, Buch K, Farris CW, Uretsky M, Tripodis Y, Baucom Z, Martin B, Palmisano J, Puzo C, et al. 2021. Structural MRI profiles and tau correlates of atrophy in autopsy-confirmed CTE. *Alzheimers Res Ther* **13**: 193.

Alquezar C, Arya S, Kao AW. 2021. Tau Post-translational Modifications: Dynamic Transformers of Tau Function, Degradation, and Aggregation. *Front Neurol* **11**. https://www.frontiersin.org/journals/neurology/articles/10.3389/fneur.2020.595532/full (Accessed July 14, 2024).

Andreadis A, Brown WM, Kosik KS. 1992. Structure and Novel Exons of the Human Tau Gene. *Biochemistry* 10626–10633.

Andronesi OC, Bergen M von, Biernat J, Seidel K, Griesinger C, Mandelkow E, Baldus M. 2008. Characterization of Alzheimer's-like Paired Helical Filaments from the Core Domain of Tau Protein Using Solid-State NMR Spectroscopy. *J Am Chem Soc* **130**: 5922–5928.

Apicco DJ, Ash PEA, Maziuk B, LeBlang C, Medalla M, Al Abdullatif A, Ferragud A, Botelho E, Ballance HI, Dhawan U, et al. 2018. Reducing the RNA binding protein TIA1 protects against tau-mediated neurodegeneration in vivo. *Nat Neurosci* **21**: 72–80.

Aronov S, Aranda G, Behar L, Ginzburg I. 2002. Visualization of translated tau protein in the axons of neuronal P19 cells and characterization of tau RNP granules. *J Cell Sci* **115**: 3817–3827.

Asada-Utsugi M, Uemura K, Ayaki T, T. Uemura M, Minamiyama S, Hikiami R, Morimura T, Shodai A, Ueki T, Takahashi R, et al. 2022. Failure of DNA double-strand break repair by tau mediates Alzheimer's disease pathology in vitro. *Commun Biol* **5**: 1–12.

Ash PEA, Lei S, Shattuck J, Boudeau S, Carlomagno Y, Medalla M, Mashimo BL, Socorro G, Al-Mohanna LFA, Jiang L, et al. 2021. TIA1 potentiates tau phase separation and promotes generation of toxic oligomeric tau. *Proc Natl Acad Sci* **118**. https://www.pnas.org/content/118/9/e2014188118 (Accessed March 26, 2021).

Aulas A, Fay MM, Lyons SM, Achorn CA, Kedersha N, Anderson P, Ivanov P. 2017. Stress-specific differences in assembly and composition of stress granules and related foci. *J Cell Sci* **130**: 927–937.

Ayhan F, Perez BA, Shorrock HK, Zu T, Banez-Coronel M, Reid T, Furuya H, Clark HB, Troncoso JC, Ross CA, et al. 2018. SCA8 RAN polySer protein preferentially accumulates in white matter regions and is regulated by eIF3F. *EMBO J* **37**: e99023.

Bai B, Hales CM, Chen P-C, Gozal Y, Dammer EB, Fritz JJ, Wang X, Xia Q, Duong DM, Street C, et al. 2013. U1 small nuclear ribonucleoprotein complex and RNA splicing alterations in Alzheimer's disease. *Proc Natl Acad Sci U S A* **110**: 16562–16567.

Bancher C, Leitner H, Jellinger K, Eder H, Setinek U, Fischer P, Wegiel J, Wisniewski HM. 1996. On the relationship between measles virus and Alzheimer neurofibrillary tangles in subacute sclerosing panencephalitis. *Neurobiol Aging* **17**: 527–533.

Bentmann E, Neumann M, Tahirovic S, Rodde R, Dormann D, Haass C. 2012. Requirements for Stress Granule Recruitment of Fused in Sarcoma (FUS) and TAR DNA-binding Protein of 43 kDa (TDP-43) *. *J Biol Chem* **287**: 23079–23094.

Berchtold D, Battich N, Pelkmans L. 2018. A Systems-Level Study Reveals Regulators of Membrane-less Organelles in Human Cells. *Mol Cell* **72**: 1035-1049.e5.

Binder LI, Frankfurter A, Rebhun LI. 1985. The distribution of tau in the mammalian central nervous system. *J Cell Biol* **101**: 1371–1378.

Bird TD, Nochlin D, Poorkaj P, Cherrier M, Kaye J, Payami H, Peskind E, Lampe TH, Nemens E, Boyer PJ, et al. 1999. A clinical pathological comparison of three families with frontotemporal dementia and identical mutations in the tau gene (P301L). *Brain J Neurol* **122 (Pt 4)**: 741–756.

Biswas S, Kalil K. 2018. The Microtubule-Associated Protein Tau Mediates the Organization of Microtubules and Their Dynamic Exploration of Actin-Rich Lamellipodia and Filopodia of Cortical Growth Cones. *J Neurosci* **38**: 291–307.

Bloom GS. 2014. Amyloid-β and tau: the trigger and bullet in Alzheimer disease pathogenesis. *JAMA Neurol* **71**: 505–508.

Boscher E, Hernandez-Rapp J, Petry S, Keraudren R, Rainone S, Loiselle A, Goupil C, Turgeon A, St-Amour I, Planel E, et al. 2020. Advances and Challenges in Understanding MicroRNA Function in Tauopathies: A Case Study of miR-132/212. *Front Neurol* **11**: 578720.

Bou Samra E, Buhagiar-Labarchède G, Machon C, Guitton J, Onclercq-Delic R, Green MR, Alibert O, Gazin C, Veaute X, Amor-Guéret M. 2017. A role for Tau protein in maintaining ribosomal DNA stability and cytidine deaminase-deficient cell survival. *Nat Commun* **8**: 693.

Boyko S, Surewicz WK. 2023. Domain-specific modulatory effects of phosphomimetic substitutions on liquid-liquid phase separation of tau protein. *J Biol Chem* **299**. https://www.jbc.org/article/S0021-9258(23)01750-7/abstract (Accessed November 23, 2024).

Braak E, Braak H, Mandelkow EM. 1994. A sequence of cytoskeleton changes related to the formation of neurofibrillary tangles and neuropil threads. *Acta Neuropathol (Berl)* **87**: 554–567.

Brion JP, Couck AM, Passareiro E, Flament-Durand J. 1985a. Neurofibrillary tangles of Alzheimer's disease: an immunohistochemical study. *J Submicrosc Cytol* **17**: 89–96.

Brion J-P, Passareiro H, Nunez J, Flament-Durand J. 1985b. Mise en évidence immunologique de la protéine tau au niveau des lésions de dégénérescence neurofibrillaire de la maladie d'Alzheimer. Arch Biol. *ArchBiol(Brux)* **95**: 229–235.

Brunello CA, Yan X, Huttunen HJ. 2016. Internalized Tau sensitizes cells to stress by promoting formation and stability of stress granules. *Sci Rep* **6**: 30498.

Buchholz S, Zempel H. 2024. The six brain-specific TAU isoforms and their role in Alzheimer's disease and related neurodegenerative dementia syndromes. *Alzheimers Dement* **20**: 3606–3628. https://onlinelibrary.wiley.com/doi/abs/10.1002/alz.13784 (Accessed February 11, 2025).

Buée-Scherrer V, Buée L, Leveugle B, Perl DP, Vermersch P, Hof PR, Delacourte A. 1997. Pathological tau proteins in postencephalitic parkinsonism: comparison with Alzheimer's disease and other neurodegenerative disorders. *Ann Neurol* **42**: 356–359.

Bugiani O, Murrell JR, Giaccone G, Hasegawa M, Ghigo G, Tabaton M, Morbin M, Primavera A, Carella F, Solaro C, et al. 1999. Frontotemporal dementia and corticobasal degeneration in a family with a P301S mutation in tau. *J Neuropathol Exp Neurol* **58**: 667–677.

Carlomagno Y, Chung D-EC, Yue M, Castanedes-Casey M, Madden BJ, Dunmore J, Tong J, DeTure M, Dickson DW, Petrucelli L, et al. 2017. An acetylation-phosphorylation switch that regulates tau aggregation propensity and function. *J Biol Chem* **292**: 15277–15286.

Castro-Alvarez JF, Uribe-Arias SA, Kosik KS, Cardona-Gómez GP. 2014. Long- and short-term CDK5 knockdown prevents spatial memory dysfunction and tau pathology of triple transgenic Alzheimer's mice. *Front Aging Neurosci* **6**.

Chaudhary AR, Berger F, Berger CL, Hendricks AG. 2018. Tau directs intracellular trafficking by regulating the forces exerted by kinesin and dynein teams. *Traffic* **19**: 111–121.

Chen C, Jin N, Qian W, Liu W, Tan X, Ding F, Gu X, Iqbal K, Gong C-X, Zuo J, et al. 2014. Cyclic AMP-dependent protein kinase enhances SC35-promoted Tau exon 10 inclusion. *Mol Neurobiol* **49**: 615–624.

Chen D, Bali S, Singh R, Wosztyl A, Mullapudi V, Vaquer-Alicea J, Jayan P, Melhem S, Seelaar H, van Swieten JC, et al. 2023. FTD-tau S320F mutation stabilizes local structure and allosterically promotes amyloid motif-dependent aggregation. *Nat Commun* **14**: 1625.

Chen D, Drombosky KW, Hou Z, Sari L, Kashmer OM, Ryder BD, Perez VA, Woodard DR, Lin MM, Diamond MI, et al. 2019. Tau local structure shields an amyloid-forming motif and controls aggregation propensity. *Nat Commun* **10**: 2493.

Chen L. 2018. What triggers tauopathy in chronic traumatic encephalopathy? *Neural Regen Res* **13**: 985.

Chung DC, Roemer S, Petrucelli L, Dickson DW. 2021. Cellular and pathological heterogeneity of primary tauopathies. *Mol Neurodegener* **16**: 57.

Chung D-EC, Deng X, Yalamanchili HK, Revelli J-P, Han AL, Tadros B, Richman R, Dias M, Naini FA, Boeynaems S, et al. 2024. The big tau splice isoform resists Alzheimer's-related pathological changes. *BioRxiv Prepr Serv Biol* 2024.07.30.605685.

Clavaguera F, Bolmont T, Crowther RA, Abramowski D, Frank S, Probst A, Fraser G, Stalder AK, Beibel M, Staufenbiel M, et al. 2009. Transmission and spreading of tauopathy in transgenic mouse brain. *Nat Cell Biol* **11**: 909–913. https://www.ncbi.nlm.nih.gov/pmc/articles/PMC2726961/ (Accessed November 30, 2024).

Cleveland DW, Hwo SY, Kirschner MW. 1977. Physical and chemical properties of purified tau factor and the role of tau in microtubule assembly. *J Mol Biol* **116**: 227–247.

Cohen TJ, Guo JL, Hurtado DE, Kwong LK, Mills IP, Trojanowski JQ, Lee VMY. 2011. The acetylation of tau inhibits its function and promotes pathological tau aggregation. *Nat Commun* **2**: 252.

Combs B, Mueller RL, Morfini G, Brady ST, Kanaan NM. 2019. Tau and Axonal Transport Misregulation in Tauopathies. *Adv Exp Med Biol* **1184**: 81–95.

Cook C, Carlomagno Y, Gendron TF, Dunmore J, Scheffel K, Stetler C, Davis M, Dickson D, Jarpe M, DeTure M, et al. 2014. Acetylation of the KXGS motifs in tau is a critical determinant in modulation of tau aggregation and clearance. *Hum Mol Genet* **23**: 104–116. https://www.ncbi.nlm.nih.gov/pmc/articles/PMC3857946/ (Accessed November 30, 2024).

Corsellis J a. N. 1951. Sub-Acute Sclerosing Leuco-Encephalitis: A Clinical and Pathological Report of Two Cases. *J Ment Sci* **97**: 570–583.

Crowther RA. 1991. Straight and paired helical filaments in Alzheimer disease have a common structural unit. *Proc Natl Acad Sci U S A* **88**: 2288–2292.

Davies JE, Rubinsztein DC. 2006. Polyalanine and polyserine frameshift products in Huntington's disease. *J Med Genet* **43**: 893–896.

Dawson HN, Ferreira A, Eyster MV, Ghoshal N, Binder LI, Vitek MP. 2001. Inhibition of neuronal maturation in primary hippocampal neurons from tau deficient mice. *J Cell Sci* **114**: 1179–1187.

Despres C, Byrne C, Qi H, Cantrelle F-X, Huvent I, Chambraud B, Baulieu E-E, Jacquot Y, Landrieu I, Lippens G, et al. 2017. Identification of the Tau phosphorylation pattern that drives its aggregation. *Proc Natl Acad Sci* **114**: 9080–9085. https://www.pnas.org/doi/10.1073/pnas.1708448114 (Accessed November 29, 2024).

Di Primio C, Quaranta P, Mignanelli M, Siano G, Bimbati M, Scarlatti A, Piazza CR, Spezia PG, Perrera P, Basolo F, et al. 2023. Severe acute respiratory syndrome coronavirus 2 infection leads to Tau pathological signature in neurons. *PNAS Nexus* **2**: pgad282.

Dickson DW. 1998. Pick's Disease: A Modern Approach. *Brain Pathol* **8**: 339–354.

Dickson DW, Rademakers R, Hutton ML. 2007. Progressive Supranuclear Palsy: Pathology and Genetics. *Brain Pathol* **17**: 74.

Dinkel PD, Holden MR, Matin N, Margittai M. 2015. RNA Binds to Tau Fibrils and Sustains Template-Assisted Growth. *Biochemistry* **54**: 4731–4740.

Drubin DG, Kirschner MW. 1986. Tau protein function in living cells. *J Cell Biol* **103**: 2739–2746.

D'Souza I, Poorkaj P, Hong M, Nochlin D, Lee VM, Bird TD, Schellenberg GD. 1999. Missense and silent tau gene mutations cause frontotemporal dementia with parkinsonism-chromosome 17 type, by affecting multiple alternative RNA splicing regulatory elements. *Proc Natl Acad Sci U S A* **96**: 5598–5603.

Dujardin S, Colin M, Buée L. 2015. Invited review: Animal models of tauopathies and their implications for research/translation into the clinic. *Neuropathol Appl Neurobiol* **41**: 59–80.

Ezerskiy LA, Schoch KM, Sato C, Beltcheva M, Horie K, Rigo F, Martynowicz R, Karch CM, Bateman RJ, Miller TM. 2022. Astrocytic 4R tau expression drives astrocyte reactivity and dysfunction. *JCI Insight* **7**: e152012.

Falcon B, Zhang W, Murzin AG, Murshudov G, Garringer HJ, Vidal R, Crowther RA, Ghetti B, Scheres SHW, Goedert M. 2018. Structures of filaments from Pick's disease reveal a novel tau protein fold. *Nature* **561**: 137–140.

Falcon B, Zivanov J, Zhang W, Murzin AG, Garringer HJ, Vidal R, Crowther RA, Newell KL, Ghetti B, Goedert M, et al. 2019. Novel tau filament fold in chronic traumatic encephalopathy encloses hydrophobic molecules. *Nature* **568**: 420–423.

Ferreira JA, Carmo-Fonseca M, Lamond AI. 1994. Differential interaction of splicing snRNPs with coiled bodies and interchromatin granules during mitosis and assembly of daughter cell nuclei. *J Cell Biol* **126**: 11–23.

Festa BP, Siddiqi FH, Jimenez-Sanchez M, Won H, Rob M, Djajadikerta A, Stamatakou E, Rubinsztein DC. 2023. Microglial-to-neuronal CCR5 signaling regulates autophagy in neurodegeneration. *Neuron* **111**: 2021-2037.e12.

Fichou Y, Lin Y, Rauch JN, Vigers M, Zeng Z, Srivastava M, Keller TJ, Freed JH, Kosik KS, Han S. 2018. Cofactors are essential constituents of stable and seeding-active tau fibrils. *Proc Natl Acad Sci* **115**: 13234–13239.

Fichou Y, Oberholtzer ZR, Ngo H, Cheng C-Y, Keller TJ, Eschmann NA, Han S. 2019. Tau-Cofactor Complexes as Building Blocks of Tau Fibrils. *Front Neurosci* **13**: 1339.

Fitzpatrick AWP, Falcon B, He S, Murzin AG, Murshudov G, Garringer HJ, Crowther RA, Ghetti B, Goedert M, Scheres SHW. 2017. Cryo-EM structures of tau filaments from Alzheimer's disease. *Nature* **547**: 185–190.

Forrest SL, Kril JJ, Stevens CH, Kwok JB, Hallupp M, Kim WS, Huang Y, McGinley CV, Werka H, Kiernan MC, et al. 2018. Retiring the term FTDP-17 as MAPT mutations are genetic forms of sporadic frontotemporal tauopathies. *Brain J Neurol* **141**: 521–534.

Garg RK, Mahadevan A, Malhotra HS, Rizvi I, Kumar N, Uniyal R. 2019. Subacute sclerosing panencephalitis. *Rev Med Virol* **29**: e2058.

Ginsberg SD, Crino PB, Lee VM, Eberwine JH, Trojanowski JQ. 1997. Sequestration of RNA in Alzheimer's disease neurofibrillary tangles and senile plaques. *Ann Neurol* **41**: 200–209.

Goate A, Chartier-Harlin MC, Mullan M, Brown J, Crawford F, Fidani L, Giuffra L, Haynes A, Irving N, James L. 1991. Segregation of a missense mutation in the amyloid precursor protein gene with familial Alzheimer's disease. *Nature* **349**: 704–706.

Goedert M, Spillantini MG. 2000. Tau mutations in frontotemporal dementia FTDP-17 and their relevance for Alzheimer's disease. *Biochim Biophys Acta BBA - Mol Basis Dis* **1502**: 110–121.

Goedert M, Spillantini MG, Jakes R, Rutherford D, Crowther RA. 1989a. Multiple isoforms of human microtubule-associated protein tau: sequences and localization in neurofibrillary tangles of Alzheimer's disease. *Neuron* **3**: 519–526.

Goedert M, Spillantini MG, Potier MC, Ulrich J, Crowther RA. 1989b. Cloning and sequencing of the cDNA encoding an isoform of microtubule-associated protein tau containing four tandem repeats: differential expression of tau protein mRNAs in human brain. *EMBO J* **8**: 393–399.

Götz J, Chen F, van Dorpe J, Nitsch RM. 2001. Formation of Neurofibrillary Tangles in P301L Tau Transgenic Mice Induced by Aβ42 Fibrils. *Science* **293**: 1491–1495.

Götz J, Gladbach A, Pennanen L, van Eersel J, Schild A, David D, Ittner LM. 2010. Animal models reveal role for tau phosphorylation in human disease. *Biochim Biophys Acta BBA - Mol Basis Dis* **1802**: 860–871. https://www.sciencedirect.com/science/article/pii/S0925443909002191 (Accessed November 29, 2024).

Götz J, Halliday G, Nisbet RM. 2019. Molecular Pathogenesis of the Tauopathies. *Annu Rev Pathol Mech Dis* **14**: 239–261.

Gratuze M, Cisbani G, Cicchetti F, Planel E. 2016. Is Huntington's disease a tauopathy? *Brain* **139**: 1014–1025.

Grundke-Iqbal I, Iqbal K, Tung YC, Quinlan M, Wisniewski HM, Binder LI. 1986. Abnormal phosphorylation of the microtubule-associated protein tau (tau) in Alzheimer cytoskeletal pathology. *Proc Natl Acad Sci U S A* **83**: 4913–4917. https://www.ncbi.nlm.nih.gov/pmc/articles/PMC323854/ (Accessed October 13, 2024).

Gu J, Chen F, Iqbal K, Gong C-X, Wang X, Liu F. 2017a. Transactive response DNA-binding protein 43 (TDP-43) regulates alternative splicing of tau exon 10: Implications for the pathogenesis of tauopathies. *J Biol Chem* **292**: 10600–10612.

Gu J, Wu F, Xu W, Shi J, Hu W, Jin N, Qian W, Wang X, Iqbal K, Gong C-X, et al. 2017b. TDP-43 suppresses tau expression via promoting its mRNA instability. *Nucleic Acids Res* **45**: 6177–6193.

Guedes-Dias P, Holzbaur ELF. 2019. Axonal transport: Driving synaptic function. *Science* **366**: eaaw9997. https://www.science.org/doi/10.1126/science.aaw9997 (Accessed February 11, 2025).

Guo JL, Lee VM-Y. 2011. Seeding of normal Tau by pathological Tau conformers drives pathogenesis of Alzheimer-like tangles. *J Biol Chem* **286**: 15317–15331.

Guthrie CR, Schellenberg GD, Kraemer BC. 2009. SUT-2 potentiates tau-induced neurotoxicity in Caenorhabditis elegans. *Hum Mol Genet* **18**: 1825–1838. https://doi.org/10.1093/hmg/ddp099 (Accessed March 27, 2024).

Haj-Yahya M, Gopinath P, Rajasekhar K, Mirbaha H, Diamond MI, Lashuel HA. 2020. Site-Specific Hyperphosphorylation Inhibits, Rather than Promotes, Tau Fibrillization, Seeding Capacity, and Its Microtubule Binding. *Angew Chem Int Ed* **59**: 4059–4067.

Hanseeuw BJ, Betensky RA, Jacobs HIL, Schultz AP, Sepulcre J, Becker JA, Cosio DMO, Farrell M, Quiroz YT, Mormino EC, et al. 2019. Association of Amyloid and Tau With Cognition in Preclinical Alzheimer Disease: A Longitudinal Study. *JAMA Neurol* **76**: 915–924.

Harada A, Oguchi K, Okabe S, Kuno J, Terada S, Ohshima T, Sato-Yoshitake R, Takei Y, Noda T, Hirokawa N. 1994. Altered microtubule organization in small-calibre axons of mice lacking tau protein. *Nature* **369**: 488–491. https://www.nature.com/articles/369488a0 (Accessed February 7, 2024).

Heneka MT, Golenbock D, Latz E, Morgan D, Brown R. 2020. Immediate and long-term consequences of COVID-19 infections for the development of neurological disease. *Alzheimers Res Ther* **12**: 69.

Hirokawa N, Shiomura Y, Okabe S. 1988. Tau proteins: the molecular structure and mode of binding on microtubules. *J Cell Biol* **107**: 1449–1459.

Hoffman LA, Vilensky JA. 2017. Encephalitis lethargica: 100 years after the epidemic. *Brain* **140**: 2246–2251.

Holmes BB, Furman JL, Mahan TE, Yamasaki TR, Mirbaha H, Eades WC, Belaygorod L, Cairns NJ, Holtzman DM, Diamond MI. 2014. Proteopathic tau seeding predicts tauopathy in vivo. *Proc Natl Acad Sci U S A* **111**: E4376-4385.

Hurtado DE, Molina-Porcel L, Carroll JC, MacDonald C, Aboagye AK, Trojanowski JQ, Lee VM-Y. 2012. Selectively Silencing GSK-3 Isoforms Reduces Plaques and Tangles in Mouse Models of Alzheimer's Disease. *J Neurosci* **32**: 7392–7402. https://www.ncbi.nlm.nih.gov/pmc/articles/PMC3368584/ (Accessed October 14, 2024).

Hutton M, Lendon CL, Rizzu P, Baker M, Froelich S, Houlden H, Pickering-Brown S, Chakraverty S, Isaacs A, Grover A, et al. 1998. Association of missense and 5'-splice-site mutations in tau with the inherited dementia FTDP-17. *Nature* **393**: 702–705.

Hyman AA, Weber CA, Jülicher F. 2014. Liquid-Liquid Phase Separation in Biology. *Annu Rev Cell Dev Biol* **30**: 39–58.

Iba M, Guo JL, McBride JD, Zhang B, Trojanowski JQ, Lee VM-Y. 2013. Synthetic tau fibrils mediate transmission of neurofibrillary tangles in a transgenic mouse model of Alzheimer's-like tauopathy. *J Neurosci Off J Soc Neurosci* **33**: 1024–1037.

Ilik İA, Malszycki M, Lübke AK, Schade C, Meierhofer D, Aktaş T. 2020. SON and SRRM2 are essential for nuclear speckle formation eds. J.P. Staley, K. Struhl, and J.P. Staley. *eLife* **9**: e60579.

Irwin DJ, Brettschneider J, McMillan CT, Cooper F, Olm C, Arnold SE, Van Deerlin VM, Seeley WW, Miller BL, Lee EB, et al. 2016. Deep clinical and neuropathological phenotyping of Pick disease. *Ann Neurol* **79**: 272–287.

Irwin DJ, Cohen TJ, Grossman M, Arnold SE, Xie SX, Lee VM-Y, Trojanowski JQ. 2012. Acetylated tau, a novel pathological signature in Alzheimer's disease and other tauopathies. *Brain* **135**: 807–818. https://doi.org/10.1093/brain/aws013 (Accessed October 13, 2024).

Iwatsubo T, Hasegawa M, Esaki Y, Ihara Y. 1992. Lack of ubiquitin immunoreactivities at both ends of neuropil threads. Possible bidirectional growth of neuropil threads. *Am J Pathol* **140**: 277–282.

Jaiswal S, Sahoo S, Dhiman V, Sachdeva N, Singh MP, Ram S, Sharma G, Bhadada SK. 2025. Long COVID psychiatric sequelae, biochemical markers & tau protein: A 3-year follow-up study. *Psychiatry Res* **347**: 116413.

Jiang L, Ash PEA, Maziuk BF, Ballance HI, Boudeau S, Abdullatif AA, Orlando M, Petrucelli L, Ikezu T, Wolozin B. 2019. TIA1 regulates the generation and response to toxic tau oligomers. *Acta Neuropathol (Berl)* **137**: 259–277.

Jiang L, Lin W, Zhang C, Ash PEA, Verma M, Kwan J, van Vliet E, Yang Z, Cruz AL, Boudeau S, et al. 2021. Interaction of tau with HNRNPA2B1 and N6-methyladenosine RNA mediates the progression of tauopathy. *Mol Cell* **81**: 4209-4227.e12.

Jiang L, Wolozin B. 2021. Oligomeric tau disrupts nuclear envelope via binding to lamin proteins and lamin B receptor. *Alzheimers Dement* **17**: e054521.

Jiang L, Zhu W, Zhao G, Cao L. 2023. Spinocerebellar ataxia type 8 presents as progressive supranuclear palsy. *Neurosci J* **28**: 199–203.

Jin M, Shepardson N, Yang T, Chen G, Walsh D, Selkoe DJ. 2011. Soluble amyloid β-protein dimers isolated from Alzheimer cortex directly induce Tau hyperphosphorylation and neuritic degeneration. *Proc Natl Acad Sci* **108**: 5819–5824.

Kampers T, Friedhoff P, Biernat J, Mandelkow EM, Mandelkow E. 1996. RNA stimulates aggregation of microtubule-associated protein tau into Alzheimer-like paired helical filaments. *FEBS Lett* **399**: 344–349.

Kanaan NM, Hamel C, Grabinski T, Combs B. 2020. Liquid-liquid phase separation induces pathogenic tau conformations in vitro. *Nat Commun* **11**: 2809.

Kapust RB, Waugh DS. 1999. Escherichia coli maltose-binding protein is uncommonly effective at promoting the solubility of polypeptides to which it is fused. *Protein Sci* **8**: 1668–1674.

Kaufman SK, Sanders DW, Thomas TL, Ruchinskas AJ, Vaquer-Alicea J, Sharma AM, Miller TM, Diamond MI. 2016. Tau Prion Strains Dictate Patterns of Cell Pathology, Progression Rate, and Regional Vulnerability In Vivo. *Neuron* **92**: 796–812.

Kavanagh T, Balcomb K, Ahmadi Rastegar D, Lourenco GF, Wisniewski T, Halliday G, Drummond E. 2024. hnRNP A1, hnRNP A2B1, and hnRNP K are dysregulated in tauopathies, but do not colocalize with tau pathology. *Brain Pathol Zurich Switz* e13305.

Kavanagh T, Halder A, Drummond E. 2022. Tau interactome and RNA binding proteins in neurodegenerative diseases. *Mol Neurodegener* **17**: 66. https://doi.org/10.1186/s13024-022-00572-6 (Accessed October 15, 2024).

Kedersha N, Panas MD, Achorn CA, Lyons S, Tisdale S, Hickman T, Thomas M, Lieberman J, McInerney GM, Ivanov P, et al. 2016. G3BP–Caprin1–USP10 complexes mediate stress granule condensation and associate with 40S subunits. *J Cell Biol* **212**: 845–860.

Kellogg EH, Hejab NMA, Poepsel S, Downing KH, DiMaio F, Nogales E. 2018. Near-atomic model of microtubule-tau interactions. *Science* **360**: 1242–1246. https://www.science.org/doi/10.1126/science.aat1780 (Accessed November 29, 2024).

Kinoshita E, Kinoshita-Kikuta E, Koike T. 2009. Separation and detection of large phosphoproteins using Phos-tag SDS-PAGE. *Nat Protoc* **4**: 1513–1521.

Kodama T, Koma Y, Arai N, Kido A, Urakawa N, Nishio M, Shigeoka M, Yokozaki H. 2020. CCL3–CCR5 axis contributes to progression of esophageal squamous cell carcinoma by promoting cell migration and invasion via Akt and ERK pathways. *Lab Invest* **100**: 1140–1157.

Kopeikina KJ, Hyman BT, Spires-Jones TL. 2012. Soluble forms of tau are toxic in Alzheimer's disease. *Transl Neurosci* **3**: 223–233. https://www.ncbi.nlm.nih.gov/pmc/articles/PMC3460520/ (Accessed February 8, 2024).

Koseoglu MM, Norambuena A, Sharlow ER, Lazo JS, Bloom GS. 2019. Aberrant Neuronal Cell Cycle Re-Entry: The Pathological Confluence of Alzheimer's Disease and Brain Insulin Resistance, and Its Relation to Cancer. *J Alzheimers Dis JAD* **67**: 1–11.

Kouri N, Whitwell JL, Josephs KA, Rademakers R, Dickson DW. 2011. Corticobasal degeneration: a pathologically distinct 4R tauopathy. *Nat Rev Neurol* **7**: 263–272.

Kovacs GG, Lukic MJ, Irwin DJ, Arzberger T, Respondek G, Lee EB, Coughlin D, Giese A, Grossman M, Kurz C, et al. 2020. Distribution patterns of tau pathology in progressive supranuclear palsy. *Acta Neuropathol (Berl)* **140**: 99.

Kow RL, Strovas TJ, McMillan PJ, Jacobi AM, Behlke MA, Saxton AD, Latimer CS, Keene CD, Kraemer BC. 2021. Distinct Poly(A) nucleases have differential impact on sut-2 dependent tauopathy phenotypes. *Neurobiol Dis* **147**: 105148.

Lasagna-Reeves CA, Castillo-Carranza DL, Sengupta U, Sarmiento J, Troncoso J, Jackson GR, Kayed R. 2012. Identification of oligomers at early stages of tau aggregation in Alzheimer's disease. *FASEB J Off Publ Fed Am Soc Exp Biol* **26**: 1946–1959.

Leroy K, Ando K, Laporte V, Dedecker R, Suain V, Authelet M, Héraud C, Pierrot N, Yilmaz Z, Octave J-N, et al. 2012. Lack of Tau Proteins Rescues Neuronal Cell Death and Decreases Amyloidogenic Processing of APP in *APP/PS1* Mice. *Am J Pathol* **181**: 1928–1940.

Leser GP, Fakan S, Martin TE. 1989. Ultrastructural distribution of ribonucleoprotein complexes during mitosis. snRNP antigens are contained in mitotic granule clusters. *Eur J Cell Biol* **50**: 376–389.

Lester E, Ooi FK, Bakkar N, Ayers J, Woerman AL, Wheeler J, Bowser R, Carlson GA, Prusiner SB, Parker R. 2021. Tau aggregates are RNA-protein assemblies that mislocalize multiple nuclear speckle components. *Neuron* **109**: 1675-1691.e9.

Lester E, Van Alstyne M, McCann KL, Reddy S, Cheng LY, Kuo J, Pratt J, Parker R. 2023. Cytosolic condensates rich in polyserine define subcellular sites of tau aggregation. *Proc Natl Acad Sci* **120**: e2217759120. https://www.pnas.org/doi/10.1073/pnas.2217759120 (Accessed February 17, 2023).

Li W, Lee V. 2006. Characterization of two VQIXXK motifs for tau fibrillization in vitro. *Biochemistry* **45**. https://pubmed.ncbi.nlm.nih.gov/17176091/ (Accessed October 12, 2024).

Lilliu E, Villeri V, Pelassa I, Cesano F, Scarano D, Fiumara F. 2018. Polyserine repeats promote coiled coil-mediated fibril formation and length-dependent protein aggregation. *J Struct Biol* **204**: 572–584.

Limorenko G, Tatli M, Kolla R, Nazarov S, Weil M-T, Schöndorf DC, Geist D, Reinhardt P, Ehrnhoefer DE, Stahlberg H, et al. 2023. Fully co-factor-free ClearTau platform produces seeding-competent Tau fibrils for reconstructing pathological Tau aggregates. *Nat Commun* **14**: 3939.

Lin Y, McCarty J, Rauch JN, Delaney KT, Kosik KS, Fredrickson GH, Shea J-E, Han S. 2019. Narrow equilibrium window for complex coacervation of tau and RNA under cellular conditions eds. Y. Shan, N. Barkai, and C. Castaneda. *eLife* **8**: e42571.

Ling S-C, Polymenidou M, Cleveland DW. 2013. Converging Mechanisms in ALS and FTD: Disrupted RNA and Protein Homeostasis. *Neuron* **79**: 416–438.

Liu C, Götz J. 2013. Profiling Murine Tau with 0N, 1N and 2N Isoform-Specific Antibodies in Brain and Peripheral Organs Reveals Distinct Subcellular Localization, with the 1N Isoform Being Enriched in the Nucleus. *PLOS ONE* **8**: e84849.

Lövestam S, Koh FA, van Knippenberg B, Kotecha A, Murzin AG, Goedert M, Scheres SH. 2022. Assembly of recombinant tau into filaments identical to those of Alzheimer's disease and chronic traumatic encephalopathy eds. E.H. Egelman, J. Chin, E.H. Egelman, F. Wang, and L.C. Serpell. *eLife* **11**: e76494.

Lövestam S, Li D, Wagstaff JL, Kotecha A, Kimanius D, McLaughlin SH, Murzin AG, Freund SMV, Goedert M, Scheres SHW. 2024. Disease-specific tau filaments assemble via polymorphic intermediates. *Nature* **625**: 119–125.

Low W-K, Dang Y, Schneider-Poetsch T, Shi Z, Choi NS, Merrick WC, Romo D, Liu JO. 2005. Inhibition of Eukaryotic Translation Initiation by the Marine Natural Product Pateamine A. *Mol Cell* 709–722.

Maina MB, Bailey LJ, Wagih S, Biasetti L, Pollack SJ, Quinn JP, Thorpe JR, Doherty AJ, Serpell LC. 2018. The involvement of tau in nucleolar transcription and the stress response. *Acta Neuropathol Commun* **6**: 70.

Martin L, Latypova X, Wilson CM, Magnaudeix A, Perrin M-L, Terro F. 2013a. Tau protein phosphatases in Alzheimer's disease: The leading role of PP2A. *Ageing Res Rev* **12**: 39–49. https://www.sciencedirect.com/science/article/pii/S1568163712000943 (Accessed February 11, 2025).

Martin L, Latypova X, Wilson CM, Magnaudeix A, Perrin M-L, Yardin C, Terro F. 2013b. Tau protein kinases: Involvement in Alzheimer's disease. *Ageing Res Rev* **12**: 289–309.

Mazroui R, Sukarieh R, Bordeleau M-E, Kaufman RJ, Northcote P, Tanaka J, Gallouzi I, Pelletier J. 2006. Inhibition of Ribosome Recruitment Induces Stress Granule Formation Independently of Eukaryotic Initiation Factor 2α Phosphorylation. *Mol Biol Cell* **17**: 4212–4219.

McKee AC, Cairns NJ, Dickson DW, Folkerth RD, Dirk Keene C, Litvan I, Perl DP, Stein TD, Vonsattel J-P, Stewart W, et al. 2016. The first NINDS/NIBIB consensus meeting to define neuropathological criteria for the diagnosis of chronic traumatic encephalopathy. *Acta Neuropathol (Berl)* **131**: 75–86.

McKee AC, Stein TD, Kiernan PT, Alvarez VE. 2015. The Neuropathology of Chronic Traumatic Encephalopathy. *Brain Pathol* **25**: 350–364.

McKee AC, Stein TD, Nowinski CJ, Stern RA, Daneshvar DH, Alvarez VE, Lee H-S, Hall G, Wojtowicz SM, Baugh CM, et al. 2013. The spectrum of disease in chronic traumatic encephalopathy. *Brain* **136**: 43–64.

McMillan PJ, Benbow SJ, Uhrich R, Saxton A, Baum M, Strovas T, Wheeler JM, Baker J, Liachko NF, Keene CD, et al. 2023. Tau–RNA complexes inhibit microtubule polymerization and drive disease-relevant conformation change. *Brain* **146**: 3206–3220.

McMillan PJ, Strovas TJ, Baum M, Mitchell BK, Eck RJ, Hendricks N, Wheeler JM, Latimer CS, Keene CD, Kraemer BC. 2021. Pathological tau drives ectopic nuclear speckle scaffold protein SRRM2 accumulation in neuron cytoplasm in Alzheimer's disease. *Acta Neuropathol Commun* **9**: 117.

Min S-W, Cho S-H, Zhou Y, Schroeder S, Haroutunian V, Seeley WW, Huang EJ, Shen Y, Masliah E, Mukherjee C, et al. 2010. Acetylation of Tau Inhibits Its Degradation and Contributes to Tauopathy. *Neuron* **67**: 953–966. https://www.ncbi.nlm.nih.gov/pmc/articles/PMC3035103/ (Accessed October 13, 2024).

Min S-W, Sohn PD, Li Y, Devidze N, Johnson JR, Krogan NJ, Masliah E, Mok S-A, Gestwicki JE, Gan L. 2018. SIRT1 Deacetylates Tau and Reduces Pathogenic Tau Spread in a Mouse Model of Tauopathy. *J Neurosci Off J Soc Neurosci* **38**: 3680–3688.

Mirbaha H, Chen D, Morazova OA, Ruff KM, Sharma AM, Liu X, Goodarzi M, Pappu RV, Colby DW, Mirzaei H, et al. 2018. Inert and seed-competent tau monomers suggest structural origins of aggregation ed. A. Akhmanova. *eLife* **7**: e36584. https://doi.org/10.7554/eLife.36584 (Accessed February 10, 2025).

Miyahara H, Akagi A, Riku Y, Sone J, Otsuka Y, Sakai M, Kuru S, Hasegawa M, Yoshida M, Kakita A, et al. 2022. Independent distribution between tauopathy secondary to subacute sclerotic panencephalitis and measles virus: An immunohistochemical analysis in autopsy cases including cases treated with aggressive antiviral therapies. *Brain Pathol* **32**: e13069.

Miyamoto K, Kowalska A, Hasegawa M, Tabira T, Takahashi K, Araki W, Akiguchi I, Ikemoto A. 2001. Familial frontotemporal dementia and parkinsonism with a novel mutation at an intron 10+11-splice site in the tau gene. *Ann Neurol* **50**: 117–120.

Montgomery KM, Carroll EC, Thwin AC, Quddus AY, Hodges P, Southworth DR, Gestwicki JE. 2023. Chemical Features of Polyanions Modulate Tau Aggregation and Conformational States. *J Am Chem Soc* **145**: 3926.

Mori H, Kondo J, Ihara Y. 1987. Ubiquitin is a component of paired helical filaments in Alzheimer's disease. *Science* **235**: 1641–1644.

Morishima-Kawashima M, Hasegawa M, Takio K, Suzuki M, Titani K, Ihara Y. 1993. Ubiquitin is conjugated with amino-terminally processed tau in paired helical filaments. *Neuron* **10**: 1151–1160. https://www.sciencedirect.com/science/article/pii/089662739390063W (Accessed May 28, 2024).

Mukrasch MD, Bibow S, Korukottu J, Jeganathan S, Biernat J, Griesinger C, Mandelkow E, Zweckstetter M. 2009. Structural Polymorphism of 441-Residue Tau at Single Residue Resolution. *PLOS Biol* **7**: e1000034.

Nakata T, Hirokawa N. 2003. Microtubules provide directional cues for polarized axonal transport through interaction with kinesin motor head. *J Cell Biol* **162**: 1045–1055.

Noble W, Olm V, Takata K, Casey E, Mary O, Meyerson J, Gaynor K, LaFrancois J, Wang L, Kondo T, et al. 2003. Cdk5 Is a Key Factor in Tau Aggregation and Tangle Formation In Vivo. *Neuron* **38**: 555–565. https://www.cell.com/neuron/abstract/S0896-6273(03)00259-9 (Accessed October 14, 2024).

Oblinger MM, Argasinski A, Wong J, Kosik KS. 1991. Tau gene expression in rat sensory neurons during development and regeneration. *J Neurosci* **11**: 2453–2459.

Odfalk KF, Bieniek KF, Hopp SC. 2022. Microglia: Friend and foe in tauopathy. *Prog Neurobiol* **216**: 102306.

Ogaki K, Li Y, Takanashi M, Ishikawa K-I, Kobayashi T, Nonaka T, Hasegawa M, Kishi M, Yoshino H, Funayama M, et al. 2013. Analyses of the MAPT, PGRN, and C9orf72 mutations in Japanese patients with FTLD, PSP, and CBS. *Parkinsonism Relat Disord* **19**: 15–20.

Okuno Y, Nakao T, Ishida N, Konno T, Mizutani H, Fukuyama Y, Sato T, Isomura S, Ueda S, Kitamura I, et al. 1989. Incidence of Subacute Sclerosing Panencephalitis Following Measles and Measles Vaccination in Japan. *Int J Epidemiol* **18**: 684–689.

Pakos-Zebrucka K, Koryga I, Mnich K, Ljujic M, Samali A, Gorman AM. 2016. The integrated stress response. *EMBO Rep* **17**: 1374–1395.

Panda D, Goode BL, Feinstein SC, Wilson L. 1995. Kinetic Stabilization of Microtubule Dynamics at Steady State by Tau and Microtubule-Binding Domains of Tau. *Biochemistry* **34**: 11117–11127. https://doi.org/10.1021/bi00035a017 (Accessed October 8, 2024).

Panda D, Samuel JC, Massie M, Feinstein SC, Wilson L. 2003. Differential regulation of microtubule dynamics by three- and four-repeat tau: Implications for the onset of neurodegenerative disease. *Proc Natl Acad Sci* **100**: 9548–9553.

Pandey S. 2012. Hummingbird sign in progressive supranuclear palsy disease. *J Res Med Sci Off J Isfahan Univ Med Sci* **17**: 197.

Parker DM, Tauber D, Parker R. 2025. G3BP1 promotes intermolecular RNA-RNA interactions during RNA condensation. *Mol Cell* **85**: 571-584.e7.

Pavlova A, Cheng C-Y, Kinnebrew M, Lew J, Dahlquist FW, Han S. 2016. Protein structural and surface water rearrangement constitute major events in the earliest aggregation stages of tau. *Proc Natl Acad Sci* **113**: E127–E136.

Piatnitskaia S, Takahashi M, Kitaura H, Katsuragi Y, Kakihana T, Zhang L, Kakita A, Iwakura Y, Nawa H, Miura T, et al. 2019. USP10 is a critical factor for Tau-positive stress granule formation in neuronal cells. *Sci Rep* **9**: 10591.

Pickering-Brown SM, Richardson AMT, Snowden JS, McDonagh AM, Burns A, Braude W, Baker M, Liu W-K, Yen S-H, Hardy J, et al. 2002. Inherited frontotemporal dementia in nine British families associated with intronic mutations in the tau gene. *Brain J Neurol* **125**: 732–751.

Piedrahita D, Hernández I, López-Tobón A, Fedorov D, Obara B, Manjunath BS, Boudreau RL, Davidson B, Laferla F, Gallego-Gómez JC, et al. 2010. Silencing of CDK5 reduces neurofibrillary tangles in transgenic alzheimer's mice. *J Neurosci Off J Soc Neurosci* **30**: 13966–13976.

Poorkaj P, Bird TD, Wijsman E, Nemens E, Garruto RM, Anderson L, Andreadis A, Wiederholt WC, Raskind M, Schellenberg GD. 1998. Tau is a candidate gene for chromosome 17 frontotemporal dementia. *Ann Neurol* **43**: 815–825.

Powell WC, Nahum M, Pankratz K, Herlory M, Greenwood J, Poliyenko D, Holland P, Jing R, Biggerstaff L, Stowell MHB, et al. 2024. Post-Translational Modifications Control Phase Transitions of Tau. *bioRxiv* 2024.03.08.583040.

https://www.ncbi.nlm.nih.gov/pmc/articles/PMC10979912/ (Accessed November 29, 2024).

Prasanth KV, Sacco-Bubulya PA, Prasanth SG, Spector DL. 2003. Sequential Entry of Components of Gene Expression Machinery into Daughter Nuclei. *Mol Biol Cell* **14**: 1043–1057.

Pratt J, Lester E, Parker R. 2021. Could SARS-CoV-2 cause tauopathy? *Lancet Neurol* **20**: 506.

Prissette M, Fury W, Koss M, Racioppi C, Fedorova D, Dragileva E, Clarke G, Pohl T, Dugan J, Ahrens D, et al. 2022. Disruption of nuclear envelope integrity as a possible initiating event in tauopathies. *Cell Rep* **40**: 111249.

Protter DSW, Parker R. 2016. Principles and Properties of Stress Granules. *Trends Cell Biol* **26**: 668–679.

Protter DSW, Rao BS, Van Treeck B, Lin Y, Mizoue L, Rosen MK, Parker R. 2018. Intrinsically Disordered Regions Can Contribute Promiscuous Interactions to RNP Granule Assembly. *Cell Rep* **22**: 1401–1412.

Qi X, Yuan S, Ding J, Sun W, Shi Y, Xing Y, Liu Z, Yao Y, Fu S, Sun B, et al. 2024. Emerging signs of Alzheimer-like tau hyperphosphorylation and neuroinflammation in the brain post recovery from COVID-19. *Aging Cell* **23**: e14352.

Qian W, Iqbal K, Grundke-Iqbal I, Gong C-X, Liu F. 2011. Splicing factor SC35 promotes tau expression through stabilization of its mRNA. *FEBS Lett* **585**: 875–880.

Qian W, Liu F. 2014. Regulation of alternative splicing of tau exon 10. *Neurosci Bull* **30**: 367–377.

Ramani A, Müller L, Ostermann PN, Gabriel E, Abida-Islam P, Müller-Schiffmann A, Mariappan A, Goureau O, Gruell H, Walker A, et al. 2020. SARS-CoV-2 targets neurons of 3D human brain organoids. *EMBO J* **39**: e106230.

Reiken S, Sittenfeld L, Dridi H, Liu Y, Liu X, Marks AR. 2022. Alzheimer's-like signaling in brains of COVID-19 patients. *Alzheimers Dement* **18**: 955–965.

Ripin N, Parker R. 2023. Formation, function, and pathology of RNP granules. *Cell* **186**: 4737–4756.

Rosso SM, van Herpen E, Deelen W, Kamphorst W, Severijnen L-A, Willemsen R, Ravid R, Niermeijer MF, Dooijes D, Smith MJ, et al. 2002. A novel tau mutation, S320F, causes a tauopathy with inclusions similar to those in Pick's disease. *Ann Neurol* **51**: 373–376.

Samelson AJ, Ariqat N, McKetney J, Rohanitazangi G, Bravo CP, Goodness D, Tian R, Grosjean P, Abskharon R, Eisenberg D, et al. 2023. CRISPR screens in iPSC-derived neurons reveal principles of tau proteostasis. *bioRxiv* 2023.06.16.545386. https://www.ncbi.nlm.nih.gov/pmc/articles/PMC10312804/ (Accessed October 15, 2024).

Sanders DW, Kaufman SK, DeVos SL, Sharma AM, Mirbaha H, Li A, Barker SJ, Foley AC, Thorpe JR, Serpell LC, et al. 2014. Distinct tau prion strains propagate in cells and mice and define different tauopathies. *Neuron* **82**: 1271–1288.

Schweighauser M, Murzin AG, Macdonald J, Lavenir I, Crowther RA, Scheres SHW, Goedert M. 2023. Cryo-EM structures of tau filaments from the brains of mice transgenic for human mutant P301S Tau. *Acta Neuropathol Commun* **11**: 160.

Sepulveda-Falla D, Sanchez JS, Almeida MC, Boassa D, Acosta-Uribe J, Vila-Castelar C, Ramirez-Gomez L, Baena A, Aguillon D, Villalba-Moreno ND, et al. 2022. Distinct tau neuropathology and cellular profiles of an APOE3 Christchurch homozygote protected against autosomal dominant Alzheimer's dementia. *Acta Neuropathol (Berl)* **144**: 589–601.

Seward ME, Swanson E, Norambuena A, Reimann A, Cochran JN, Li R, Roberson ED, Bloom GS. 2013. Amyloid-β signals through tau to drive ectopic neuronal cell cycle re-entry in Alzheimer's disease. *J Cell Sci* **126**: 1278–1286.

Shi Y, Zhang W, Yang Y, Murzin AG, Falcon B, Kotecha A, Beers M van, Tarutani A, Kametani F, Garringer HJ, et al. 2021. Structure-based Classification of Tauopathies. *Nature* **598**: 359.

Siahaan V, Krattenmacher J, Hyman AA, Diez S, Hernández-Vega A, Lansky Z, Braun M. 2019. Kinetically distinct phases of tau on microtubules regulate kinesin motors and severing enzymes. *Nat Cell Biol* **21**: 1086–1092.

Sibille N, Sillen A, Leroy A, Wieruszeski J-M, Mulloy B, Landrieu I, Lippens G. 2006. Structural impact of heparin binding to full-length Tau as studied by NMR spectroscopy. *Biochemistry* **45**: 12560–12572.

Sisniega DC, Reynolds AS. 2021. Severe Neurologic Complications of SARS-CoV-2. *Curr Treat Options Neurol* **23**: 14.

Skoglund L, Viitanen M, Kalimo H, Lannfelt L, Jönhagen ME, Ingelsson M, Glaser A, Herva R. 2008. The tau S305S mutation causes frontotemporal dementia with parkinsonism. *Eur J Neurol* **15**: 156–161.

Sperfeld AD, Collatz MB, Baier H, Palmbach M, Storch A, Schwarz J, Tatsch K, Reske S, Joosse M, Heutink P, et al. 1999. FTDP-17: an early-onset phenotype with parkinsonism and epileptic seizures caused by a novel mutation. *Ann Neurol* **46**: 708–715.

Spillantini MG, Murrell JR, Goedert M, Farlow MR, Klug A, Ghetti B. 1998. Mutation in the tau gene in familial multiple system tauopathy with presenile dementia. *Proc Natl Acad Sci U S A* **95**: 7737–7741.

Spillantini MG, Tolnay M, Love S, Goedert M. 1999. Microtubule-associated protein tau, heparan sulphate and alpha-synuclein in several neurodegenerative diseases with dementia. *Acta Neuropathol (Berl)* **97**: 585–594.

Spillantini MG, Yoshida H, Rizzini C, Lantos PL, Khan N, Rossor MN, Goedert M, Brown J. 2000. A novel tau mutation (N296N) in familial dementia with swollen achromatic neurons and corticobasal inclusion bodies. *Ann Neurol* **48**: 939–943.

Stanford PM, Halliday GM, Brooks WS, Kwok JB, Storey CE, Creasey H, Morris JG, Fulham MJ, Schofield PR. 2000. Progressive supranuclear palsy pathology caused by a novel silent

mutation in exon 10 of the tau gene: expansion of the disease phenotype caused by tau gene mutations. *Brain J Neurol* **123 (Pt 5)**: 880–893.

Strang KH, Golde TE, Giasson BI. 2019. MAPT mutations, tauopathy, and mechanisms of neurodegeneration. *Lab Invest* **99**: 912–928. https://www.sciencedirect.com/science/article/pii/S0023683722026009 (Accessed February 11, 2025).

Su JH, Cummings BJ, Cotman CW. 1992. Localization of heparan sulfate glycosaminoglycan and proteoglycan core protein in aged brain and Alzheimer's disease. *Neuroscience* **51**: 801–813.

Sun X, Eastman G, Shi Y, Saibaba S, Oliveira AK, Lukens JR, Norambuena A, Thompson JA, Purdy MD, Dryden K, et al. 2024. Structural and functional damage to neuronal nuclei caused by extracellular tau oligomers. *Alzheimers Dement* **20**: 1656–1670.

Takei Y, Teng J, Harada A, Hirokawa N. 2000. Defects in Axonal Elongation and Neuronal Migration in Mice with Disrupted tau and map1b Genes. *J Cell Biol* **150**: 989–1000. https://www.ncbi.nlm.nih.gov/pmc/articles/PMC2175245/ (Accessed February 7, 2024).

Tanaka H, Kondo K, Chen X, Homma H, Tagawa K, Kerever A, Aoki S, Saito T, Saido T, Muramatsu S-I, et al. 2018. The intellectual disability gene PQBP1 rescues Alzheimer's disease pathology. *Mol Psychiatry* **23**: 2090–2110.

Therriault J, Vermeiren M, Servaes S, Tissot C, Ashton NJ, Benedet AL, Karikari TK, Lantero-Rodriguez J, Brum WS, Lussier FZ, et al. 2023. Association of Phosphorylated Tau Biomarkers With Amyloid Positron Emission Tomography vs Tau Positron Emission Tomography. *JAMA Neurol* **80**: 188–199.

Tochio N, Murata T, Utsunomiya-Tate N. 2019. Effect of site-specific amino acid D-isomerization on β-sheet transition and fibril formation profiles of Tau microtubule-binding repeat peptides. *Biochem Biophys Res Commun* **508**: 184–190.

Tommasi NS, Gonzalez C, Briggs D, Properzi MJ, Gatchel JR, Marshall GA, Initiative ADN. 2021. Affective symptoms and regional cerebral tau burden in early-stage Alzheimer's disease. *Int J Geriatr Psychiatry* **36**: 1050.

Torii T, Miyamoto Y, Nakata R, Higashi Y, Shinmyo Y, Kawasaki H, Miyasaka T, Misonou H. 2023. Identification of Tau protein as a novel marker for maturation and pathological changes of oligodendrocytes. *Glia* **71**: 1002–1017.

Tracy TE, Sohn PD, Minami SS, Wang C, Min S-W, Li Y, Zhou Y, Le D, Lo I, Ponnusamy R, et al. 2016. Acetylated Tau Obstructs KIBRA-Mediated Signaling in Synaptic Plasticity and Promotes Tauopathy-Related Memory Loss. *Neuron* **90**: 245–260. https://www.ncbi.nlm.nih.gov/pmc/articles/PMC4859346/ (Accessed October 13, 2024).

Trivedi R, Nagarajaram HA. 2022. Intrinsically Disordered Proteins: An Overview. *Int J Mol Sci* **23**: 14050.

Trivellato D, Floriani F, Barracchia CG, Munari F, D'Onofrio M, Assfalg M. 2023. Site-directed double monoubiquitination of the repeat domain of the amyloid-forming protein tau impairs self-assembly and coacervation. *Bioorganic Chem* **132**: 106347. https://www.sciencedirect.com/science/article/pii/S004520682300007X (Accessed November 30, 2024).

Van Alstyne M, Nguyen VL, Hoeffer CA, Parker R. 2024. Polyserine peptides are toxic and exacerbate tau pathology in mice. 2024.10.10.616100. https://www.biorxiv.org/content/10.1101/2024.10.10.616100v1 (Accessed October 12, 2024).

Van Swieten J, Spillantini MG. 2007. Hereditary Frontotemporal Dementia Caused by Tau Gene Mutations. *Brain Pathol* **17**: 63–73.

Vanderweyde T, Apicco DJ, Youmans-Kidder K, Ash PEA, Cook C, Lummertz da Rocha E, Jansen-West K, Frame AA, Citro A, Leszyk JD, et al. 2016. Interaction of tau with the RNA-Binding Protein TIA1 Regulates tau Pathophysiology and Toxicity. *Cell Rep* **15**: 1455–1466.

Vanderweyde T, Yu H, Varnum M, Liu-Yesucevitz L, Citro A, Ikezu T, Duff K, Wolozin B. 2012. Contrasting Pathology of the Stress Granule Proteins TIA-1 and G3BP in Tauopathies. *J Neurosci* **32**: 8270–8283. https://www.ncbi.nlm.nih.gov/pmc/articles/PMC3402380/ (Accessed October 13, 2024).

Varvel NH, Bhaskar K, Patil AR, Pimplikar SW, Herrup K, Lamb BT. 2008. Aβ Oligomers Induce Neuronal Cell Cycle Events in Alzheimer's Disease. *J Neurosci* **28**: 10786–10793.

Violet M, Delattre L, Tardivel M, Sultan A, Chauderlier A, Caillierez R, Talahari S, Nesslany F, Lefebvre B, Bonnefoy E, et al. 2014. A major role for Tau in neuronal DNA and RNA protection in vivo under physiological and hyperthermic conditions. *Front Cell Neurosci* **8**: 84.

Virhammar J, Nääs A, Fällmar D, Cunningham JL, Klang A, Ashton NJ, Jackmann S, Westman G, Frithiof R, Blennow K, et al. 2021. Biomarkers for central nervous system injury in cerebrospinal fluid are elevated in COVID-19 and associated with neurological symptoms and disease severity. *Eur J Neurol* **n/a**: 3324–3331.

Vogler TO, Wheeler JR, Nguyen ED, Hughes MP, Britson KA, Lester E, Rao B, Betta ND, Whitney ON, Ewachiw TE, et al. 2018. TDP-43 and RNA form amyloid-like myo-granules in regenerating muscle. *Nature* **563**: 508–513.

Wang C, Terrigno M, Li J, Distler T, Pandya NJ, Ebeling M, Tyanova S, Hoozemans JJM, Dijkstra AA, Fuchs L, et al. 2023. Increased G3BP2-Tau interaction in tauopathies is a natural defense against Tau aggregation. *Neuron* **111**: 2660-2674.e9. https://www.sciencedirect.com/science/article/pii/S0896627323004348 (Accessed October 15, 2024).

Wardell MR, Brennan SO, Janus ED, Fraser R, Carrell RW. 1987. Apolipoprotein E2-Christchurch (136 Arg----Ser). New variant of human apolipoprotein E in a patient with type III hyperlipoproteinemia. *J Clin Invest* **80**: 483–490.

Webber CJ, Spek SJF van de, Cruz AL, Puri S, Zhang C, Aw JTM, Papadimitriou G-Z, Roberts R, Jiang K, Tran TN, et al. 2024. TIA1 Mediates Divergent Inflammatory Responses to Tauopathy in Microglia and Macrophages. 2024.11.06.622325. https://www.biorxiv.org/content/10.1101/2024.11.06.622325v1 (Accessed November 27, 2024).

Wegmann S, Biernat J, Mandelkow E. 2021. A current view on Tau protein phosphorylation in Alzheimer's disease. *Curr Opin Neurobiol* **69**: 131–138. https://www.sciencedirect.com/science/article/pii/S0959438821000222 (Accessed November 29, 2024).

Wei Y, Qu M-H, Wang X-S, Chen L, Wang D-L, Liu Y, Hua Q, He R-Q. 2008. Binding to the Minor Groove of the Double-Strand, Tau Protein Prevents DNA from Damage by Peroxidation. *PLoS ONE* **3**: e2600.

Weigand AJ, Bangen KJ, Thomas KR, Delano-Wood L, Gilbert PE, Brickman AM, Bondi MW, Initiative ADN. 2019. Is tau in the absence of amyloid on the Alzheimer's continuum?: A study of discordant PET positivity. *Brain Commun* **2**: fcz046.

Weingarten MD, Lockwood AH, Hwo SY, Kirschner MW. 1975. A protein factor essential for microtubule assembly. *Proc Natl Acad Sci U S A* **72**: 1858–1862.

Wesseling H, Mair W, Kumar M, Schlaffner CN, Tang S, Beerepoot P, Fatou B, Guise AJ, Cheng L, Takeda S, et al. 2020. Tau PTM Profiles Identify Patient Heterogeneity and Stages of Alzheimer's Disease. *Cell* **183**: 1699-1713.e13.

Wheeler JM, McMillan P, Strovas TJ, Liachko NF, Amlie-Wolf A, Kow RL, Klein RL, Szot P, Robinson L, Guthrie C, et al. 2019. Activity of the poly(A) binding protein MSUT2 determines susceptibility to pathological tau in the mammalian brain. *Sci Transl Med* **11**: eaao6545. https://www.science.org/doi/10.1126/scitranslmed.aao6545 (Accessed March 27, 2024).

Wisniewski HM, Dymecki J, Wegiel J, Kulczycki J, Schmidt-Sidor B, Grundke-Iqbal I, Strojny P. 1991. Neurofibrillary Pathology in Subacute Sclerosing Panencephalitis. *Dementia* **2**: 133–141.

Wolozin B. 2012. Regulated protein aggregation: stress granules and neurodegeneration. *Mol Neurodegener* **7**: 56.

Wolozin B, Ivanov P. 2019. Stress granules and neurodegeneration. *Nat Rev Neurosci* **20**: 649–666.

Wszolek ZK, Pfeiffer RF, Bhatt MH, Schelper RL, Cordes M, Snow BJ, Rodnitzky RL, Wolters EC, Arwert F, Calne DB. 1992. Rapidly progressive autosomal dominant parkinsonism and dementia with pallido-ponto-nigral degeneration. *Ann Neurol* **32**: 312–320.

Xia Y, Prokop S, Gorion K-MM, Kim JD, Sorrentino ZA, Bell BM, Manaois AN, Chakrabarty P, Davies P, Giasson BI. 2020. Tau Ser208 phosphorylation promotes aggregation and reveals neuropathologic diversity in Alzheimer's disease and other tauopathies. *Acta Neuropathol Commun* **8**: 88.

Yang H, Yuan P, Wu Y, Shi M, Caro CD, Tengeiji A, Yamanoi S, Inoue M, DeGrado WF, Condello C. 2023. EMBER multidimensional spectral microscopy enables quantitative determination of disease- and cell-specific amyloid strains. *Proc Natl Acad Sci* **120**: e2300769120.

Yonenobu Y, Beck G, Kido K, Maeda N, Yamashita R, Inoue K, Saito Y, Hasegawa M, Ito H, Hasegawa K, et al. 2023. Neuropathology of spinocerebellar ataxia type 8: Common features and unique tauopathy. *Neuropathology* **43**: 351–361.

Yoshiyama Y, Higuchi M, Zhang B, Huang S-M, Iwata N, Saido TC, Maeda J, Suhara T, Trojanowski JQ, Lee VM-Y. 2007. Synapse Loss and Microglial Activation Precede Tangles in a P301S Tauopathy Mouse Model. *Neuron* **53**: 337–351.

Zetterberg H. 2022. Biofluid-based biomarkers for Alzheimer's disease–related pathologies: An update and synthesis of the literature. *Alzheimers Dement* **18**: 1687–1693. https://www.ncbi.nlm.nih.gov/pmc/articles/PMC9514308/ (Accessed November 27, 2024).

Zhang W, Tarutani A, Newell KL, Murzin AG, Matsubara T, Falcon B, Vidal R, Garringer HJ, Shi Y, Ikeuchi T, et al. 2020a. Novel tau filament fold in corticobasal degeneration. *Nature* **580**: 283–287.

Zhang X, Chen Y, Tan Y, Pan T, Wei G. 2025. Recent Advances in Co-Condensation and Co-Aggregation of Amyloid Proteins Linked to Neurodegenerative Diseases. *Curr Protein Pept Sci*.

Zhang X, Lin Y, Eschmann NA, Zhou H, Rauch JN, Hernandez I, Guzman E, Kosik KS, Han S. 2017. RNA stores tau reversibly in complex coacervates. *PLOS Biol* **15**: e2002183.

Zhang X, Vigers M, McCarty J, Rauch JN, Fredrickson GH, Wilson MZ, Shea J-E, Han S, Kosik KS. 2020b. The proline-rich domain promotes Tau liquid–liquid phase separation in cells. *J Cell Biol* **219**: e202006054.

Zubair AS, McAlpine LS, Gardin T, Farhadian S, Kuruvilla DE, Spudich S. 2020. Neuropathogenesis and Neurologic Manifestations of the Coronaviruses in the Age of Coronavirus Disease 2019: A Review. *JAMA Neurol* **77**: 1018.

Zwierzchowski-Zarate AN, Mendoza-Oliva A, Kashmer OM, Collazo-Lopez JE, White CL, Diamond MI. 2022. RNA induces unique tau strains and stabilizes Alzheimer's disease seeds. *J Biol Chem* **298**: 102132.

2024. 2024 Alzheimer's disease facts and figures. *Alzheimers Dement* **20**: 3708–3821.